TRW



TRW 23499.000
P241-83-6192
27 April 1983

TRW CONTRACTS - DATA TRANSMITTAL COVER SHEET

CONTRACT NO. NAS5-20682 - SEMI-ANNUAL REPORT, NO. 6

TITLE: PLASMA WAVE EXPERIMENT FOR THE ISEE-3 MISSION

DATE: 28 April 1983

| COPIES | ADDRESSEE |
|---|---|
| 1 | K. R. Fairbrother, Code 286 (Contracting Officer) |
| 2 | R. Wales, Code 602 (Tech. Officer) |
| 1 | Publications Branch, Code 253.1 |
| 1 | Patent Counsel, Code 204 |
| Letter | AFPRO/TRW |


TRW INC.
SPACE & TECHNOLOGY GROUP

K. P Stidham /bc

K. P. Stidham
Contract Administrator
Applied Technology Division
Telephone: 213/536-3837
Mail Station: R1/2004

KPS:bc

cc: F L. Scarf, TRW Program Manager

TRW Tech Report No. 23499-6030-UT-00



# PLASMA WAVE EXPERIMENT FOR THE ISEE-3 MISSION

by

F. L. Scarf,
Principal Investigator

Semi-Annual Report
(For Period: October 1, 1982 - March 30, 1983)

Prepared for
NASA Goddard Space Flight Center
Greenbelt, Maryland 20771

Contract No. NAS5-20682

28 April 1983

Bldg R-1, Rm 1176
Applied Technology Division
TRW Space and Technology Group
One Space Park
Redondo Beach, California 90278
(213) 536-2015

# PREFACE

## 1. OBJECTIVE

The purpose of this report is to summarize the performance of work for the period 1 October 1982 through 30 March 1983, in compliance with Modification 19 to Article XXI of Contract NAS5-20682, entitled "Plasma Wave Experiment for ISEE-C (Heliocentric) Mission" dated 20 November 1974.

The objective of this contract is to provide analysis of data from a scientific instrument designed to study solar wind and plasma wave phenomena on the ISEE-3 Mission.

## 2. SCOPE OF WORK

Project activities during this past six months have included successful return of data from the instrument, continuing analysis of all data, publication of results, and deposit in National Space Science Data Center of the data.

## 3. CONCLUSIONS

Not applicable.

## 4. SUMMARY OF RECOMMENDATIONS

Not applicable.

## 1.0 INTRODUCTION

The purpose of this report is to summarize the various activities and tasks accomplished on the data analysis phase of the contract during the last six months.

## 2.0 WORK ACTIVITIES FOR THE SIX-MONTH PERIOD

### 2.1 Research

During this interval, there was much research activity involving the ISEE-3 Plasma Wave Investigation and the (unfunded) counterparts on ISEE-1 and -2. The paper entitled "Computer-Constructed Imagery of Distant Plasma Interaction Boundaries" by Greenstadt et al., was published in Advances in Space Rearch (2, 7, 163, 1983). Several new papers were completed: "Plasma Boundaries and Shocks" (Russell and Greenstadt), submitted to Revs. of Geophys. and Space Phys., February 1983; "Transfer of Pulsation-Related Wave Activity Across the Magnetopause: Observations of Corresponding Spectra by ISEE-1 and ISEE-2" (Greenstadt et al.), prepared for the special issue of Geophysical Research Letters covering the AGU Chapman Conference on Waves in Magnetospheric Plasmas (Kona Coast, Hawaii, February 1983) and submitted to the journal, March 1983; "Science Return from ISEE-3 at Comet Giacobini-Zinner" (Scarf et al.), to be published in the proceedings of the International Conference on Cometary Exploration (Budapest, Hungary, November 1982); and "The Interplanetary Shock Event of November 11/12 1978 -- A Comprehensive Test of Acceleration Theory" (K.-P. Wenzel et al.), submitted to the International Cosmic Ray

Conference (to be held in Bangalore, India, August 1983). Two other papers are in the process of being revised and readied for submission to the journals: "Collisionless Snock Lengths" (Mellott and Greenstadt), for Physical Review Letters; and "Plasma and Energetic Particle Structure of a Collisionless Quasi-Parallel Shock" (Kennel et al.), prepared for Journal of Geophysical Research."

## 2.2 Other Activities

During this six-month period, Dr. Scarf participated in the International Conference on Cometary Exploration (held in Budapest, Hungary, November 1982), and the attached ISEE-3 manuscript was submitted for publication in the proceedings of the conference. Dr. Scarf also discussed the ISEE-3 mission to Giacobini-Zinner at the Inter-Agency Consultative Group meeting and at the meeting of the IACG Plasma Science Working Group. Dr. Scarf attended the ISEE Science Working Team meeting at Goddard Space Flight Center on March 7-8, 1983, and he submitted ISEE-3 plasma wave data covering the first one and one-half crossings of the distant geomagnetic tail (October 1, 1982 through January 8, 1983) to NSSDC at this meeting. Mr. Greenstadt attended the AGU Fall Meeting held in San Francisco (December 1982) and presented a talk entitled "A Storm-Time, Pc 5 Event Observed in the Outer Magnetosphere by ISEE-1 and -2: Wave Properties". In February he traveled to Kona Coast, Hawaii, to participate in the Chapman Conference and to present a talk on "Transfer of Pulsation-Related Wave Activity Across the Magnetopause: Observations of Favorable Conditions by ISEE-1 and -2".

TRW Tech. Report No. 40789-6002-UT-00

D/



# PLASMA BOUNDARIES AND SHOCKS

C.T. Russell, Institute of
Geophysics and Planetary
Physics, University of
Los Angeles, California 90024

E.W. Greenstadt, TRW Space
and Technology Group,
One Space Park, Redondo Beach,
California 90278

FOR

Reviews of Geophysics and
Space Physics

February 3, 1983

Contribution to the 1983

US National Report to IUGG

# Plasma Boundaries and Shocks

C. T. Russell, Institute of Geophysics and Planetary Physics, University of California, Los Angeles, California 90024
and
E. W. Greenstadt, TRW Space and Technology Group, One Space Park Redondo Beach, California 90278

## INTRODUCTION

The quadrennium has seen an explosive growth in our knowledge and understanding of the various plasma and magnetic field boundaries in the terrestrial magnetosphere. Nowhere is that more evident than at the magnetopause and bow shock. In the 1975 and 1979 quadrennial reports the magnetopause was covered in a single paragraph each year. The bow shock received one paragraph in 1975 and none in 1979! The reason for the resurgence of interest in these boundaries was the availability of new and exciting measurements from the ISEE-1 and -2 spacecraft. Not only did these spacecraft carry sensitive high-time resolution, three-dimensional plasma instrumentation as well as high-time resolution and accurate magnetic and electric field data, but also the variable separation of the two spacecraft allowed the velocity of structures to be measured and thereby allowed time profiles to be converted to spatial profiles. Simultaneously numerical simulationists were benefiting from larger and faster computers and to development of ever increasingly sophisticated codes. During this period the simulation field began to blossom. The combination of good data and realistic models led to not only empirical knowledge but theoretical understanding of many of the processes at work.

The quadrennium interval 1979 through 1982 spanned the transition from exploratory work with preliminary data from ISEE-1 and 2 [e.g. Bame et al., 1979; Russell and Greenstadt, 1979; 1981] to detailed investigations with fully calibrated and updated measurements from these satellites and ISEE-3 as well. Published contributions therefore included the last of the ISEE preliminary papers, announcements of new discoveries, and follow-up accounts of plasma boundary phenomenology,--plus reports based on Voyager and Pioneer-Venus data.

Progress in the field was aided by many workshops and conferences devoted to the magnetospheric boundaries. The first of these, the Chapman Conference on Magnetospheric Boundary

Layers, held in Alpach Austria in June 1979 covered mainly the magnetopause and boundary layer. The proceedings of this conference has been published as an ESA special publication, SP-148. There were two coordinated data analysis workshops, CDAW-3 and CDAW-4, devoted to the bow shock and the magnetopause as observed by ISEE-1 and -2. These have been described by Ogilvie [1982] and Paschmann [1982], respectively. The latter workshop spawned a series of papers in a special issue of the Journal of Geophysical Research [April, 1982]. A Gordon Conference on collisionless shocks was held in June 1981 but as is their policy no proceedings were published; however, a workshop on upstream particles and waves held at JPL produced a special issue of the Journal of Geophysical Research: ISEE: Upstream Waves and Particles, Vol. 86, No. A6, June 1, 1981, which contains many of the articles cited here, including overviews by Tsurutani and Rodriguez [1981] and Kennel [1981].

In this review we will proceed from the outside in. We will discuss first the bow shock and foreshock and say a little about interplanetary shocks. Then we discuss the magnetosheath, magnetopause and boundary layer. After a section on reconnection we treat the plasma and neutral sheets, polar cusp and the injection of plasma into the inner magnetosphere.

## SHOCKS

### General

Broadly speaking, studies have divided themselves into two categories: careful documentation of more or less anticipated features of the shock using the high-quality instrumentation and two-point measurements of the ISEE-1,2 spacecraft, and intensive investigation of the [quasi-parallel] foreshock inspired by the discovery of the array of return ion distributions reported in the last IUGG interval [Gosling et al., 1978]. Both categories have benefited from reawakened interest in, and support of, theoretical calculations and large-scale computer simulations of shock and foreshock phenomena. As might be imagined, routine documentation is proceding slowly because of the care required in quantifying shock features reliably and because of frequent diversion of a limited number of researchers to the exciting area of foreshock dynamics.

Figure 1 illustrates conceptually the items of shock structure that have been the principal

foci of activity to the present. Figure 1 is an adaptation of a sketch used in an earlier review prepared at the beginning of this IUGG interval; the hatched areas indicate those combinations of shock geometry and structure that have been the subjects of intense and detailed investigation. We see that substantial areas of the figure are unshaded, and that only a minor fraction of the shock's features have been studied. Nevertheless, much has been learned and a substantial foundation for continued study has been laid. We note here that an additional area of investigation has been opened by identification of electrostatic shocks in the magnetosphere between 2.5 and 7 $R_E$ on auroral field lines [Mozer, 1981].

Hydromagnetic Modeling

Refinement of bow shock location and shape continued with efforts to compare measurements and models at the terrestrial planets [Slavin and Holzer, 1981; Slavin et al., 1983; Mihalov et al. 1982], and the analytic description of the bow shock system was advanced by Zhuang and Russell [1981] in a comprehensive study of magnetosheath thickness. Encounters with the Jovian bow shock were described by Lepping et al. [1981]. Harvey et al. [1981] and Bonifazi et al. [1980b, c, 1982] found they could routinely use simple MHD formulas for approximating the bow shock location needed in their studies of upstream conditions.

Bow Shock Front or Thermalization Layer.

By either term above we mean that feature of the shock wherein a substantial portion of the solar streaming energy of any plasma component is converted into thermal, although not necessarily isotropic or maxwellian, energy. The thicknesses and the diagnostics by which the layer is defined, as well as the kinetic details of the conversion are the subjects of inquiry.

An overview of the "typical" quasi-perpendicular shock was given by Greenstadt et al. [1980a], in which the relationships of the various diagnostics to each other could be seen at medium resolution, by current standards. Rapid heating of electrons in the magnetic foot and ramp of the shock was apparent, along with generation of a secondary distribution of accelerated protons, while thermalization of both proton distributions was seen to occur through a more prolonged series of magnetic oscillations behind the principal shock ramp and overshoot.

The overshoots themselves were studied by Russell et al. [1982a] and Livesy et al. [1982], who found that the overshoots grow with Mach number above critical [M>3]; this result is consistent with that of simulations showing the association of overshoots with trapped, reflected particles constituting the secondary distribution of protons present in the shock front above M~3 [Leroy et al.,1981; 1982].

High resolution views of electron heating at the bow shock were described by Bame et al. [1979]. Further details of electron distributions typical of the q-perpendicular shock have been displayed by Feldman et al. [1982]: Electron distributions are skewed and anisotropized by the shock potential, producing distribution envelopes with "bumps", i.e. free-energy components defined by nonmonotonic df/dE, offset along the ambient field toward or away from the shock,depending on location up- or downstream. Such distributions can be expected to excite the plasma instabilities responsible for thermalizing the particles, as discussed in the Feldman et al. paper and elaborated theoretically by [Thomsen et al., 1982]. A careful analysis of the energy gain of electrons in the observed reference frame has been undertaken by Scudder and Goodrich [1982], and an extensive treatment of microinstabilities in the bow shock has been prepared by Wu et al. [1982].

High-resolution observations of ion heating and related behavior in the bow shock emerged with a paper by Paschmann et al. [1982], who displayed two-dimensional ion velocity distributions through the foot, ramp, and overshoot of a nearly perpendicular shock, at 6-sec resolution. Figure 2 [taken from Figure 1 of Paschmann et al.] illustrates schematically the ion behavior inferred from the spacecraft data, which agrees well with the results from simulations already cited [Leroy et al., 1981; 1982]. The first simulation report [Leroy et al., 1981] showed that the "overall shock structure consists of several distinct regions whose properties are closely connected to the dynamics of the reflected ions." The second simulation report [Leroy et al., 1982] described the effects on perpendicular shock configuration of a wide range of parameters: Scaling, stationarity, and reflection were all studied as functions of beta and Mach number. Perhaps the most striking result was the variation in numbers of ions reflectioned, from none at subcritical Mach numbers to 30-40% at M(Alfven])12-13.

A related look at observational details of ion dissipation with the ISEE spacecraft was provided by Formisano and Torbert [1982], who correlated large-amplitude electrostatic waves in the frequency range 2-512 Hz with the presence of doubly-peaked ion energy shock profiles. The results lend support to the long-standing belief that ion-ion streaming produces the instability generating ion acoustic waves responsible for ion heating in supercritical collisionless shocks.

The general picture of quasi-perpendicular shock structure has been enhanced by a description of the variable plasma wave turbulence at different planetary shocks, where a progressively more distinct spectral peak between the Buneman and ion plasma frequencies was found in going from Venus to Saturn [Scarf et al.,1981]. It was speculated that this progression followed the increase in Mach number with distance in the solar wind away from the sun. At an opposite extreme, Russell et al. [1982b] have been attempting to analyze Earth's bow shock in its simplest form at low Mach number and low beta. They find that laminar, quasi-perpendicular shocks defined by these conditions have thicknesses close to the ion inertial length c/ωpi and that thickness increases as θBn drops toward 55 deg. Figure 3 sketches the rough dependence of Q-perpendicular shocks on Mach number and angle.

Study of quasi-parallel shock structure is progressing very slowly, A great amount of data has been examined, but almost nothing has been published that doesn't center on the associated foreshock, reviewed separately below. Recent examination of foreshock ions, however, has found evidence of specularly reflected ions in or just ahead of quasi-parallel transition, implying the presence in q-parallel structures of potential layers capable of causing such reflection [Gosling et al., 1982]. Fresh simulations of q-parallel shocks [Quest et al., 1982] have generated specularly reflected ions and have also found strong ion heating, stronger than electron heating, at low Mach number, for a specific parameter set chosen to be similar to that of the cases observed by Gosling et al., [1982]. Thus, simulations show considerable promise of improving our understanding of quasi-parallel structures in the near future, with return ions becoming valuable as diagnostics of q-parallel structure. The first quantitative attack on Q-parallel macro-structure with ISEE-1, 2 was reported by Greenstadt et al. [1982a], who computed the correlation between large-amplitude

magnetic pulsations at the two spacecraft at the outer edge of the shock structure, finding a sharp drop from high to low correlation at a satellite-separation of about 1000 km. The drop appeared to be compatible with Larmor radii of protons typically observed in the foreshock just upstream from the outermost pulsations.

Figure 4 summarizes, by shading portions of a familiar table of structural designations, the types of shock structure where the principal activity has been taking place.

## Foreshock

Particles. Starting with the well-defined, energy-dependent electron boundaries found near the field line tangent to the bow shock [Anderson et al.,1979], foreshock, i.e. return, particles have commanded major attention. The distinguishable distributions of 1-40kev return ions discovered earlier--beams, diffuse, and intermediate [Gosling et al.,1979]--have been tied by simultaneous IMF directions to Q-perpendicular, Q-parallel, and transition shock structures, in the same order [Greenstadt et al.,1980b]. The characteristic of the reflected beams appeared to be consistent with a model proposed earlier by Sonnerup [1969], based on preservation of magnetic moment in the reflection process [Paschmann et al., 1980] and all the various particle classes have been characterized in phase space [Eastman et al., 1981; Sentman et al. 1981a; Gurgiolo et al., 1981; Formisano et al., 1980], and the deceleration of the solar wind by diffuse distributions has been noted [Bame et al., 1980] and confirmed by comparison of data from two satellites [Bonifazi et al., 1980c]. At last, theoretical instability computations have been performed using realistic ion and electron distributions in the solar wind [Gary,1981; Gary et al.,1981; Sentman et al., 1981b; Feldman et al., 1982b], and consequences of these are being tested with further data.

Additional interest has centered on higher energy return protons in the 30kev to 1Mev range, particularly on their detection and occurrence far upstream at ISEE-3 as well as near the shock at ISEE-1 [Anderson, 1981; Gloeckler, 1979; Ipavich et al., 1979a,b; 1981a,b; Sanderson et al., 1981]. Although some sunward streaming ions have been attributed to the magnetosphere [Scholer and Hovestadt, 1981], anisotropies and spectral shapes of most of these ions, together with their link to the quasi-parallel bow shock via correlation with the appropriate IMF

directions [Scholer et al., 1979a,b; 1980a,b; 1981a] have awakened interest in seeking observational evidence near the earth's shock that cosmic rays can be fashioned out of the plasma background by reflection, or at least ejection, from relatively weak shocks like the earth's. Association of 40kev and 30Mev protons and, indeed, the entire range of ion energies from 1Kev to 1.6 Mev, with both upstream and downstream regions of interplanetary shocks [Gosling et al., 1980-1981; Evenson et al., 1982], most of which are even weaker than the earth's at 1AU, have strengthened this interest, to be discussed again in a later paragraph. Alpha particles have also been found to participate in the reflection of solar wind particles from the bow shock [Scholer et al., 1981b].

Waves. Athough foreshock waves are derived from interactions of foreshock particles with the solar wind, they were the phenomena from which the foreshock was originally defined, because of their ease of detection and processing compared to backstreaming particles. Waves have continued to be the pioneer tool in investigating upstream effects. In particular, they have served to demonstrate the existence of foreshocks of other planets. Hoppe and Russell [1981] showed the universality of the various foreshock ULF waves at Mercury, Venus, and Jupiter, including discrete wave packets and the incipient shock-like wave gradients underlying them at Venus. Indeed, the dependence of upstream wave periods on IMF magnitude at Earth [Russell and Hoppe, 1981] was extended to a common relationship for the waves at four planets, implying resonance with beams of ions of essentially the same energy at each of the planets, and perhaps in other astrophysical systems as well [Hoppe and Russell, 1982a]. The wave foreshock concept was also extended to interplanetary [IP] shocks, where VLF electromagnetic and plasma waves were found to precede IP shocks for many hours ahead of actual shock arrival if the local geometry was Q-parallel with respect to the IMF overtaken by the front [Kennel et al., 1982; Greenstadt et al., 1982a].

Wave properties in the earth's foreshock were also explored further. Wave packets attached to the largest amplitude ULF waves were found to be whistlers by correlating ISEE-1 and -2 data [Hoppe and Russell, 1980], and small waves in the foot of a Q-perpendicular shock, a

"mini foreshock", so to speak, were shown to be consistent with phase and group velocity properties of whistlers in the local solar wind [Greenstadt et al., 1981]. Upstream plasma waves were described by Filbert and Kellogg [1979] and Gurnett et al. [1979].

Particles and waves. The physics of the foreshock lies, of course, in neither particles nor waves, but in the relationships between them. Fundamental to these relationships is the correspondence between particle and wave types [Paschmann et al., 1979; Hoppe et al., 1981; 1982a,b], according to which beams, intermediate, and diffuse ion distributions are associated respectively with small, 1Hz whistlers, larger transverse narrow band, .1-.01Hz waves, and still larger [$\delta B^{\sim} B/2$], compressional, .1-.01Hz waves and connected whistler-wave packets. Figure 5, from Hoppe and Russell [1982b] summarizes this correspondence. Dependences of properties of the ion distributions, e.g. densities, velocities, temperatures, on position within the foreshock and its wave structure have been extensively developed by Bonifazi and Moreno [1981a,b], and Bonifazi et al., [1980a,b, 1982]. Instabilities caused by beams [Gary et al., 1981] and diffuse distributions [Sentman et al., 1981b] have been proposed to explain the associated waves, as mentioned earlier, but neither theory has correctly provided all the observed properties of the waves. In any case, skewed foreshock electron distributions offer a better and more likely explanation for the 1Hz waves than the ion beams [Feldman et al., 1982a], which are not always seen with these waves [Hoppe et al., 1982]. In the VLF range, narrow- banded ion acoustic waves are associated with backstreaming protons under about 1.5keV, while electron plasma oscillations, whistlers, ion acoustic waves, and low frequency electrostatic waves accompany electrons between .2 and 1.5keV [Anderson et al., 1981]. The upstream plasma waves are closely allied with spatial gradients of foreshock particles and bursts of wave noise appear at the edges of particle enhancements [Anderson et al.,op.cit.; Parks et al., 1981].

Special attention has focused on documenting the properties of foreshock ions in hope of discovering the origin of the diffuse ion distributions and ULF waves accompanying them. The puzzle of the foreshock centers on the source and maintenance of the ULF/diffuse foreshock, which is doubtless the product of some particle interaction. since the waves cannot by themselves

propagate upstream. It has been suggested [1] that the diffuse ions evolve out of an interaction of the reflected beams with the solar wind that produces waves which in turn disrupt the beams and scatter the beam particles into their diffuse distributions [Bame et al., 1980; Gary et al., 1981; Paschmann et al., 1981], and [2] that the diffuse ions derive from inherent properties of the q-parallel shock structure with whose geometry their occurrence is so intimately connected [Greenstadt et al., 1980b; Eastman et al., 1981]. The first hypothesis is supported in part by weakening of the beams with distance [Bonifazi and Moreno, 1981b]; the second by the association of specularly, as opposed to magnetic moment-conserving, reflected ions specifically with q-parallel structures [Gosling et al., 1982; Quest et al., 1982]. It may reasonably be expected at this time that resolution of the problem will involve a combination of both models, facilitated by new theoretical approaches differentiating source populations [Schwartz et al., 1982].

Among the most exciting results in the foreshock has been the development of both theory and observation of the higher energy, 40keV-1MeV, protons. These have been treated by Monte Carlo simulation [Ellison, 1982] and as products of a Fermi process in which the upstream ULF waves serve as reflecting and scattering centers, together with the shock downstream, to produce incipient cosmic rays [Terasawa, 1979; 1981]. A number of observations have supported the energization of return ions from the shock by repeated reflection between the scattering centers upstream and the shock or other scattering centers downstream [Scholer et al., 1979b; 1980a]. The upstream centers appear to scatter protons with a mean free path of about 4 $R_E$ and to lie within about 30 $R_E$ of the bow shock [Scholer et al., 1980b]. A self-consistent model of ion energization using reflected beams as feedstock to generate waves, which in turn reflect and scatter the ions until they leave a "free escape" boundary beyond 10 or 20 Re upstream from the Q-parallel shock [Lee et al., 1981; Lee, 1982], has succeeded in predicting energy spectra consistent with measured distributions [Ipavich et al., 1981a,b].

## Interplanetary Shocks

The growing theory and evidence that energetic ions are produced out of the thermal plasma by the earth's bow shock has stimulated fresh

attention to IP shocks, where suprathermal particles, both electrons [Potter, 1981] and ions [Gosling et al., 1980, 1981] have been recorded, along with precursor plasma wave noise that might be indicative of forward particle escape [Kennel et al., 1982; Greenstadt et al, 1982b]. The structure of IP shocks has enjoyed renewed scrutiny [Pesses et al., 1979; 1981; Russell and Greenstadt, 1981], and an interesting instance of bidirectional electron streaming suggestive of closed field lines in the driver gas has been described [Bame et al., 1980]. Finally, coronal transient phenomena have been reviewed generally by Dryer [1982], and the interaction of IP shocks with the bow shock, magnetosheath, and magnetopause have been modelled and observed [Zhuang et al., 1981; Winterhalter et al., 1981].

Magnetosheath

As usual, the magnetosheath has been the focus of massive inattention relative to other shock-related subjects, with a few notable exceptions. Early evaluation of ion and electron measurements demonstrated the existence of "quiet" and "disturbed" local states in the sheath, the latter distinguished by the presence of energetic ions, 3-40KeV, long period density fluctuations, and turbulent flow [Asbridge et al., 1978; Ogilvie and Scudder, 1979]. The disturbed state is probably the same as that identified with protons of energy > 100 KeV by West and Buck [1976]. The average electron heat flux in the sheath was found to be double that in the solar wind and directed away from the shock [Ogilvie ans Scudder 1979]. In a broad look at the magnetosheath, Crooker et al. [1981] compared the appearance of energetic ions in the sheath with IMF orientation to produce patterns of these ions downstream. Because of the known correlation of the ions with enhanced magnetic sheath turbulence, ion patterns probably approximated the patterns of downstream Q-parallel structure, or so the comparisons suggest: IMF across the solar wind flow removed the ions to the outside lanks of the sheath; stream angle IMF placed them mostly in the morning sheath; IMF parallel to the solar wind filled the subsolar sheath with energetic ions. Figure 6, from the Crooker et al. paper, illustrates these configurations. The possibility that trapped, magnetospheric ions may provide some of the energetic ions found in the sheath was argued by Speiser et al. [1982], and a generation mechanism for lion roars in the sheath was proposed by Thorne and Tsurutani [1981].

"Festoon"-shaped electric field emissions between 0.1 and 4 KHz in f-t spectrograms have been identified as doppler-shifted ion acoustic waves convected through the sheath from the bow shock [Gallagher, 1982].

## Magnetospheric Boundaries

Magnetopause. The amount of research done on the magnetopause over the last few years has been great and we cannot do it justice in the space provided here. Readers interested in further details are referred to the various excellent reviews available. Fairfield [1979] summarizes work on the magnetopause prior to the ISEE results. Paschmann [1982] provides an up-to-date review of the ISEE results and Sonnerup [1979] reviews the theory of reconnection which is a key process at the magnetopause. Finally, Cowley [1982] provides a detailed and up-to-date review of reconnection at the magnetopause, flux transfer events, and the boundary layer in the guise of examining the causes of connection.

Location. There is very little work being done on the average location and shape of the magnetopause at present. However, magnetopause motions are still of quite some interest. One of the puzzles about the shape of the magnetopause was why it appeared to be symmetric despite the fact the $\underline{J} \times \underline{B}$ forces would cause an additional deflection of the post shock solar wind. Zhuang et al. [1981b] developed an analytic model of the magnetosheath to examine this problem and found that, while the flow deflection did take place in front of the magnetosphere, the thermal and magnetic pressure of the magnetosheath maintained a nearly symmetric magnetosphere.

The interaction of interplanetary shocks with the magnetopause was examined by Grib et al. [1979] and Zhuang [1981a]. The observed response of the magnetopause to shocks was well explained by these models. Another cause of magnetopause motion was examined by Crooker and Siscoe [1979]. They found that substorms caused large excursions of the tail magnetopause.

One postulate that has attracted some vociferous support but little experimental evidence is that of impulsive injections through the magnetopause [ef. Heikkila, 1979, 1982a]. The advocates of this model suppose that over dense regions or blobs in the solar wind are blown against (and through) the magnetopause. These models ignore the fact that the stagnation streamline paints the entire magnetopause. The

subsolar magnetosheath spreads the normal stresses over the entire magnetopause.

Gasdynamic simulations of the solar wind interaction with the magnetosphere have been available for many years, but only recently have there been magnetohydro dynamic models. Most recently these models have developed in three dimensions [Leboeuf et al., 1981; Wu et al., 1981]. Presently they do little more than determine the location of boundaries and the flow field and field line geometry around the obstacle but even this is useful especially at low Mach numbers where the gasdynamic solutions are expected to be inappropriate.

Motion and Structure. The earliest ISEE measurements revealed the magnetopause to be in irregular and constant motion [Russell and Elphic, 1978; Paschmann et al., 1978; Elphic and Russell, 1979]. As shown in Figure 7 the velocities ranged from kilometers per second to hundreds of kilometers per second [Berchem and Russell, 1982a] but the thickness was much more constant at about 400-1000 km or a few ion gyro radii. One of the surprises of the magnetopause was the variation in structure in short distances along the boundary. During a rapid interplanetary shock-induced motion of the magnetopause the currents on the magnetopause cannot be simply described in terms of MHD discontinuities. Although occasionally the magnetopause has the magnetic and plasma signatures of a rotational discontinuity [Paschmann el al., 1979, it also can be found with a clear tangential discontinuity signature even though the magnetosheath and magnetospheric fields are antiparallel (Papamastorakis et al., 1982]. Contrary to common belief the magnetic field rotation is not controlled by the gyration of ions or electrons so that it follows a particular path dependent on the sign of the normal component of the field crossing the boundary. Rather the path the magnetic field follows from the magnetosheath to the magnetosphere is the shortest path [Berchem and Russell, 1982b]. Computer simulations have been performed of both the tangential discontinuity and rotational discontinuity by Lee and Kan [1979; 1092]. These originally favored the electron polarization but recent simulations [Swift and Lee, unpublished manuscript, 1982] reproduce these new observations.

Flux Transfer Events. Frequently when ISEE-1 and -2 are near the magnetopause, the

magnetic field will oscillate in a manner that resembles that occurring during a magnetopause crossing but with some significant differences. Thse differences suggest that a tube of magnetic flux in the magnetosphere has reconnected with some magnetosheath magnetic field and is being pulled tailward [Russell and Elphic, 1978, 1979; Elphic and Russell, 1979]. A sketch of the configuration of an FTE is shown in Figure 8. During these events the low energy plasma resembles the magnetosheath plasma and the energetic particles resemble the magnetospheric population. Daly et al. [1981] have shown that the energetic ions are streaming out of the mangetosphere. The electron signature is, however, more confusing. These results were confirmed by Scholer et al. [1982a]. Paschmann et al., [1982] have examined the over-pressure in the flux transfer event and find that it is equal to the Maxwell stress imposed by the twist and draping of the magnetic field around the tube. Modeling the leakage of particles out of the magnetosphere through an FTE has shown that the ISEE observations can easily be replicated thus lending further support to the FTE interpretation [Speiser and Williams, 1982]. Initially all FTE's had the same signature in the component of the magnetic field normal to the magnetopause, outward then inward. However, Rijnbeek et al., [1982] have discovered reversed FTE's on August 9, 1978 a period when Sonnerup et al., [1981] showed that ISEE was probably observing steady-state reconnection below the merging line. This is very important for two reasons. First, it shows that the sign of the FTE signature reverses from north to south across the merging line. Second, it shows that the magnetosphere may be undergoing steady-state reconnection and patchy reconnection simultaneously or nearly so. The statistical accuracy of these results have been extended using three years of data by Berchem and Russell [unpublished manuscript, 1982] who show that the magnetospheric equator essentially divides the FTE signatures into two groups, normal and reversed. This pattern is consistent with FTE's being created by reconnection at the magnetospheric equator and the being pulled poleward away from the equator by field line tension and magnetosheath convection.

Remote Sounding of the Magnetopause.

Williams [1979, 1980] and Williams et al., [1979] note that the near presence of the magnetopause is associated with gyro phase asymmetries in the

3-D energetic ion observations. In other words, particles which intersect the magnetopause (or some boundary near the magnetopause) in their cyclotron motion about a field line appear to be lost. While Williams and coworkers originally identified this boundary with the magnetopause, it need not be so. It is perhaps more correct to call it the trapping boundary which could, for example, be the boundary between open and closed field lines. This technique has also be used to measure magnetopause velocity [Fahnenstiel, 1981; Fritz and Fahnenstiel, 1982; Fritz et al., 1982] but because the technique, at least as applied to ISEE-1 data, returns a magnetopause location once every 36 seconds care must be exercised in the interpretation of the data. Most recently Daly [1982] has critically examined the remote sounding technique and concludes that the simple absorbing wall model overestimates the distance to the boundary.

Boundary Layer. The boundary layer is perhaps the outstanding enigma of the magnetosphere. It is a region of density and temperature intermediate between that of the magnetosheath and that of the magnetosphere just inside the magnetopause. The thickness of the boundary layer is extremely variable [Eastman and Hones, 1979]. It also often is flowing away from the sun but occasionally flows the other way. Sonnerup [1979, 1980a] has developed a simple model of a viscous boundary layer coupled to the earth by field-aligned currents. Field-aligned currents certainly are present but they don't obey the simple Sonnerup model [Sckopke et al., 1981; Hones et al., 1982]. In fact, the boundary layer studied by Sckopke et al. [1981] seems to be associated with the magnetospheric roots of flux transfer events [Cowley, 1982]. This should not be surprising since Paschmann et al. [1982] find that flux transfer events in the magnetosheath contain a mixture of magnetosheath and magnetospheric plasma having temperatures higher and densities lower than the magnetosheath. Such properties are very similar to those of the boundary layer. Reiff [1979] has reviewed the properties of what is thought to be the low altitude extension of the boundary layer. The low altitude measurements reveal two distinct plasma populations on the dayside: one predominatly on open field lines with low electron temperature (~15 eV), decreasing proton energy with increasing latitude and correlated with the IMF; the other on closed filed lines with a V-shaped ion distribution and an electron

temperature of about 50 eV warmer than the above layer but cooler than the plasma sheet.

Miscellaneous. A very attractive postulate about the location of the merging line was put forth by Crooker [1979a,b; 1980] who assumed that merging was most likely to occur at those places on the magnetopause where the magnetospheric and magnetosheath fields were exactly antiparallel. The resulting merging line depended on the relative orientation of the magnetospheric and magnetosheath magnetic fields and was in the equator and passed through the subsolar point only when the interplanetary magnetic field was exactly southward. Otherwise the merging line was at high north and south latitudes. However, observations of steady-state merging [Sonnerup et al., 1981] and FTE's, as discussed above, support a near equatorial merging line at all times.

If reconnection is taking place, the plasma flows into the magnetopause from both the magnetosheath and the magnetosphere. This is equivalent to a tangential electric field. Such a tangential electric field has been reported by Mozer et al. [1978, 1979] and Fahleson et al. [1979] using ISEE-1 measurements on November 20, 1979. However, this was a very turbulent period with extremely violent and irregular magnetopause motion. Heikkila [1982] has pointed out that these variations cause inductive effects in the data so that the interpretation of the measurements is not as simple as first believed.

Most of the work on the energetic electron layer which surrounds the magnetopause was done prior to the ISEE results [Bieber and Stone, 1979; Meng, 1979]. Scholer et al. [1982b] have examined high resolution energetic electron measurements for one ISEE pass through the subsolar magnetopause. They find a very filamentary structure with scale size of a few electron gyro radii. Ion composition measurements have been performed in the boundary layer, magnetopause and adjacent magnetosheath [Peterson et al., 1928]. All three regions contain both ionospheric and solar wind components. Plasma waves are intense near the magnetopause [Gurnett et al., 1979; Tsurutani et al., 1981; Anderson et al., 1982]. In flux transfer events, the dominant plasma wave features are an intense low frequency continuum, a dramatic increase in the frequency of occurrence of short wavelength spikes, quasi-periodic electron cyclotron harmonics correlated with ~1 Hz magnetic field fluctuations and enhanced electron plasma oscillations [Anderson et al., 1982].

## RECONNECTION

There has long been little doubt that reconnection as described by Dungey [1961] is an important process in the magnetosphere [cf. Russell, 1976]. However, until the launch of ISEE, the existing plasma data lack sufficient time resolution and 3-D coverage to monitor the variations in plasma behavior predicte in a reconnecting magnetopause. As expected ISEE-1 and -2 soon encountered the expected signatures of merging or reconnection in the plasma data [Paschmann et al., 1979] as shown in Figure 9. However, the quasi-steady state merging signature was clearly found on only a few occasions in two seasons of observations [Sonnerup et al., 1981]. On the other hand, when conditions are right, the reconnection process can proceed continually for many hours [Gosling et al., 1982]. Further, some of the reconnection must be taking place in an unsteady manner in FTE's. On the other hand, Papamastorakis et al. [1982] show that reconnection doesn't always occur when you might expect it to.

Eastman and Frank [1982] have questioned Paschmann et al.'s [1979] identification of reconnection. Their criticism in turn has been examined in detail by Scholer et al. [1982] and Daly and Fritz [1982], and successfully countered by the later two authors.

Despite the success of ISEE observations in demonstrating the reality of reconnecton, there still remains the problem of understanding how it operates and what controls it. This problem is being attacked not just through observational programs but also through analytic theory [Coroniti, 1980; Grenly and Sonnerup, 1981; Quest and Coroniti, 1981a,b], computer modeling [Cheng, 1979; Sato and Hasegawa, 1980; Birn and Hones, 1981; Brecht et al. 1982; Matthaeus, 1982; Sato and Walker, 1982] and laboratory studies [Gekelman and Stenzel, 1981; Gekelman et al., 1982; Stenzel and Gekelman, 1981, Stenzel et al., 1982a, b; Baum and Bratenahl, 1982]. The experiment of Baum and Bratenahl is directed more to dayside reconnection, whereas the experiment of Stenzel, Gekelman and co-workers is more appropriate to the magnetotail. The latter experiment has yielded a rich harvest of results including the observation of double layers in the current sheet of the reconnecting plasma.

If reconnection occurs on the dayside, then reconnection must also occur on the nightside of the magnetosphere also becuase dayside reconnection if left unchecked and unreplenished

would drive all the magnetic flux into the magnetotail. Observations in the tail assure us that indeed reconnection takes place there. Caan et al. [1979], Hones and Schindler [1979], Hones [1980], Nishida et al. [1981] and Hayakawa et al. [1982] observe the expected joint field and plasma behavior. Bieber and Stone [1980; 1982] observe the expected streaming electrons and plasma behavior. Forbes et al. [1981a,b] observe the tailward retreat of the neutral line and the expected plasma sheet drift. There can be little doubt from the in situ tail data that reconnection is also occuring there.

## PLASMA SHEET AND NEUTRAL SHEET

The magnetotail is extremely important in magnetospheric physics as the site of energy storage for substorm related processes. Thus, some of the tail related papers will be discussed in the reviews of Burch [this issue, 1982] and Hughes [this issue, 1982]. However, some of these works merit the risk of repetition. Fairfield et al. [1981a] combined IMP-6 field and plasma data to study the accumulation and release of energy in the tail. Coroniti et al. [1980] combined IMP-7 plasma field, energetic particle nd plasma wave data to take a detailed look at plasma sheet behavior during substorms. Rapid flows and highly turbulent fields were observed. Erickson and Wolf [1980] questioned on theoretical ground whether steady-state reconnection is even possible in the tail. Hones et al. [1982] report observations of the three-dimensional plasmoid that is formed during reconnecton in the tail.

The neutral sheet has long been known to be pulled north and south by the diurnal wobble of the earth's magnetic equator as if the neutral sheet were hinged to the magnetic equator at about 10 Re. Fairfield [1980] has used IMP tail observations to refine the model of how the neutral sheet responds to this diurnal torquing.

Hardy et al. [1979a] have examined the plasma mantle and boundary layer plasma as seen in the surface of the moon with the suprathermal ion detector experiment. They find that the appearance of these ions is controlled by the interplanetary magnetic field. The probability of appearance is greater for southward fields and in the northern lobe is greater on the dawn side of the tail when the solar magnetospheric Y-component of the IMF is positive. In the south a positive Y-component increases the probability in the dusk sector. Closer to the earth

Fairfield et al. [1981] report that the plasma sheet can become as thin as 1000 km during substorms. The energetic ion composition of the plasma sheet has been investigated by Peterson et al. [1981]. They find that the plasma sheet has a variable ionospheric component representing from 10% to more than 50% of the total number density and that there must be more than one process responsible for the energization of solar wind plasma to plasma sheet energies.

A thin layer of earthward streaming energetic protons and alpha particles has been observed by several groups just external to the plasma sheet [Mobius, 1980; Spjeldvik and Fritz, 1981; Williams, 1981]. The layer appears to be about two gyro radii thick and can be seen to reflect from the earth and stream tailward. Another important observation in this same region of space is the detection of large electric field spikes [up to ~80 mV $m^{-1}$] usually within one minute of the plasma sheet boundary [Cattell et al., 1982]. These strong electric fields occur in regions of enhanced low frequency turbulence and in regions of field-aligned current. Individual electric field spikes are well-correlated with small-scale gradients in particle fluxes and small-scale currents.

Sharp et al. [1981] have examined low energy ion streams in the magnetotail boundary layer, lobes, and plasma sheet. They find that the boundary layer or plasma mantle consists of plasma of solar wind origin but that the streams in the lobe and plasma sheet have ionospheric composition. Finally, we note that Meng [1981] has presented a statistical survey of the energetic particle population of the magnetotail.

## OTHER PLASMA BOUNDARIES

Other plasma boundaries that were the object of intensive investigation in the past received little attention over the last four years. The polar cusp has been studied mainly with low altitude satellites and rockets. Atmospheric Explorer-D low energy electron and ion data have been examined by Reiff et al. [1980] and Burch et al. [1980] to determine the effect of the interplanetary magnetic field on the cusp. When the interplanetary magnetic field is southward the average energy of ions decreases towards the pole. When the interplanetary magnetic field is northward it decreases and then increases. The former signature is interpreted to be consistent with merging and the latter with diffusion. Ion composition measurements from S3-3 show that at

times the magnetosheath plasma enters adiabatically while on other occasions the ions appear to have passed through an electrostatic potential in reaching low altitudes [Shelley, 1979]. These ion composition data, however, also show that ionospheric ions are continuously being accelerated to energies of the order of keV with the cusp region. Meng [1980] has examined the variation in polar cusp position during a geomagnetic storm. Curtis et al. [1979] have examined high altitude observations of plasma waves in the cusp during substorms. A region almost devoid of plasma has been discovered by Calvert [1981] at high invariant latitudes in the night magnetosphere on the basis of inferred density determined from natural plasma wave observations. This auroral plasma cavity, as it has been called, has densities below 1 $cm^{-3}$ at distances of 2 Re and above and is believed to be a transient phenomenon associated with the generation of AKR.

Another topic that has recieved very little attention lately is the injection boundary of substorm particles and the nose events of Explorer 45. This appears to be in part because it is now fairly well understood and in part because new and exciting plasma injection mechanisms have been discovered. In the steady-state electric and magnetic fields of the magnetosphere plasma can drift from the plasma sheet and around outside of some demarcation boundary. Inside this boundary which varies with pitch angle and energy, plasma circulates onclosed paths and does not intersect with the plasma sheet. During substorms the convection electric field in the magnetosphere increases and decreases on time scales comparable to the drift time of this plasma. Kaye and Kivelson [1979], Southwood and Kaye [1979], Kivelson et al. [1980] and Ejiri et al. [1980] successfully use simple electric field models and time variations of these models to replicate the observed substorm-associated features of the low energy plasma. The more comprehensive Rice model is discussed by Walker [this issue, 1982].

In the area of understanding ion injection in the magnetosphere attention is now being focussed on field-aligned flows from the ionosphere. When these ion beams peak at some angle intermediate between $0^{\circ}$ and $90^{\circ}$ pitch angle they are termed conics. Such distributions have been seen deep in the magnetosphere with the ISEE-1 plasma composition experiment in all three primary ionospheric species [Horwitz et al., 1982]. Measurements with the ATS-6 plasma

spectrometer also reveal field-aligned thermal ions in the midnight region [Olsen, 1982]. An even more exotic pitch angle distribution has been discovered with the ion analyzers on the P78-2 satellite [a.k.a. SCATHA] and termed ion 'zippers' [Fennell et al., 1981]. These ions are predominantly field-aligned at low energies and predominantly peaked perpendicular to the field at high energies with a very narrow transition in energy. They have been called zipper events because of their appearance on energy-time spectorgrams made using a detector that scans in pitch angle. The two components of the zipper are quite distinct in their magnetospheric drift paths. The low energy component drifts to the dayside via local morning and the high energy component by local evening. Ion composition measurements show that the low energy parallel component is mainly composed of oxygen and the high energy perpendicular component consists mainly of hydrogen. Lyons and Moore [1981] attribute this difference to the effects of charge exchange.

## THE FUTURE

While much has been learned about the outer magnetospheric boundaries from the ISEE-1 and -2 missions, the analysis of data from these spacecraft has far to go. Thus, we should expect many new results still from this mission. The Dynamics Explorer mission has just been launched and we should learn much auroral plasmas at mid and low altitudes in the near future. However, we will not learn much about the distant polar cusp until new spacecraft are launched. Hopefully, the Polar Plasma Laboratory of the OPEN mission which is now being planned will fill this void.

## ACKNOWLEDGEMENTS

The preparation of this review was supported by the National Aeronautics and Space Administration under research contracts NAS5-25772 [UCLA], and NASW-3690,-3499 [TRW].

## REFERENCES


### Shocks General

Kennel, C.F., Collisionless shocks and upstream waves and particles: Introductory remarks, J. Geophys. Res., 86, 4325-4329, 1981.

Mozer, F.S., ISEE 1 Observations of elecrostatic shocks on auroral zone field lines between 2.5 and 7 earth radii, Geophys. Res., Lett., 8, No. 7 823-826, July 1981.

Tsurutani, B.T., P. Rodriquez, Upstream waves and particles: An overview of ISEE results, J. Geophys. Res., 86, 4319-4324, 1981.

### Hydromagnetic Modeling

Lepping, R.P., L.F. Burlaga, and L.W. Klein, Jupiter's magnetopause, bow shock, and 10-hour modulated magnetosheath: Voyagers 1 and 2, Geophys. Res. Lett., 8, 99-102, 1981.

Mihalov, J.D., J.R. Spreiter, and S.S. Stahara, Comparison of gas dynamic model with steady solar wind flow around venus, J. Geophys. Res. 87, 10363-10371, 1982.

Slavin, J.A., and R.E. Holzer, Solar wind flow about the terrestrial planets, 1. Modeling bow shock position and shape, J. Geophys. Res., \86, 11401-11418, 1981.

Slavin, J.A., R.E. Holzer, J.R. Speiter, S.S. Stahara, and D. S. Chaussee, Solar wind flow about the terrestrial planets, J. Geophys. Res., submitted 1982.

Slavin, J.A., R.E. Holzer, J.R. Spreiter, S.S. Stahara, and D.S. Chaussee, Solar wind flow about the terrestrial planets, 2. Comparison with gasdynamic theory and implications for solar-planetary interactions, J. Geophys. Res., in press 1983.

Zhuang, H.C., C.T. Russell, Analytic treatment of the structure of the bow shock and magnetosheath, J. Geophys. Res., 86, 2191-2205, 1981.

Shock Front Thermalizaton

Bame, S.J., J.R. Asbridge, J.T. Gosling, M. Halbig, G. Paschmann, N. Sckopke, and H. Rosenbauer, High temporal resolution observations of electron heating at the bow shock, Space Sci. Rev., 23, 75, 1979.

Feldman, W.C., S.J. Bame, S.P. Gary, J.T. Gosling D. McComas, and M. Thomsen, G. Paschmann, N. Sckopke, and M.M. Hoppe, Electron heating by field-aligned free energy within the earth's bow shock, Pre-print.

Formisano, V., Measurement of the potential drop across the earth's collisionless bow shock, Geophys. Res. Lett., 9, 1033-1036, 1982.

Formisano, V. and R. Torbert, Ion acoustic wave forms generated by ion-ion streams at the earth's bow shock, Geophys Res., Lett., 9, 207-210, 1982.

Gosling, J.T., M.F. Thomsen, S.J. Bame, W.C. Feldman, G. Paschmann, N. Sckopke, Evidence for specularly reflected ions upstream from the quasi-parallel bow shock, Geophys. Res. Lett., in press, 1982.

Greenstadt, E.W., C.T. Russell, J.T. Gosling, S.J. Bame, G. Paschmann, G.K. Parks, K.A. Anderson, F.L. Scarf, R.R. Anderson, D.A. Gurnett, R.P. Lin, C.S. Lin and H. Rime, A macroscopic profile of the typical quasi-perpendicular bow shock: ISEE 1 and 2, J. Geophys. Res., 85, 2124-2130, 1980a.

Greenstadt, E.W., M.M. Hoppe and C.T. Russell, Large-amplitude magnetic variations in quasi-parallel shocks: Correlation lengths measured by ISEE 1 and 2, Geophys. Res. Lett., 9, 781-784, 1982a.

Leroy, M.M., C.C. Goodrich, D. Winske, C.S. Wu and K. Papadopoulos, Simulation of a perpendicular bow shock, Geophys. Res. Lett.,8, 12, 1269-1272, 1981.

Leroy, M.M., D. Winske, C.C. Goodrich, C.S. Wu and K. Papadopoulos, The structure of perpendicular bow shocks, J. Geophys. Res., 87, 5081-5094, 1982.

Livesey, W.A., C.F.Kennel and C.T. Russell, ISEE-1 and -2 Observations of magnetic field strength overshoots in quasi-perpendicular bow shocks, Geophys. Res. Lett., 9, 1037-1040, 1982.

Paschmann, G., N. Sckopke, S.J. Bame and J.T. Gosling, Observations of gyration ions in the foot of the nearly perpendicular bow shock, Geophys. Res. Lett., 9, 881-884, 1982.

Quest, K.B., D.W. Forslund, J.U. Brackbill and K. Lee, Collisionless disspation processes in quasi-parallel shocks, Geophys. Res. Lett., in press, 1982.

Russell, C.T., M.M. Hoppe and W.A. Livesey, Overshoots in planetary bow shocks, Nature, 296, 45-48, 1982.

Russell, C.T., M.M. Hoppe, W.A. Livesey, J.T. Gosling, and S.J. Bame, ISEE 1 and 2 observations of laminar bow shocks: Velocity and thickness, Geophys. Res. Lett., 9, 1171-1174, 1982b.

Scarf, F.L., D.A. Gurnett and W.S. Kurth, Plasma wave turbulence at planetary bow shocks, Nature, 292, 747-750, 1981.

Scudder, J.D. and C.C. Goodrich, The energy gain of plasma electrons at collisionless shock waves, J. Geophys. Res., submitted, 1982.

Scudder, J.D. and C.C. Goodrich, The energy gain of plasma electrons at collisionless shock waves, J. Geophys. Res., submitted, 1983.

Thomsen, M.F., H.C. Barr, S.P. Gary, W.C. Feldman and T.E. Cole, Stability of electron distributions within the earth's bow shock, J. Geophys. Res., in press, 1982.

Wu, C.S., D. Winske, Y.M. Zhou, S.T. Tsai, P. Rodriguez, M. Tanaka, K. Papadopoulos, K. Akimoto, C.S. Lin, M. Leroy, and C.C. Goodrich, Microinstabilities associated with a high-mach number, perpendicular bow shock, Pre-print, Inst. for Phys. Sci. & Tech., Univ. of Maryland, 1983.

Foreshock

Anderson, K.A., R.P. Lin, F. Martel, C.S. Lin, G.K. Parks and H. Reme, Thin sheets of energetic electrons upstream from the earth's bow shock, Geophys. Res. Lett., 6, 401-404, 1979.

Anderson, K.A., Measurements of bow shock particles far upstream from the earth, J. Geophys. Res., 86, 4445-4454, 1981.

Anderson R.R., G.K. Parks, T.E. Eastman, D.A. Gurnett and L.A. Frank, Plasma waves associated with energetic particles streaming into the solar wind from the earth's bow shock, J. Geophys. Res., 86, 4493-4510, 1981.

Bame, S.J., J.R. Asbridge, W.K. Feldman J.T. Gosling G. Paschmann and N. Sckopke, Deceleration of the solar wind upstream from the earth's bow shock and the origin of diffuse upstream ions, J. Geophys. Res., 85, 2981, 1980.

Bonifazi, C., G. Moreno, A.J. Lazarus, J.D. Sullivan, M.M. Hoppe and C.T. Russell, Solar wind deceleration and MHD turbulence in the earth's foreshock region: ISEE-1-2 and IMP 8 observations, J. Geophys. Res., in press, 1982.

Bonifazi, C. and G. Moreno, Reflected and diffuse ions backstreaming from the earth's bow shock: 2, Origin, J. Geophys. Res. Lett., 86, 4405-4413, 1981b.

Bonifazi, C. and G. Moreno, Reflected and diffuse ions backstreaming from the earth's bow shock: 2, Origin, J. Geophys. Res. Lett., 86, 4397-4404, 1981a.

Bonifazi, C., P. Cerulli-Irelli, M. Dobrowolny, A. Egidi, G. Moreno, and S. Orsini, Observations of backstreaming protons in the solar wind near the earth's bow shock, Nuovo Cimento, 2c, No. 6, 772-780, Nov.-Dec. 1979.

Bonifazi, C., P. Cerulli-Irelli, M. Dobrowolny, A. Egidi, G. Moreno, and S. Orsini, Observations of backstreaming protons in the solar wind near the earth's bow shock and their interactions with the solar wind, J. Geophys. Res., 85, 3461-3472, 1980a.

Bonifazi, C., G. Moreno, A.J. Lazarus and J. Sullivan, Deceleration of the solar wind in the earth's foreshock region: ISEE 2 and IMP 8 observations, J. Geophys. Res., 85,6031-6038, 1980b.

Eastman, T.E., R.R. Anderson L.A. Frank and G.K. Parks Upstream particles observed in the earth's foreshock region, J. Geophys. Res., 86, 4379-4395, 1981.

Ellison, D.C., Monte carlo simulation of charged particles upstream of the earth's bow shock, Geophys. Res. Lett., 8, 991-994, 1981.

Feldman, W.C., R.R. Anderson, J.R. Asbridge, S.J. Bame, J.T. Gosling, R.D. Zwickl, Plasma electron signature of magnetic connection to the earth's bow shock: ISEE 3, J. Geophys. Res., 87, 632-642, 1982a.

Filbert, P.C. and P.J. Kellogg, Electrostatic noise at the plasma frequency beyond the earth's bow shock, J. Geophys. Res., 84, 1369-1381, 1979.

Formisano, V., S. Orsini, C. Bonifazi, A. Egidi, and G. Moreno, High time resolution observations of the solar wind and backstreaming ions in the earth's foreshock region, Geophys. Res. Lett., 7, 385-388, 1980.

Formisano, V. and S. Orsini, Acceleration process at the earth's bow shock, J. Geophys. Res., 50, 114-122, 1981.

Gary, S.P., Microinstabilities upstream of the earth's bow shock - A brief review, J. Geophys. Res., 86, 4331-4336, 1981.

Gary, S.P., J.T. Gosling and D.W. Forslund, The electromagnetic ion beam instability upstream of the earth's bow shock, J. Geophys. Res., 86, 6691-6696, 1981.

Gloeckler, G., Observations of energetic particles in the near and far interplanetary medium, Aip Conf. Proc.,56, 43, 1979.

Gosling, J.T., J.R. Asbridge, S.J. Bame, G. Paschmann and N. Sckopke, Observations of two distinct populations of bow shock ions, Geophys. Res. Lett., 5, 957-960, 1978.

Gosling, J.T., J.R. Asbridge, S.J. Bame and W.C. Feldman, Ion acceleration at the earth's bow shock: A review of observations in the upstream region, Proc. workshop on particle acceleration mechanisms in astrophysics, 1979.

Greenstadt, E.W., C.T. Russell and M.M. Hoppe, Magnetic field orientation and suprathermal ion streams in the earth's foreshock, J. Geophys. Res., 85, 3473-3479, 1980b.

Greenstadt, E.W., R.W. Fredricks, C.T. Russell, F.L. Scarf, R.R. Anderson and D. A. Gurnett, Whistler mode wave propagation in the solar wind near the bow shock, J. Geophys. Res., 86, 4511-4516, 1981.

Gurgiolo, C., G.K. Parks, B.H. Mauk, C.S. Lin, K.A. Anderson, R.P. Lin and H. Reme, Non-E X B ordered ion beams upstream of the earth's bow shock, J. Geophys. Res., 86, 4415-4424, 1981.

Gurnett, D.A., R.R. Anderson, F.L. Scarf, R.W. Fredricks and E.J. Smith, Initial results from the ISEE-1 and-2 plasma wave investigation, Space Sci. Rev., 23, 103-122, 1979.

Harvey, C.C., M.B. Bavassano-Cattaneo, M. Dobrowolny, S. Orsini, A. Mangeney and C.T. Russell, Correlated wave and particle observations upstream of the earth's bow shock, J. Geophys. Res., 86, 4517-4529, 1981.

Hoppe, M.M. and C.T. Russell, Particle acceleration at planetary bow shocks, Nature, 295, 41-42, 1982a.

Hoppe, M.M., C.T. Russell, L.A. Frank, T.E. Eastman and E.W. Greenstadt, Upstream hydromagnetic waves and their association with backstreaming ion populations: ISEE 1 and ISEE 2 observations, J. Geophys. Res., 86, 4471-4492, 1981.

Hoppe, M.M. and C.T. Russell, Upstream waves and particles, Presented to COSPAR, Ottawa, 1982, submitted to Space Sci. Rev., 1982b.

Hoppe, M.M., C.T. Russell, T.E. Eastman and L.A. Frank, Characteristics of the ULF waves associated with upstream ion beams, J. Geophys. Res., 87, 643-650, 1982.

Hoppe, M.M. and C.T. Russell, Whistler mode wave packets in the earth's foreshock region, Nature, 287, 407-420, 1980.

Hoppe, M.M. and C.T. Russell, On the nature of ULF waves upstream of planetary bow shocks, Adv. Space Res., 1, 327, 1981.

Ipavich, F.M., G. Gloeckler, C.Y. Fan, L.A. Fisk, D. Hovestadt, B. Klecker, J.J. O'Gallagher and M. Scholer, Initial observations of low energy charged particles near the earth's bow shock on ISEE-1, Space Sci. Rev., 23, 93-101, 1979a.

Ipavich, F.M., A.B. Galvin, G. Gloeckler, D. Hovestadt, M. Scholer, C.Y. Fan, L.A. Fisk and J.J. O'Gallagher, Composition and energy spectra of low energy ions observed upstream of the earth's bow shock on ISEE-1, Proc. 16th Intern. Cosmic Ray Conf., Vol. 3, 140-144, 1979b.

Ipavich, F.M., A.B. Galvin, G. Gloeckler, M. Scholer and D. Hovestadt, Statistical survey of ions observed upstream of the earth's bow shock - Energy spectra, Composition, and Spatial Variation, J. Geophys. Res., 86, 4337-4342, 1981a.

Ipavich, F.M., M. Scholer and G.Gloeckler, Temporal development of composition, spectra and anisotropies during upstream particle events, J. Geophys. Res., 86, 11153-11160, 1981b.

Lee, M.A., G. Skadron and L.A. Fisk, Acceleration of energetic ions at the earth's bow shock, Geophys. Res. Lett., 8, 401-404, 1981.

Lee, M.A., Coupled hydromagnetic wave excitation and ion acceleration upstream of the earth's bow shock, J. Geophys. Res., 87, 5063-5080, 1982.

Parks, G.K., E.W. Greenstadt, C.S. Wu, C.S. Lin, A. St.-Marc, R.P. Lin, K.A. Anderson, C. Gurgiolo, B. Mauk, H. Reme, R. Anderson and T.E. Eastman, Upstream particle spatial gradients and plasma waves, J. Geophys. Res., 86, 4343-4354, 1981.

Paschmann, G., N. Sckopke, S.J. Bame, J.R. Asbridge, J.T. Gosling, C.T. Russell and E.W. Greenstadt, Association of low-frequency waves with suprathermal ions in the upstream solar wind, Geophys. Res. Lett., 6, 209-212, 1979.

Paschmann, G., N. Sckopke, J.R. Asbridge, S.J. Bame and J.T. Gosling, Energization of solar wind ions by reflection from the earth's bow shock, J. Geophys. Res., 85, 4689-4693, 1980.

Paschmann, G., N. Scopke, J. Papamastorakis, J.R. Asbridge, S.J. Bame and J.T. Gosling, Characteristics of reflected and diffuse ions upstream from the earth's bow shock, J. Geophys. Res., 86, 4355-4364, 1981.

Russell, C.T. and M.M. Hoppe, Dependence of upstream wave periods on the interplanetary magnetic field strength, Geophys. Res. Lett., 8, 615-617, 1981.

Sanderson, T.R., R. Reinhard and K.P. Wenzel, Propagation of upstream protons between the earth's bow shock and ISEE-3, J. Geophys. Res., 86, 4425-4434, 1981.

Scholer, M. and D. Hovestadt, Upstream energetic ions and electron: Bow shock-associated or magnetospheric origin?, J. Geophys. Res.,86 9040-9046, 1981.

Scholer, M., G. Gloeckler, F.M. Ipavich, D. Hovestadt and B. Klecker, Pitch angle distributions of energetic protons near the earth's bow shock, Geophys. Res. Lett., 6, 707-710, 1979a, 28-45 KeV only when B aligned with shock; Anisotropic alkong B, acceleration between shock and scattering centers upstream suggested.

Scholer, M., F.M. Ipavich, G. Gloeckler, C.Y. Fan, L.A. Fisk, D. Hovestadt, B. Klecker and J.J. O'Gallagher, Energetic ions upstream of the earth's bow shock observed on ISEE-1 and ISEE-3, In Proc. 16th Int. Cosmic Ray Conf., 5, 287-291, 1979b.

Scholer, M., G. Gloeckler, F.M. Ipavich, D. Hovestadt and B. Klecker, Upstream particle events close to the bow shock and 200 $R_E$ upstream: ISEE-1 and ISEE-1 observations, Geophys. Res. Lett., 7, 73-76, 1980a, 28-145 KeV isotrophic near shcok, sunward streaming at ISEE-3, scattering from multiple reflection from scattering centers closer than ISEE-3 [200$R_E$].

Scholer, M., G. Gloeckler, F.M. Ipavich and B. Klecker, Conditions for acceleration of energetic ions >= 30 KeV associated with the earth's bow shock, J. Geophys. Res. 85,4602-4606, 1980b, E> 30 KeV statistic give high probabilty when $\lambda_{XB}$ small, implying time of connection mfp ~ $4R_E$, scattering at r< 30 $R_E$ from shock.

Scholer, M., F.M. Ipavich and G. Gloeckler, Beams of protons and alpha particles greater than 30 KeV/charge from the earth's bow shock, J. Geophys. Res., 86, 4374-4378, 1981b, 2 examples, both species present; beam like events; protons explainable by simple reflection.

Scholer, M., F.M. Ipavich, G. Gloeckler and D. Hovestadt, Simultaneous observations of energetic protons close to the bow shock and far upstream, J. Geophys. Res., 49, 186-191, 1981a.

Schwartz, S.J., M.F. Thomsen and J.T. Gosling, Ions upstream of the earth's bow shock: a theoretical comparison of alternative source populations, J. Geophys. Res., in press, 1982.

Sentman, D.D., C.F. Kennel and L.A. Frank, Plasma rest frame distributions of suprathermal ions in the earth's foreshock region, J. Geophys. Res., 86, 4365-4373, 1981b.

Sentman, D.D., J.P. Edmiston and L.A. Frank, Instabilities of low frequency, parallel propagating electromagnetic waves in the earth's foreshock region, J. Geophys. Res., 86, 7487-7497, 1981b.

Sonnerup, B.U.O., Acceleration of particles reflected at a shock front, J. Geophys. Res., 74, 1301-1304, 1969.

Terasawa, T., Origin of 30 to 100 KeV protons observed in the upstream region of the earth's bow shock, Planet. Space Sci., 27, 365, 1979.

Terasawa, T., Energy spectrum of ions accelerated through fermi process at the terrestrial bow shock, J. Geophys. Res., 86, 7595-7606, 1981.

Bame, S.J., J.R. Asbridge, W.C. Feldman, J.T. Gosling, and R.D. Zwickl, Bi-directional streaming of solar wind electrons greater than 80 eV: ISEE evidence for a closed-field structure within the driver gas of an interplanetary shock, Geophys. Res. Lett., 8, 2981-2990, 1980.

Dryer, M., Coronal transient phenomena, Space Sci. Rev., in press, Feb. 1982.

Evenson P., P. Meyer and S. Yanagita, Solar flare shocks in interplanetary space and solar flare particle events, J. Geophys. Res., 87, 625-631, 1982.

Gosling, J.T., J.R. Asbridge, S.J. Bame and W.C. Feldman, G. Paschmann, N. Sckopke, Solar wind ions accelerated to 40 KeV by shock wave disturbances, J. Geophys. Res., 85, 744-752, 1980.

Gosling, J.T., J.R. Asbridge, S.J. Bame, W.C. Feldman, R.D. Zwickl, G. Paschmann, N. Sckopke and R. J. Hynds, Interplanetary ions during an energetic storm particle event: The distribution function from solar wind thermal energies to 1.6 Mev, J. Geophys. Res., 86, 547-554, 1981.

Greenstadt, E.W., F.L. Scarf, C.F. Kennel, E.J. Smith and R.W. Fredricks, Plasma wave levels and IMF orientations preceding observations of interplanetary shocks by ISEE-3, Geophys. Res. Lett., 9, 668-671, 1982b.

Kennel, C.F., F.L. Scarf and F.V. Coroniti, E. J. Smith and D. A. Gurnett, Non-local plasma turbulence associated with interplanetary shocks, J. Geophys. Res., 87, 17-34, 1982.

Presses, M.E., B.T. Tsurutani, J.A. Van Allen and E.J. Smith, Acceleration of energetic protons by interplanetary shocks, J. Geophys. Res., 84, 7297-7301, 1979.

Presses, M.E., J.R. Jokipii and D. Eichler, Cosmic ray drift, shock wave acceleration, and the anomalous component of cosmic rays, The Astrophys. J., 246, 85, June, 1981.

Potter, D.W., Acceleration of electrons by interplanetary shocks, J. Geophys. Res., 86, 11111-11116, 1981.

Russell, C.T. and E.W. Greenstadt, ISEE 1 and 2 observations of interplanetary shocks, solar wind IV, H. Rosenbauer[ed.], 191-198, MPI for Astronomy, Lindau 1981.

Winterhalter, D., M.G. Kivelson and C.T. Russell, ISEE-1, -2, and -3, observations of the interaction between an interplanetary shock and the earth's magnetosphere: A rapid traversal of the magnetopause, Geophys. Res. Lett., 8, 911-914, 1981.

Zhuang, H.C., C.T. Russell, E.J. Smith and J.T. Gosling, Three dimensional interaction of interplanetary shock waves with the bow shock and magnetopause: A comparison of theory with ISEE observations, J. Geophys. Res., 86, 5590-5600, 1981.

Magnetosheath

Asbridge, J.R., S.J. Bame, J.T. Gosling, G. Paschmann and N. Sckopke, Energetic plasma ions within the earth's magnetosheath, Geophys. Res. Lett., 5, 953-955, 1978.

Crooker, N., T.E. Eastman, L.A. Frank, E.J. Smith and C.T. Russell, Energetic magnetosheath ions and the interplanetary magnetic field orientation, J. Geophys. Res., 86, 4455-4460, 1981.

Gallagher, D.L., Short wavelength electrostatic waves in the earth's magnetosheath, J. Geophys. Res., 81, submitted, 1982.

Ogilvie, K. W. and J.D. Scudder, First results from the six-axis electron spectrometer on ISEE-1, Space Sci. Rev., 23, 123-133, 1979.

Speiser, T.W., D.J. Williams and H.A. Garcis, Magnetopherically trapped ions as a source of magnetosheath energetic ions, J. Geophys. Res., 86, 723-732, 1981.

Thorne, R.M. and B.T. Tsurutani, Generation mechanism for magnetosheath lion roars, Nature, 293, 384-386, 1981.

West, H.I. and R.M. Buck, Observations of > 100 KeV protons in the earth's magnetosheath, J. Geophys. Res., 81, 569-584, 1976.

Magnetopause

Anderson, R.R., C.C. Harvey, M.M. Hoppe, B.T. Tsurutani, T.E. Eastman and J. Etcheto, Plasma waves near the magnetopause, J. Geophys. Res., 87, 2087-2107, 1982.

Berchem, J. and C.T. Russell, The thickness of the magnetopause current layer: ISEE-1 and 2 observations, J. Geophys. Res., 87, 2108-2114, 1982a.

Berchem, J. and C.T. Russell, Magnetic field rotation through the magnetopause: ISEE-1 and 2 observations, J. Geophys. Res., 87,8139-8148, 1982b.

Bieber J.W. and E.C. Stone, Energetic electron bursts in the magnetopause electron layer and in interplanetary space, in Magnetospheric Boundary Layers, [B. Battrick, ed.], 131-141, ESA SP-148, 1979.

Cowley, S.W.H., The causes of convection in the earth's magnetosphere: A review of develoments during the IMS, Rev. Geophys. Space Phys., 20, 531-565, 1982.

Crooker, N.U. and G.L. Siscoe, Large amplitude substorm motion of the magnetotail boundary, Geophys. Res. Lett., 6, 105-108, 1979.

Daly, P. W., Remote sensing of energetic particle boundaries, Geophys. Res. Lett, in press, 1982.

Daly, P.W., D.J. Williams, C.T. Russell and E. Keppler, Particle signature of magnetic flux transfer events at the magnetopause, J. Geophys. Res., 86, 1628-1632, 1981.

Dungey, J.W., Interplanetary magnetic field and the auroral zones, Phys. Rev. Lett., 6, 47-48, 1961,

Eastman, T.E. and E.W. Hones, Jr., Characteristics of magnetospheric boundary layer as observed by IMP 6, J. Geophys. Rev., 84, 2019-2028, 1979.

Elphic, R.C. and C.T. Russell, ISEE-1 and 2 magnetometer observations of the magnetopause in Magnetospheric Boundary Layers, [B. Battrick, ed.] 43-50, ESA SP-148, Paris, 1979.

Fahleson, U.V., C.G. Falthammar, P.A. Lindqvist, F.S. Mozer, R.B. Torbert, A. Gonfalone and A. Pedersen, Quasistatic electric fields observed during a number of magnetopause crossings by ISEE-1, in Magnetospheric Boundary Layers [B. Battrick, ed.], 51-65, ESA SP-148, Paris, 1979.

Fahnenstiel, S.C., Standing waves observed at the dayside magnetopause, Geophys. Res. Lett., 8, 1155-1158, 1981.

Fairfield, D.H., Global aspects of the earth's magnetopause, in Magnetospheric Boundary Layers [B. Battrick, ed.], 5-1, ESA SP-148, Paris, 1979.

Fairfield, D.H., A statistical determination of the shape and position of the geomagnetic neutral sheet, J. Geophys. Res., 85, 775-780, 1980.

Fritz, T.A. and S.C. Fahnenstiel, High temporal resolution energetic particle soundings at the magnetopause on November 8, 1977, using ISEE-2, J. Geophys. Res., 87, 2125-2132, 1982.

Fritz, T.A., D.J. Williams, G. Paschmann, C.T. Russell, and W.N. Spjeldvik, The magnetopause as sensed by energetic particles, magnetic fields and plasma measurements on November 20, 1977, J. Geophy. Res., 87, 2133-2138, 1982.

Gary, S.P. and T.E. Eastman, The lower hybrid drift instability at the magnetopause, J. Geophys. Res., 84, 7378-7381, 1979.

Grib, S.A., B.E. Brunelli, M. Dryer, and W.W. Shen, Interaction of interplanetary shock waves with the bow shock magnetopause, J. Geophys. Res., 84, 5907-5922, 1979.

Gurnett, D.A., R.R. Anderson, B.T. Tsurutani, E.J. Smith, G. Paschmann, G. Haerendel, S.J. Bame and C.T. Russell, Plasma wave turbulence at the magnetopause: Observations from ISEE 1 and 2, J. Geophys. Res. 84, 7043-7058, 1979.

Heikkila, W.J., Impulsive penetration and viscous interaction, in Magnetospheric Boundary Layers [B. Battrick, ed.], 375-380, ESA SP-148, Paris, 1979.

Heikkila, W.J., Impulsive plasma transport through the magnetopause, Geophys. Res. Lett., 9, 877-880, 1982a.

Heikkila, W.J., Inductive electric field at the magnetopause, Geophys. Res. Lett., 9, 159-162, 1982b.

Heppner, J.P., N.C. Maynard, and T.L. Aggson, Early results from ISEE-1 measurements, Space Sci. Rev., 22, 777-789, 1978.

Hill, T.W., Rates of mass momentum and energy transfer at the magnetopause, in Magnetospheric Boundary Layers, [B. Battrick, ed.], 325-332, ESA SP-148, Paris, 1979.

Holzer, R.E. and J.A. Slavin, A correlative study of magnetic flux transfer in the magnetosphere, J. Geophys. Res., 84, 2573-2578, 1979.

Hones, Jr., E.W., B.U.O. Sonnerup, S.J. Bame, G. Paschmann and C.T. Russell, "Reverse draping" of magnetic field lines in the boundary layer, Geophys. Res. Lett., 9, 523-526, 1982.

Knott, K., D.H. Fairfield, A. Kurth and D.T. Young, Observations near the magnetopause at the onset of the July 29, 1977 sudden storm commencement, J. Geophys. Res., 87, 5883-5894, 1982.

Lanzerotti, L.J., S.M. Krimigis, C.D. Bostrom, W.I. Axford, R.P. Lepping and N.F. Ness, measurements of plasma flow at the dawn magnetopause by Voyager 1, J. Geophys. Res., 84, 6483-6488, 1979.

Lanzerotti, L.J., C.G. Maclennan, R.P. Lepping and S.M. Krimigis, Intensity variations in plasma flow at the dawn magnetopause, Planet Space Sci., 28, 1163-1169, 1980.

Leboeuf, J.N., T. Tajima, C.F. Kennel and J.M. Dawson, Global simulations of the three-dimensional magnetosphere, J. Geophys. Res., 86, 257-260, 1981.

Lee, L.C. and J.R. Kan, A unified kinetic model of the tangential magnetopause structure, J. Geophys. Res., 84, 6417-6426, 1979.

Lee, L.C. and J.R. Kan, Field-aligned currents in the magnetospheric boundary layer, J. Geophys. Res., 85, 37-40, 1980.

Lee, L.C. and J.R. Kan, Structure of the magnetopause rotational discontinuity, J. Geophys. Res., 87, 139-143, 1982.

Lee, L.C. and J. G. Roederer, Solar wind energy transfer through the magnetopause of an open magnetosphere, J. Geophys. Res., 87, 1439-1444, 1982.

Lee, L.C., R.K. Albano and J.R. Kan, Kelvin-Helmholtz instability in the magnetopause boundary layer region, J. Geophys. Res., 86, 54-58, 1981.

Lepping, R.P. and L.F. Burlaga, Geomagnetopause surface fluctuations observed by Voyager 1, J. Geophys. Res., 84, 7099-7106, 1979.

Meng, C.I., L.A. Frank and K.L. Ackerson, Particle and field characteristic of the dayside magnetopause energetic electron layer, in Magnetospheric Boundary Layers [B. Battrick, ed.], 143-148, ESA SP-148, Paris, 1979.

Mozer, F.S., R.B. Torbert, U.V. Fahleson, C.F. Falthammar, A. Gonfalone, A. Pedersen and C.T. Russell, Direct observation of a tangential electric field component at the magnetopause, Geophys. Res. Lett., 6, 305-308, 1979.

Ogilvie, K.W., ISEE work on collisionless shocks: CDAW3: The meeting and the results, in The IMS Source Book, [C.T. Russell and D.J. Southwood, eds.], 264-271, American Geophysical Union, Washington D.C., 1982.

Papamastorakis, I., G. Paschmann, N. Sckopke, S.J. Bame and J. Berchem, The magnetopause as a tangentially discontinuity for large field rotation angles, J. Geophys. Res., in press, 1982.

Parks, G.K., C. Gurgiolo, C.S. Lin, K.A. Anderson, R.P. Lin, F. Martel and H. Reme, Dual spacecraft observations of energetic particles in the vicinity of the magnetopause, bow shock, and interplanetary medium, Space Sci. Rev., 22, 765-776, 1978.

Parks, G.K., C.S. Lin, K.A. Anderson, R.P. Lin, H. Reme, F. Coroniti, C. Meng and R. Pellat, Particle boundary structures at the magnetopause and the plasma sheet, in Magnetospheric Boundary Layers [B. Battrick, ed.], 151-156, ESA SP-148, Paris, 1979.

Parks, G.K., C.S. Lin, K.A. Anderson, R.P. Lin and H. Reme, ISEE-1 and 2 particle observations of outer plasma sheet boundary, J. Geophys. Res., 84, 6471-6476, 1979.

Paschmann, G., ISEE magnetopause observations: Workshop results, in The IMS Source Book [C.T. Russell and D.J. Southwood, eds.], 272-284, American Geophysical Union, Washingto,n D.C., 1982.

Paschmann, G., N. Sckopke, G. Haerendel, I. Papamastorakis, S.J. Bame, J.R. Asbridge, J.T. Gosling, E.W. Hones, Jr. and E.B. Tech, ISEE plasma observations near the subsolar magnetopause, Space Sci. Rev., 22, 717-713, 1978.

Paschmann, G., G. Haerendel, I. Papamastorakis, N. Sckopke, S.J. Bame, J.T. Gosling and C.T. Russell, Plasma and magnetic field characteristics of magnetic flux transfer events, J. Geophys. Res., 87, 2159-2168, 1982.

Peterson, W.K., E.G. Shelley, G. Haerendel, and G. Paschmann, Energetic ion composition in the subsolar magnetopause and boundary layer, J. Geophys. Res. 87, 2139-2146, 1982.

Potemra, T.A., Current systems in the earth's magnetosphere, Rev. Geophys. Space Phys., 17, 640-656, 1979.

Rijnbeek, R.P., S.W.H. Cowley, D.H. Southwood, and C.T. Russell, Observations of "reverse polarity" flux transfer events at the earth's dayside magnetopause, Nature, in press, 1982.

Russell, C.T., Magnetospheric physics: Magnetic fields, Rev. Geophys. Space Phys., 13, 952-955, 1975.

Russell, C.T., The control of the magnetopause by the interplanetary magnetic field, in Dynamics of the magnetosphere, [S-I. Akasofu, ed.], 3-22, D. Reidel Publ. Co., Dordrecht, Holland, 1980.

Russell, C.T. and R.C. Elphic, Initial ISEE magnetometer results: Magnetopause observations, Space Sci. Rev., 22, 681-715, 1978.

Russell, C.T. and R.C. Elphic, ISEE observations of flux transfer events at the dayside magnetopause, Geophys. Res. Lett., 6, 33-36, 1979.

Scholer, M., F.M. Ipavich, G. Gloeckler, D. Hovestadt and E. Klecker, Leakage of magnetospheric ions into the magnetosheath along reconnected field lines at the dayside magnetopause, J. Geophys. Res., 87, 2169-2176, 1982.

Scholer, M., D. Hovestadt, F.M. Ipavich and G. Gloeckler, Energetic protons, alpha particles, and electrons in magnetic flux transfer events, J. Geophys. Res., 87, 2169-2176, 1982a.

Scholer, M., D. Hovestadt, F.M. Ipavich, B. Klecker and G. Gloeckler, Unusual structure of the dayside low-latitude magnetopause energetic electron layer, J. Geophys. Res., 87, 2255-2262, 1982b.

Sckopke, N., G. Paschmann, G. Haerendel, B.U.O. Sonnerup, S.J. Bame, T.G. Forbes, E.W. Hones, Jr. and C.T. Russell, Structure of the low-latitude boundary layer, J. Geophys. Res., 86, 2099-2110, 1981.

Sonnerup, B.U.O., Theory of the low-latitude boundary layer, in Magnetospheric Boundary Layers, [B. Battrick, ed.], 395-397, ESA SP-148, Paris, 1979.

Sonnerup, B.U.O., Theory of the low-latitude boundary layer, J. Geophys. Res., 85, 2017-2026, 1980.

Sonnerup, B.U.O., Transport mechanisms at the magnetopause, in Dynamics of the magnetosphere, [S-I. Akasofu, ed.] 77-100, D. Reidel Publ. Co., Dordrecht, Holland, 1980.

Sonnerup, B.U.O. and B.G. Ledley, OGO-5 magnetopause structure and classical reconnection, J. Geophys. Res., 84, 399-405, 1979a.

Sonnerup, B.U.O. and B.G. Ledley, electromagnetic structure of the magnetopause and boundary layer, in Magnetospheric Boundary Layer, [B. Battrick ed.] 401-411, ESA SP-148, Paris, 1979B.

Speiser, T.W. and D.J. Williams, Magnetopause modeling: Flux transfer events and magnetosheath quasi-trapped distributions, J. Geophys. Res., 87, 2177-2186, 1982.

Speiser, T.W., D.J. Williams, and H.A. Garcia, Magnetospherically trapped ions as a source of magnetosheath energetic ions, J. Geophys. Res., 86, 723-732, 1981.

Tsurutani, B.T., E.J Smith, R.M. Thorne, R.R. Anderson, D.A. Gurnett, G.K. Parks, C.S. Lin and C.T. Russell, Wave-particle interactions at the magnetopause: Contributions to the dayside aurora, Geophys. Res. Lett., 8, 183-186, 1981.

Williams, D.J. Magnetopause characteristics inferred from three-dimensional energetic particle distributions, J. Geophys. Res., 84, 101-104, 1979.

Williams, D.J. Magnetopause characteristics at 0840-1040 hours local time, J. Geophys. Res., 85, 3387-3395, 1980.

Williams, D.J. and L.A. Frank, ISEE-1 charged particle observations indicative of open magnetospheric field lines near the subsolar region, J. Geophys. Res., 85, 2037-2042, 1980.

Williams, D.J., T.A. Fritz, E. Keppler, B. Wilken and G. Wibberenz, Three-dimensional energetic ion observations and tangential magnetopause electric field, Space Sci. Rev., 22, 805-811, 1978.

Williams, D.J., T.A. Fritz, B. Wilken and E. Keppler, An energetic particle perspective of the magnetopause, J. Geophys. Res., 84, 6385-6396, 1979.

Wu, C.C., R.J. Walker and J.M. Dawson, A three-dimensional MHD model of the earth's magnetosphere, Geophys. Res. Lett., 8, 523-526, 1981.

Zhuang, H-C., C.T. Russell and R.J. Walker, The influence of the interplanetary magnetic field and thermal pressure on the position and shape of the magnetopause, J. Geophys. Res., 86, 10009-10021, 1981b.

Reconnection

Baum, P.J. and A. Bratenahl, The laboratory magnetosphere Geophys. Res. Lett., 9, 435-437, 1982.

Bieber, J.W. and E.C. Stone, Streaming energetic electrons in earth's magnetotail: Evidence for substorm-associated magnetic reconnection, Geophys. Res. Lett., 7, 945-948, 1980.

Bieber, J.W., E.C. Stone, E.W. Hones, Jr., D.N. Baker, and S.J. Bame, Plasma behavior during energetic electron steaming events: Further evidence for substorm-associated magnetic reconnection, Geophys. Res. Lett., 9, 644-667, 1982.

Birn, J. and E.W. Hones,Jr., Three-dimensional computer modeling of dynamic reconnection in the geomagnetic tail, J. Geophys. Res., 86, 6802-6808, 1981.

Brecht, S.H., J.G. Lyon, J.A. Fedder and K. Hain, A time dependent three-dimensional simulation of the earth's magnetosphere: Reconnection events, J. Geophys. Res., 87, 6098-6108, 1982.

Caan, M.N., D.H. Fairfield and E.W. Hones, Jr., Magnetic fields in flowing magnetotail plasmas and their significance for magnetic reconnection, J. Geophys. Res., 84, 1971-1976, 1979.

Cheng, A.F., Unsteady magnetic merging in one-dimension, J. Geophys. Res., 85, 2129-2134,1979.

Coroniti, F.V., On the tearing mode in quasi-neutral sheets, J. Geophys. Res., 85, 6719-6728, 1980.

Coroniti, F.V., L.A. Frank, D.J. Williams, R.P. Lepping, F. L. Scarf, S.M. Krimigis and G. Gloeckler, Variability of plasma sheet dynamics, J. Geophys. Res., 85, 2957-2977, 1980.

Crooker, N.U., Anti-parallel merging, the half-wave rectifier response of the magnetosphere and convection, in Magnetospheric Boundary Layers, [B. Battrick, ed.] 343-348, ESA SP-148, Paris, 1979a.

Crooker, N.U., Dayside merging, and cusp geometry, J. Geophys. Res., 84, 951-959, 1979b.

Crooker, N.U., The half-wave rectifier response of the magnetosphere and anti-parallel merging, J. Geophys. Res., 85, 575-578, 1980a.

Crooker, N.U., The configuration of dayside merging, in Dynamics of the magnetosphere, [S-I. Akasofu, ed.], 101-120, D. Reidel Publ. Co., Dordrecht, Holland, 1980b.

Eastman, T.E. and L.A. Frank, Observations of high speed flows ner the earth's magnetopause: Evidence for reconnection?, J. Geophys. Res., 87, 2187-2202, 1982.

Daly, P.W. and T.A. Fritz, Trapped electron distributions on open magnetic field lines, J. Geophys. Res., 87, 6081-6088, 1982.

Gekelman, W. and R.L. Stenzel, Magnetic field line reconnection experiments, 2, Plasma parameters, J. Geophys. Res., 86, 659-666, 1981.

Gekelman, W, R.L. Stenzel and N. Wild, Magnetic field line reconnection experiment, 3, Ion acceleration, flows and anomalous scattering, J. Geophys. Res., 87, 101-110, 1982.

Gosling, J.T., J.R. Asbridge, S.J. Bame, W.C. Feldman, G. Paschmann, N. Sckopke and C.T. Russell, Evidence for quasi-stationary reconnection at the dayside magnetopause, J. Geophys. Res., 86, 2147-2158, 1982.

Greenly, J.B. and B.U.O. Sonnerup, Tearing modes at the magnetopause, J. Geophys. Res., 86, 1305-1312, 1981.

Kirkland, K.B. and B.U.O. Sonnerup, Contact discontinuities in a cold collision free two-beam plasma, J. Geophys. Res., submitted, 1982.

Matthaeus, W.H., Reconnexion in two dimensions: Localization of vorticity and current near magnetic x-points, Geophys. Res. Lett., 9, 660-663, 1982.

Paschmann, G., B.U.O. Sonnerup, I. Papamastorakis, N. Sckopke, G. Haerendel, S.J. Bame, J.B. Asbridge, J.T. Gosling, C.T. Russell and R.C. Elphic, Plasma acceleration at the earth's magnetopause: Evidence for reconnection, Nature, 282, 243-246, 1979.

Quest, K.B. and F.V. Coroniti, Tearing at the dayside magnetopause, J. Geophys. Res., 86, 3289-3298, 1981a.

Quest, K.B. and F.V. Coroniti, Linear theory of tearing in high- plasma, J. Geophys. Res., 86, 3299-3306, 1981b.

Russell, C.T., Reconnexion, in Physics of Solar Planetary Environments, [D.J. Williams, ed.], 526-640, American Geophysical Union, Washington, D.C. 1976.

Sato, T. and A. Hasegawa, Externally driven magnetic reconnection versus tearing mode instability, Geophys. Res. Lett., 9, 55-55, 1982.

Sato, T. and R.J. Walker, Magnetotail dynamics excited by the streaming tearing mode, J. Geophys. Res., in press, 1982

Scholer, M., P.W. Daly, G. Paschmann and T.A. Fritz, Field line topology determined by energetic particles during a possible magnetopause reconnection event, J. Geophys. Res., 87, 6073-6080, 1982a.

Sonnerup, B.U.O., Magnetic field reconnection, in Solar System Plasma Physics, Vol. III, [L.J. Lanzerotti, C.F. Kennel and E.V. Parker, eds.], 45-108, North-Holland Publ. Co., 1979.

Sonnerup, B.U.O., G. Paschmann, I. Papamastorakis, N. Sckopke, G. Haerendel, S.J. Bame, J.R. Asbridge, J.T. Gosling and C.T. Russell, Evidence for magnetic field reconnection at the earth's magnetopause, J. Geophys. Res., 86, 10049-10067, 1981.

Stenzel, R.L. and W. Gekelman, Magnetic field line reconnection experiments, 1, Field topologies, J. Geophys. Res., 86, 649-658, 1981.

Stenzel, R.L.. W. Gekelman and N. Wild, Magnetic field line reconnection experiments, 4, Resistivity, heating and energy, J. Geophys. Res., 87, 111-118, 1982.

Stenzel, R.L., W. Gekelman and N. Wild, Double layer formation during current sheet disruptions in a reconnection experiment, Geophys. Res. Lett., 9, 680-683, 1982.

Stern, D.P., The role of 0-type neutral lines in magnetic merging during substorms and solar flares, J. Geophys. Res., 84, 63-71, 1979.

Vasyliunas, V.M., Upper limit on the electric field along a magnetic 0 line, J. Geophys. Res., 84. 4616-4620, 1980.

Plasma Sheet and Neutral Sheet

Akasofu, S-I. and D.N. Covey, Effects of the interplanetary magnetotail structure: Large-scale changes of the plasma sheet during magnetospheric substorms, Planet. Space Sci., 28, 757-762, 1980.

Cattell, C.A., M. Kim, R.P. Lin and F.S. Mozer, Observation of large electric fields near the plasma sheet boundary by ISEE-1, Geophys. Res. Lett., 9, 539-542, 1982.

Erickson, G.M., R.A. Wolf, Is steady convection possible in the earth's magnetotail?, Geophys. Res. Lett., 7, 897-900, 1980.

Fairfield, D.H., R.P. Lepping, E.W. Hones, Jr., S.J. Bame and J.R. Asbridge, Simultaneous measurements of magnetotail dynamics by IMP spacecraft, J. Geophys. Res., 86, 1396-1414, 1981a.

Fairfield, D.H., E.W. Hones, Jr. and C.I. Meng, Multiple crossings of a very thin plasma sheet in the earth's magnetotail, J. Geophys. Res., 86, 11189-11200, 1981b.

Forbes, T.G., E.W. Hones, S.J. Bame, J.R. Asbridge, G. Paschmann, N. Sckopke and C.T. Russell, Evidence for the tailward retreat of a magnetotail neutral line in the magnetotail during substorm, Geophys. Res. Lett., 8, 261-264, 1981a.

Forbes, T.G., E.W. Hones, Jr., S.J. Bame, J.R. Asbridge, G. Paschmann, N. Sckopke and C.T. Russell, Substorm-related plasma sheet motions as determined from differential timing of plasma changes at the ISEE satellites, J. Geophys. Res., 86, 3459-3569, 1981b.

Hada, T., A. Nishida, T. Terasawa, E.W. Hones, Jr., Bi-directional electron pitch angle anisotropy in the plasma sheet, J. Geophys. Res., 84, 11211-11224, 1981.

Hardy, D.A., H.K. Hills, and J.W. Freeman, Occurrence of lobe plasma at lunar distance, J. Geophys. Res., 84, 72-78, 1979a.

Hardy, D.A., P.H. Reiff and W.J. Burke, Response of magnetotail plasma at lunar distance to changes in the interplanetary magnetic field, the solar wind plasma and substorm activity, J. Geophys. Res., 84, 1382-1290, 1979b.

Hayakawa, H., A. Nishida, E.W. Hones, Jr., and S.J. Bame, Statistical characteristics of plasma flow in the magnetotail, J. Geophys. Res., 87, 277-283, 1982.

Hones, Jr., E.W., Plasma flow in the magnetotail and its implication for substorm theories, in Dynamics of the magnetosphere, [S-I. Akasofu, ed.], 545-562, D. Reidel Publ. Co., Dordrecht, Holland, 1980.

Hones, Jr., E.W. and K. Schindler, Magnetotail plasma flow during substorms: A survey with IMP6 and IMP8 satellites, J. Geophys. Res., 84, 7155-7169, 1979.

Hones, Jr., E.W., J. Birn, S.J. Bame, J.R. Asbridge, G. Paschmann, N. Sckopke and G. Haerendel, Further determination of the characteristic of magnetospheric plasma vortices with ISEE-1 and 2, J. Geophys. Res., 86, 814-820, 1981.

Hones, Jr., E.W., J. Birn, S.J. Bame, G. Paschmann and C.T. Russell, On the three-dimensional magnetic structure of the plasmoid created in the magnetotail at substorm onset, Geophys. Res. Lett., 9, 203-206, 1982.

Meng, C-I., A.T.Y. Lui, S.M. Krimigis, S. Ismail and D.J. Williams, Spatial distribution of energetic particles in the distant magnetotail, J. Geophys. Res., 86, 5682-5700, 1981

Mobius, E., F.M. Ipavich, M. Scholer, G. Gloecker, D. Hovestadt and B. Klecker, Observations of a nonthermal ion layer at the plasma sheet boundary during substorm recovery, J. Geophys. Res., 85, 5143-5148, 1980.

Nishida, A., H. Hayakawa and E.W. Hones, Jr., Observed signatures of reconnection in the magnetotail, J. Geophys Res., 86, 1422-1436, 1981.

Peterson, W.K., R.D. Sharp, E.G. Shelley, R.G. Johnson and H. Balsiger, Energetic ion composition of the plasma sheet, J. Geophys. Res., 86, 761-767, 1981

Sarris, E.T., S.M. Krimigis, A.T.Y. Lui, K.L. Ackerson, L.A. Frank and D.J. Williams, Relationship between energetic particles and plasma in the distant plasma sheet, Geophys. Res. Lett., 8, 349-352, 1981.

Sharp, R.D., D.L. Carr, W.K. Peterson and E.G. Shelley, Ion streams in the magnetotail, J. Geophys. Res., 86, 4639-4648, 1981.

Shull, P., Jr., Fast plasma flows in the translunar magnetotail, J. Geophys. Res., 86, 4708-4714, 1981.

Spjeldvik, W.N. and T.A. Fritz, Energetic ion and electron observations of the geomagnetic plasma sheet boundary layer: Three-dimensional results from ISEE-1, J. Geophys. Res., 86, 2480-2486, 1981.

Swift, D.W., Numerical simulation of the interaction of the plasma sheet with the lobes of the earth's magnetotail, J. Geophys. Res., 87, 2287-2300, 1982.

Swift, D.W. and L.C. Lee, The magnetotail boundary and energy transfer processes, Geophys. Res. Lett., 9, 527-530, 1982.

Wagner, J.S., J.R. Kan and S-I., Akasofu, Particle dynamics in the plasma sheet, J. Geophys. Res., 84, 891-897, 1979

Williams, D.J., Energetic ion beams at the edge of the plasma sheet: ISEE-1 observations plus a simple explanatory model, J. Geophys. Res., 86, 5507-5518, 1981.

Other Plasma Boundaries

Arnoldy, R.L., T.E. Moore and S-I. Akasofu, Plasma injection events at synchronous orbit related to positive J. Geophys. Res., 87, 77-84, 1982.

Birmingham, T.J., The effect of injection location on the spectrum of energetic magnetospheric particles, J. Geophys. Res., 85, 607-612, 1980.

Burch, J. L., P. H. Reiff, R. W. Spiro, R. A. Heelis and S. A. Fields, Cusp region particle precipitation and ion convection for northward interplanetary magnetic field, Geophys. Res. Lett., 7, 393-396, 1980.

Calvert, W., The auroral plasma cavity, Geophys. Res. Lett., 8, 919-921, 1981.

Carlson, C. W. and R. B. Torbert, Solar wind ion injections in the morning auroral oval, J. Geophys. Res., 85, 2903-2908, 1980.

Curtis, S. A., C. S. Wu and D. H. Fairfield, Electromagnetic and electrostatic emissions at the cusp-magnetosheath interface during substorms, J. Geophys. Res., 84, 898-909, 1979.

Fjiri, M., R. A. Hoffman, and P. H. Smith, Energetic particle penetrations into the inner magnetosphere, J. Geophys. Res., 85, 653-663, 1980.

Fennell, J. F., D. R. Croley, Jr. and S. M. Kaye, Low-energy ion pitch angle distributions in the outer magnetosphere: Ion zipper distributions, J. Geophys. Res., 86, 3375-3382, 1981.

Fennell, J. F., R. G. Johnson, D. T. Young, R. B. Torbert and T. E. Moore, Plasma and electric field boundaries at high and low altitudes on July 29, 1977, J. Geophys. Res., 87, 5933-5942, 1982.

Horwitz, J. L., C. R. Baugher, C. R. Chappell, E. G. shelley and D. A. Young, Conical pitch angle distributions of very low-energy ion fluxes observed by ISEE-1 J. Geophys. Res., 87, 2311-2320, 1982.

Kaye, S. M. and M. G. Kivelson, Time dependent convection electric fields and plasma injection, J. Geophys. Res. 84, 4183-4188, 1979.

Kaye, S. M., E. G. Shelley, R. D. Sharp and R. G. Johnson, Ion composition of zipper events, J. Geophys. Res., 86, 3383-3388, 1981.

Kivelson, M. G., S. M. Kaye and D. J. Southwood, The physics of plasma injection events, in Dynamics of the magnetosphere, [S-I. Akasofu, ed.], 385-406, D. Reidel Publ. Co., Dordrecht, Holland, 1980.

Meng, C. I., Latitudinal variation of the polar cusp during a geomagnetic storm, Geophys. Res. Lett., 9, 60-63, 1982.

Lyons, L. R. and T. E. Moore, Expects of charge exchange in the distribution of ionospheric ions trapped in the radiation belts near synchronous orbit, J. Geophys. Res., 86, 5885-5888, 1981.

Olsen, R. C., Field-aligned ion streams in the earth's midnight region, J. Geophys. Res., 87, 2301-2310, 1982.

Parks, G. K., B. Mauk, C. Gurgiolo and C. S. Lin, Observations of plasma injection, in Dynamics of the Magnetosphere, [S-I. Akasofu, ed.], 371-384, D. Reidel Publ. Co., Dordrecht, Holland, 1980.

Reiff, P. H., Low altitude signatures of the boundary layers, in Magnetospheric Boundary Layers, [B. Battrick, ed.], 167-173, ESA SP-148, Paris, 1979.

Reiff, P. H., J. L. Burch and R. W. Spiro, Cusp proton signatures and the interplanetary magnetic field, J. Geophys. Res., 85, 5997-6005, 1980.

Shelley, E. G., Ion composition in the dayside cusp: Injection of ionospheric ions into the high latitude boundary layer, in Magnetospheric Boundary layers, [B. Battrick, ed.], 187-192, ESA SP-148, Paris, 1979.

Southwood, D. J. and S. M. Kaye, Drift approximations in simple magnetospheric convection models, J. Geophys. Res., 84, 5773-5780, 1979.

Williams, D. J., Ring current composition and sources, in Dynamics of the magnetosphere, [S-I. Akasofu, ed.], 407-424, D. Reidel Publ. Co., Dordrecht, Holland, 1980.

TRW Tech. Report No. 36116-6004-UT-00



# TRANSFER OF PULSATION-RELATED WAVE ACTIVITY ACROSS THE MAGNETOPAUSE: OBSERVATIONS OF CORRESPONDING SPECTRA BY ISEE-1 AND ISEE-2

by

E. W. Greenstadt

Space Sciences Department
TRW Space and Technology Group
Redondo Beach, California 90278

M. M. Mellott, R. L. McPherron, and C. T. Russell

Institute of Geophysics and Planetary Physics
University of California at Los Angeles
Los Angeles, California 90024

H. J. Singer and D. J. Knecht

Plasma, Particles and Fields Branch
Air Force Geophysics Laboratory
Hanscom Air Force Base, Massachusetts 01731

March 9, 1983

Submitted for publication in Geophysical Research Letters
[special issue on Chapman Conference on Waves in Magnetospheric Plasmas]

Bldg R-1, Rm 1176
TRW Space and Technology Group
One Space Park
Redondo Beach, California 90278
(213) 536-2015

# TRANSFER OF PULSATION-RELATED WAVE ACTIVITY ACROSS THE MAGNETOPAUSE: OBSERVATIONS OF CONJUGATE SPECTRA BY ISEE-1 AND ISEE-2

by

R. L. Greenstadt

Space Sciences Department
TRW Space and Technology Group, Redondo Beach, California 90278

M. M. Mellott, R. L. McPherron, and C. T. Russell

Institute of Geophysics and Planetary Physics
University of California at Los Angeles, Los Angeles, California 90024

H. J. Singer and D. J. Knecht

Plasma, Particles and Fields Branch
Air Force Geophysics Laboratory, Hanscom Air Force Base, Massachusetts 01731

Abstract. Comparison of power spectra of magnetic field data from ISEE-1 and -2 recorded simultaneously on both sides of the magnetopause showed that power level inside the magnetosphere varied with power level outside in the magnetosheath and suggested that the same frequencies were enhanced on the two sides of the boundary. Power levels were two to three orders of magnitude lower inside than outside the magnetosphere, indicating that wave energy was transmitted inside from the sheath.

## INTRODUCTION

A persistent and significant, although weak and disordered, correlation between solar wind properties and daytime geomagnetic pulsation activity in the Pc 3,4,5 range, periods T=10 to 500sec, has been established by many reports, of which we cite a sampling [Bol'shakova and Troitskaya, 1968; Gul'elmi, 1974; Webb and Orr, 1976; Saito et al., 1979; Greenstadt et al., 1979; Wolfe et al., 1980]. These correlations, together with the need to understand pulsaton phenomena in general, have also led to a number of models attempting to explain the observations [Southwood, 1968; Greenstadt, 1972; Vinogradov and Parkhomov, 1974; Chen and Hasegawa, 1974; Kovner, 1976]. Both observation and theory have been concerned with the sources of the waves, the modulation of the waves by the complex media

through which they travel, and the control of wave properties directly or indirectly by solar wind conditions. A more comprehensive summary and reference list can be found in a paper by Greenstadt et al. [1980].

Regardless of the specifics of either models or observations, however, there are, in the most general terms, three possible sources of pulsations in the magnetosphere: Waves are produced inside the magnetosphere, waves enter the magnetosphere from the magnetosheath, or waves emanate from the boundary surface separating the magnetosheath and the magnetosphere (i.e. from the magnetopause). None of these possible sources excludes either of the others, but certainly if waves enter the magnetosphere from outside, they must cross the boundary somewhere at some time, and it should be possible to establish by observation a physical similarity between waves detected simultaneously on both sides of the magnetopause. This is the approach we pursue in the present study; the preliminary results reported here support the transfer of wave energy inward from the magnetosheath to the magnetosphere.

We define as a "straddle" a situation in which one spacecraft is on one side of the magnetopause and a second is on the opposite side. The ISEE-1 and -2 satellites provided many such straddle crossings, but we have concentrated on the magnetometer data of 1978, when the spacecraft were separated by hundreds to thousands of km for several months, giving straddles long enough for unequivocal analyses of waves with periods up to several minutes. Our approach is to compute concurrent power spectra on both sides of clearly defined magnetopause crossings and to seek similarities or differences in the spectra from the two spacecraft. We require reasonably continuous data from both satellites over minimal intervals of 15 minutes and preferably much longer. We found four potentially suitable straddles of which we have developed two for this preliminary report, supplemented by two single-spacecraft crossings, as explained later. We present only spectra of the total field magnitude at this time, derived from vector samples every two seconds.

## DATA

The two cases we describe occurred on 8 October and 27 November 1978. The 8 October crossing occurred in early afternoon, the 27 November crossing in late morning. The daytime surface field for our cases was measured by the AFGL ground stations in a sector spanning the United States near 55 degrees magnetic latitude. Ground station data processed for this report were recorded by the Newport station at the western edge of the sector, which fell before and after noon during the two intervals of interest, so that the morning-afternoon local times on the ground were reversed from those of our crossings at the magnetopause. We used ground station data as a rough guide to the presence of traditional pulsations on the ground, since it is waves related to the origin of such pulsations that we wish to be studying. The two straddle intervals of this report took place during IMF conditions favorable to the presence of enhanced wave activity in the subsolar magnetosheath convected from quasi-parallel bow shock structure.

Power spectra presented in this study were calculated with the fast Fourier transform. Figure 1 places one spectrum, dotted curve, on the same scales used by Fairfield [1976] to display the characteristics of magnetosheath magnetic noise from several spacecraft. The dotted curve is a power spectrum for the total ambient field recorded by ISEE-1 immediately outside the magnetopause on 8 October. All spectra are for the total field magnitude; details of the earlier spectra can be found in Fairfield's review [op.cit.].

The figure illustrates four principal points: magnetosheath spectra typically show either an enhancement or a slope change, or both, at or below the local proton gyrofrequency (highlighted by the dashed lines); second, magnetosheath spectra are highly variable, both in absolute power level and in the frequencies that might be enhanced in any particular sample; third, spectra taken from ISEE data years later are reasonably representative of the same wave behavior that prevailed during the earlier measurements. Fourth, and most importantly for this report, spectra obtained from ISEE close to the magnetopause do not appear to define a special region in any way unrepresentative of the magnetosheath at other locations.

Figure 2a is an example of our first straddle case. The upper panels of the figure display plots of field magnitude from ISEE-1 and ISEE-2, for the magnetopause crossing of 8 October 1978. ISEE-2, lower field plot, entered the magnetosphere first at 1805:50 and finally at 1813; ISEE-1, top, encountered the magnetosphere later, initially at 1831 and entered finally at 1835:40. Thus, there were 18 minutes during which data were acquired simultaneously from one satellite outside and one inside the magnetopause.

Spectrum A shows the wave power in the total field in the magnetosheath just outside the magnetopause, at ISEE-1. The next spectrum below, B, shows the wave power in the magnetosphere just inside the magnetopause, at ISEE-2, for the same time interval as that of the first spectrum. The power was appreciably lower and the decrease in power with frequency clearly much steeper inside than outside the magnetopause, beginning with about one third the outside power at the lowest frequencies. At 0.1 Hz, there were three orders of magnitude difference between the two spectra.

Spectrum G, at bottom, represents the power on the ground at the AFGL station at Newport, Washington, for the same intervals as in the depicted satellite samples. The ground station was a few hours west of the satellites, about local noon. The shaded vertical strips in the spectral panels draw attention to the enhancements in power at the satellites and on the ground that appear to bind wave activity together in the inner magnetosheath, the outermost magnetosphere, and at the earth's surface. All the spectra show some concentration of power between .02 and .07 Hz in the form of a plateau or peaks in the respective curves.

Figure 2a shows a progressive decline in power from the magnetosheath to the earth's surface. Each spectral curve is contained in, i.e. accounts for a fraction of the power of, the next spectrum above it. The magnetospheric spectra are well below that of the magnetosheath and are closer to one another than to the latter, the discrepancy being greatest at the highest frequencies.

Figure 2b superposes spectra from a second straddle case on 27 November 1978, when ISEE-1

was just outside the magnetopause. ISEE-2 was deeper inside the magnetosphere, having entered at 2000 UT, than it had been on 8 Oct., and the Newport station was below and east of the satellite meridian (in the early afternoon sector). In this instance, the power in the sheath (A) displayed enhancement and a plateau between .011 and .05 Hz, as did also the power in the magnetosphere (B), while the corresponding power on the ground (G) was relativily featureless, but essentially at the same level as at ISEE-2. Whether the apparent lack of frequency enhancement on the ground at this time was because of a delayed effect not yet visible, an unfavorable position in the afternoon sector, or a poor choice of representation of the surface record is still to be determined. The small graph at the bottom shows the power distribution in By at Newport for the local noon and afternoon interval including the 22-minute segment of the upper graph; clearly, there was some activity in the surface field within the longer interval and within the enhanced portion of the spectrum at the satellites. The attenuation of wave power across the magnetopause is obvious here, as in the previous case, but we also see that the frequency range of enhancement was shifted to somewhat lower frequencies, in all locations, than in the case of 8 October, as indicated by the shading in Figure 2.

The magnetosheath spectra of 8 Oct. and 27 Nov. are superposed in Fig. 3, showing that the power of the 27 Nov. spectrum peaked at lower frequency and dropped more rapidely than the power on 8 Oct. This difference corresponds to the slightly different regions of the frequency scale that seemed to be show enhanced power in the magnosphere, as shaded in Figure 2 . Unfortunately, the absolute power levels in the magnetosheath in the two cases examined above did not differ appreciably from each other, considering the wide range of power exhibited in the curves of Figure 1. In order to study whether power inside the magnetosphere is related generally to power in the magnetosheath, it was necessary to examine nonstraddle cases. On the premise that the sheath spectrum remained substantially unchanged from one interval to the next over an hour's time, we selected cases with significantly different power levels and compared spectra before and after magnetopause crossing, rather than simultaneous spectra on opposite sides of the boundary. Corresponding

magnetosheath and magnetosphere spectra are superposed in Figure 4 for three days, 8 October, and 10 and 17 September 1978. The 8 October curves are already familiar. The new ones show that progressively lower power in the sheath corresponded to progressively lower power in the magnetosphere, suggesting, with these few cases and the necessary assumption of stationarity on the 10th and 17th, that the powers inside and outside the magnetopause were directly related.

## SUMMARY

The data presented above may be summarized as follows, with the understanding that we refer essentially to the frequency range $0.01 < f < 0.1$ Hz (periods $10 < T < 100$ sec.):

The power within the magnetosheath was 10 to 1000 times the power in the magnetosphere;

The power within the magnetosphere varied less than a factor of 10 from the magnetopause to the surface;

The power level inside the magnetosphere correlated overall with power level outside the magnetopause;

The frequency of power enhancement in the magnetosphere appeared to shift with the frequency of power enhancement in the magnetosheath.

The power outside the magnetopause appered to be representative of power in the magnetosheath generally.

In addition to the foregoing, we have found evidence that the variable presence of a frequency range of enhanced power in the magnetosheath was correlated with the variable presence of an IMF orientation favorable to the occurrence of quasi-parallel structure in the bow shock around the subsolar point. This result will be treated in a separate report.

## DISCUSSION

Similarity between spectra in the magnetosheath and magnetosphere may be explained,

excluding coincidence, in the three ways defined in the INTRODUCTION. The observations listed in the SUMMARY suggest that internal magnetospheric origin may be excluded from consideration because of the higher power observed outside the boundary. Moreover, a principal criterion by which we selected cases was the appearance of a clear magnetopause allowing us easily to determine that one spacecraft was inside, the other outside the boundary. This would eliminate wave propagation outward along field lines locally interconnecting the solar wind to the magnetosphere. In fact, we have established that in one case the boundary was well approximated by a tangential discontinuity.

Surface waves are an unlikely explanation because of the overwhelming power in the magnetosheath compared to the magnetosphere. The newest calculations of surface wave effects [Pu and Kivelson, 1983] require that the magnetic wave power inside the boundary exceed that outside, opposite our results. Also, the frequencies expected for surface waves tend to be lower than those with which we have been dealing.

We conclude therefore that our preliminary results are consistent with external wave origin, specifically with the transfer of a small fraction of magnetosheath wave power, possibly derived from quasi-parallel shock structure, into the magnetosphere to appear as waves in the Pc 3-4 range.

The asserted commonality of frequency enhancement across the boundary, as illustrated here in Figure 2, is subtle at best. This is hardly surprising, since we are dealing with a global phenomenon notoriously elusive to sharply defined correlations, which we chance to sample as a few straddles at a few points in space. We chose the two examples here as the purest straddle cases. Other spectra, with more persuasive enhancement profiles, were obtained in data contexts requiring more exposition than could be included in this letter and will be the subject of a separate report. The component-by-component details of the transfer process, the global picture describing where the most effective transfer takes place, and the pathways whereby broadband energy in the magnetosheath is recorded as monochromatic pulsations in the magnetosphere remain to be determined.

Acknowledgements. Support for this report was provided by USAF contract F49620-81-C-003 and NASA contract NAS7-3090 (at TRW); NASA Grant NAS5-25772 (at UCLA).

REFERENCES

Bol'shakova, O. V., and V. A. Troitskaya, Relation of the interplanetary magnetic field direction to the system of stable oscillations, Dokl. Akad. Nauk SSSR, 180, 4, 1968.

Chen, L., and A. Hasegawa, A theory of long-period magnetic pulsations, 1, Steady state excitation of field line resonance, J. Geophys. Res., 79, 1024,1974.

Crooker, N., T. Eastman, L. Frank, E. Smith, and C. T. Russell, Energetic magnetosheath ions and the interplanetary magnetic field orientation, J. Geophys. Res., 86, 4455, 1981.

Fairfield, D. H., Magnetic fields of the magnetosheath, Rev. Geophys. Space Phys., 14, 117, 1976.

Greenstadt, E. W., Field-determined oscillations in the magnetosheath as possible source of medium-period, daytime micropulsations, in Proceedings of Conference on Solar Terrestrial Relations, 515, Univ. of Calgary, April 1972.

Greenstadt, E. W., H. J. Singer, C. T. Russell, and J. V. Olson, IMF orientation, solar wind velocity, and Pc3-4 signals: a joint distribution, J. Geophys. Res., 84, 527, 1979.

Greenstadt, E. W., R. L. McPherron, and K. Takahashi, Solar wind control of daytime, mid-period geomagnetic pulsations, J. Geomag. Geoelectr., 32, Suppl. II, SII 89, 1980.

Gul'ielmi, A. V., Diagnostics of the magnetosphere and interplanetary medium by means of pulsations, Space Sci. Rev., 16, 331, 1974.

Kovner, M. S., Pc 2-4 pulsations and low frequency oscillations in the solar wind ahead of a shock wave front, Geomag. and Aeronomy, XIV, 725, 1974.

Pu, Z.-y., and M. G. Kivelson, Kelvin-Helmholtz instability at the magnetopause: Energy flux

into the magnetosphere, J. Geophys. Res., 88, 853, 1983.

Saito, T. I. Yumoto, K. Takahashi, T. Tamura, and T. Sakurai, Solar wind control of Pc 3, magnetospheric study 1979, in Proceedings of International Workshop on Selected Topics of Magnetospheric Physics, 155, Japanese IMS Committee, Tokyo, 1979.

Southwood, D. J., The hydromagnetic stability of the magnetospheric boundary, Planet. Space Sci., 16, 587, 1968.

Vinogradov, Pl A., and V. A. Parkhomov, MHD waves in the solar wind--a possible source of geomagnetic Pc 3 pulsations, Geomagn. Aeron., USSR, 15, 109, 1974.

Webb, D., and D. Orr, Geomagnetic pulsations (5-50 mHz) and the interplanetary magnetic field, J. Geophys. Res., 81, 5941, 1976.

Wolfe, A., L. J. Lanzerotti, and C. G. Maclennan, Dependence of hydromagnetic energy spectra on solar wind velocity and interplanetary magnetic field direction, J. Geophys. Res., 85, 114, 1980.

## FIGURE CAPTIONS

Figure 1. An ISEE-1 magnetosheath spectrum obtained near the magnetopause (dots), superposed on a selection af spectra from earlier spacecraft in the magnetosheath.

Figure 2. Magnetic field magnitude records and superposed spectra for two cases of ISEE-1, ISEE-2 straddles of the magnetopause: (a) 8 Oct., (b) 27 Nov., 1978; A, B, and C signify spectra for the indicated intervals at ISEE-1, ISEE-2, and the AFGL Newport ground station. The insert at bottom right covers a longer interval at Newport, as noted.

Figure 3. Superposed magnetosheath spectra from 8 Oct. and 27 Nov.

Figure 4. Superposed power spectra for three different power levels in the magnetosheath and magnetosphere on three different days.

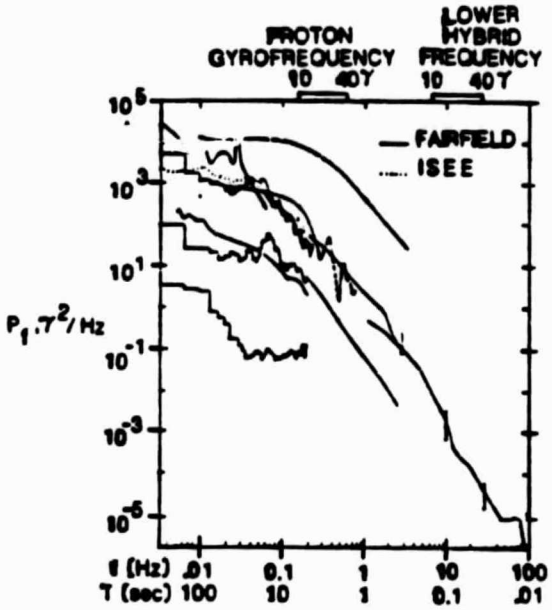


Figure 1. An ISEE-1 magnetosheath spectrum obtained near the magnetopause (dots), superposed on a selection af spectra from earlier spacecraft in the magnetosheath.

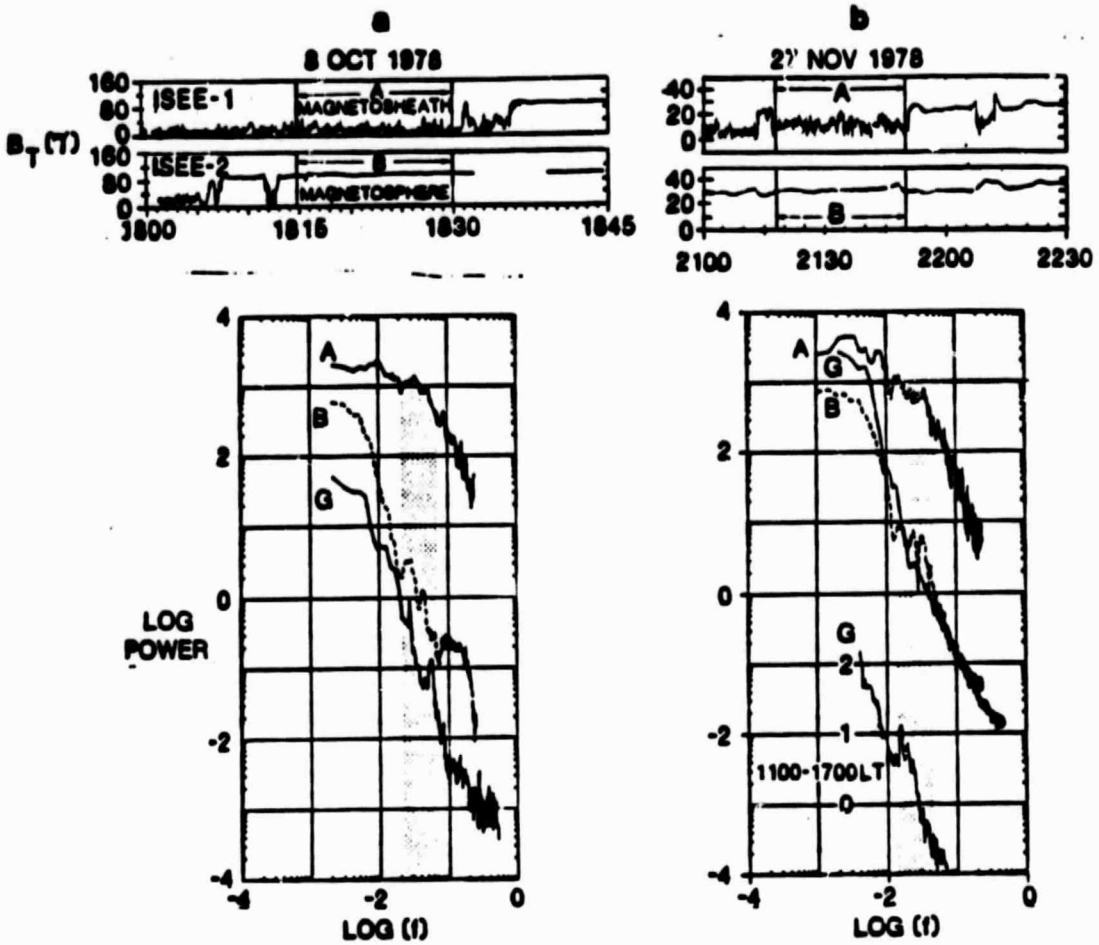


Figure 2. Magnetic field magnitude records and superposed spectra for two cases of ISEE-1, ISEE-2 straddles of the magnetopause: (a) 8 Oct., (b) 27 Nov., 1978; A, B, and G signify spectra for the indicated intervals at ISEE-1, ISEE-2, and the AFGL Newport ground station. The insert at bottom right covers a longer interval at Newport, as noted.

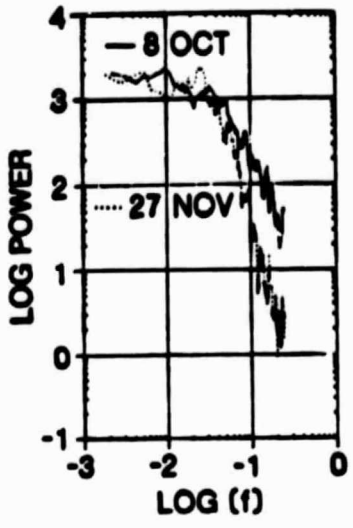


Figure 3. Superposed magnetosheath spectra from 8 Oct. and 27 Nov.

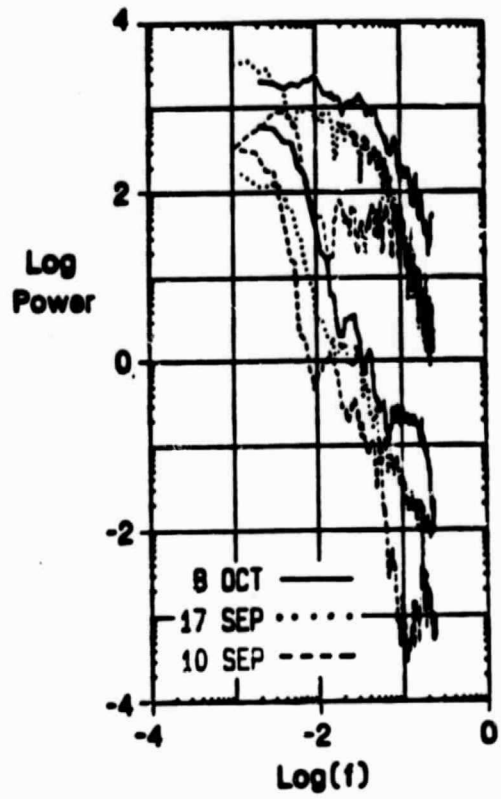


Figure 4. Superposed power spectra for three different power levels in the magnetosheath and magnetosphere on three different days.

D3

TRW Tech. Report No. 40789-6001-UT-00

N83 35854

# SCIENCE RETURN FROM ISEE-3 AT COMET GIACOBINI-ZINNER*

by

F. L. Scarf[1], E. J. Smith[2], and R. W. Farquhar[3]

[1]TRW Space and Technology Group, Redondo Beach, California 90278

[2]Jet Propulsion Laboratory, California Institute of Technology, Pasadena, California 91109

[3]NASA Goddard Space Flight Center, Greenbelt, Maryland 20771

December 1982

*To be published in the Proceedings of the International Conference on Cometary Exploration, Budapest, Hungary, November 15-20, 1982.

Bldg R-1, Rm 1176
TRW Space and Technology Group
One Space Park
Redondo Beach, California 90278
(213) 536-2015

# SCIENCE RETURN FROM ISEE-3 AT COMET GIACOBINI-ZINNER

F.L. SCARF[1], E.J. SMITH[2], AND R.W. FARQUHAR[3]

[1]TRW SPACE AND TECHNOLOGY GROUP, REDONDO BEACH, CALIFORNIA 90278

[2]JET PROPULSION LABORATORY, CALIFORNIA INSTITUTE OF TECHNOLOGY, PASADENA, CALIFORNIA 91109

[3]NASA GODDARD SPACE FLIGHT CENTER, GREENBELT, MARYLAND 20771

The spacecraft ISEE-3 will be sent to encounter Giacobini-Zinner in September 1985 during the period of intense Halley observations. This mission provides a unique opportunity for comparative study of important dynamical processes at both short and long-period comets. The ISEE-3 payload includes a vector Helium magnetometer and a high-sensitivity plasma wave search coil that give complete information on the magnetic field profile and the B-field fluctuation spectrum up to 1 kHz. Long electric dipoles (90 meters, tip-to-tip) are used by the plasma wave instrument and the radio mapping receiver to detect wave phenomena over the spectral range 17 Hz to 2 MHz, and the electron section of the ISEE-3 plasma probe measures the plasma density, the flow speed, and other important characteristics of the electron distribution function. These instruments can readily identify the position and strength of the bow shock, provide data on the nature of ionosheath/coma flow and turbulence, and yield direct information on the plasma phenomena that develop at the contact surface and in the foreshock region. As ISEE-3 flies across the comet tail, identification of the upper hybrid resonance emissions or trapped continuum radiation by the two wave instruments should provide unambiguous and absolute data on the local electron density profile, similar to the science return from the Voyager 1 wave instruments in the wake and tail of Titan. Other ISEE-3 instruments that measure characteristics of energetic particles and ion composition will also yield very significant information on the solar wind-comet interaction.

ISEE-3 (the third in the series of International Sun-Earth Explorers) was launched on August 12, 1978, and Figure 1 contains a drawing of the spacecraft with all booms and antenna systems deployed. Figure 1 also has a drawing of Comet Giacobini-Zinner. This sketch is based on photographs taken by E. Roemer during the 1959 apparition (see Figure 6) and it shows that this active short-period comet has many very interesting characteristics including an extensive visible coma (outer diameter ≈ 50,000 km) and a long, narrow ion tail (length of visible portion ≈ 350,000 km at 1 AU).

The ISEE-3 encounter with Giacobini-Zinner will represent the third extended mission phase for the spacecraft. During its primary mission (August 1978 through August 1981) the spacecraft was stationed in an elliptical orbit around the $L_1$ libration point (approximately

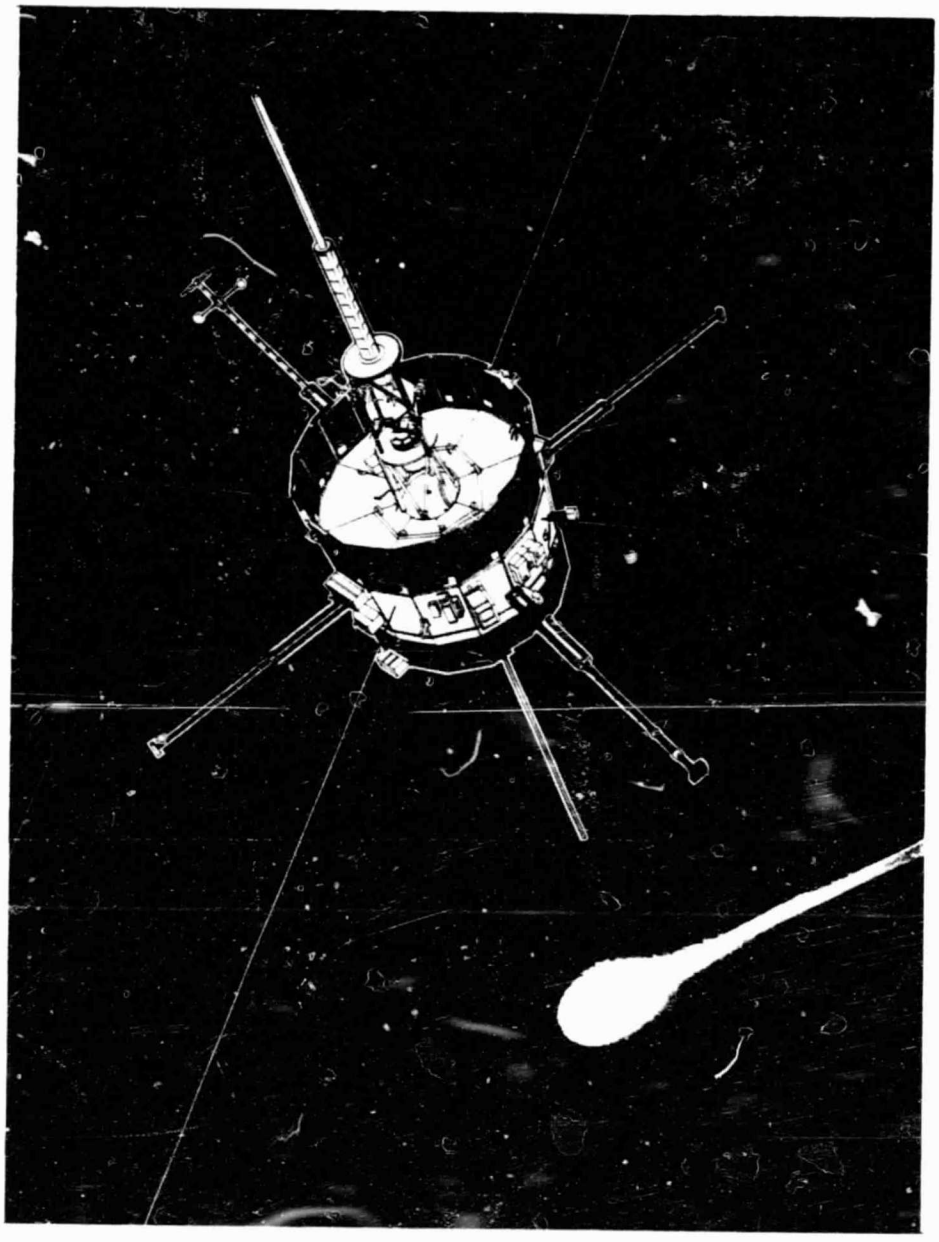

Figure 1. ISEE-3 and Comet Giacobini-Zinner

250 $R_e$ upstream from earth), and from this upstream position it monitored solar wind phenomena and processes and provided early warning of interplanetary storms. During the first phase of the extended mission it remained in the upstream halo orbit, but in June 1982 the thrusters were

fired, sending ISEE-3 back to the earth's geomagnetic tail. The first tail crossing beyond the lunar orbit occurred during October 1982, and ISEE-3 will continue to explore the distant geomagnetic tail out to $L_2$ (250 $R_e$ downstream) until December 1983, when a close lunar flyby will launch the spacecraft into its mission phase toward Comet Giacobini-Zinner. The trajectory for this phase is shown in Figure 2. Here the coordinate system is earth-centered and sun-oriented, and it can be seen that when ISEE-3 encounters the comet on September 11, 1985 (six days after Giacobini-Zinner perihelion), the viewing from earth will be excellent. Figure 2 also shows that ISEE-3 should be able to provide significant information on solar wind conditions upstream from Halley's comet after the Giacobini-Zinner encounter; the Halley-related observations will represent a fourth extended mission phase.

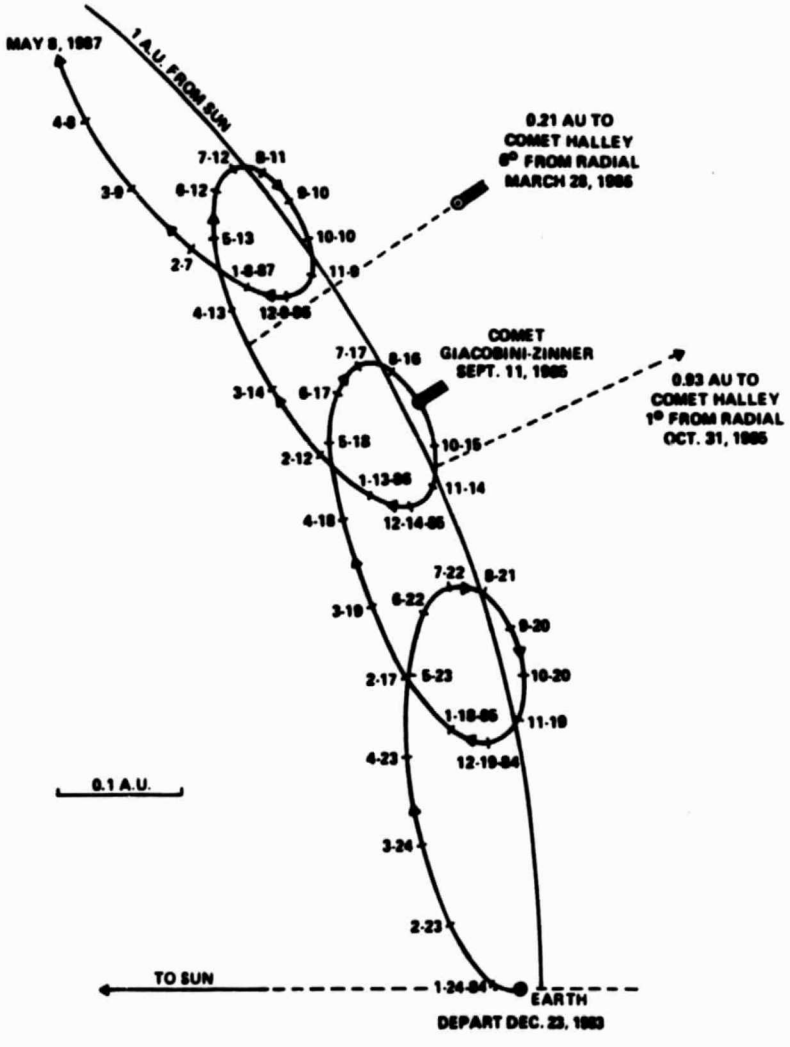


Figure 2. ISEE-3 Trajectory Relative to Fixed Sun-Earth Line

The Giacobini-Zinner encounter will occur as the comet crosses the ecliptic plane (descending node) at a heliocentric distance of 1.03 AU and a geocentric distance of 0.46 AU. In the frame of reference of the comet, the spacecraft will be traveling at a speed of 20.7 km/sec, primarily from south to north. It is planned to target ISEE-3 to pass downstream of the nucleus, and Figure 3 shows two views of the planned encounter. We expect that ISEE-3 will have inbound and outbound crossings of the bow shock, the contact surface, and the boundaries of the outer coma or inner plasma sheet. In addition, ISEE-3 will traverse the foreshock, the subsonic sheath regions, and the tail lobes. ISEE-3 will be targeted to fly by at a downstream distance which is deemed to be safe in terms of the dust hazard. A distance of 10,000 km has been tentatively proposed, but the dust hazard has not yet been carefully evaluated. Nevertheless, it is clear that for Giacobini-Zinner, the dust problem is considerably less than the corresponding problem at Halley. For Giacobini-Zinner, the flyby speed is 3.5 to 4 times lower, the rate of production of dust is perhaps two orders of magnitude less, and observations of the Giacobinid meteor stream suggest that dust particles from Giacobini-Zinner may have a mean mass density two orders of magnitude lower than the average for the Halley dust particles.

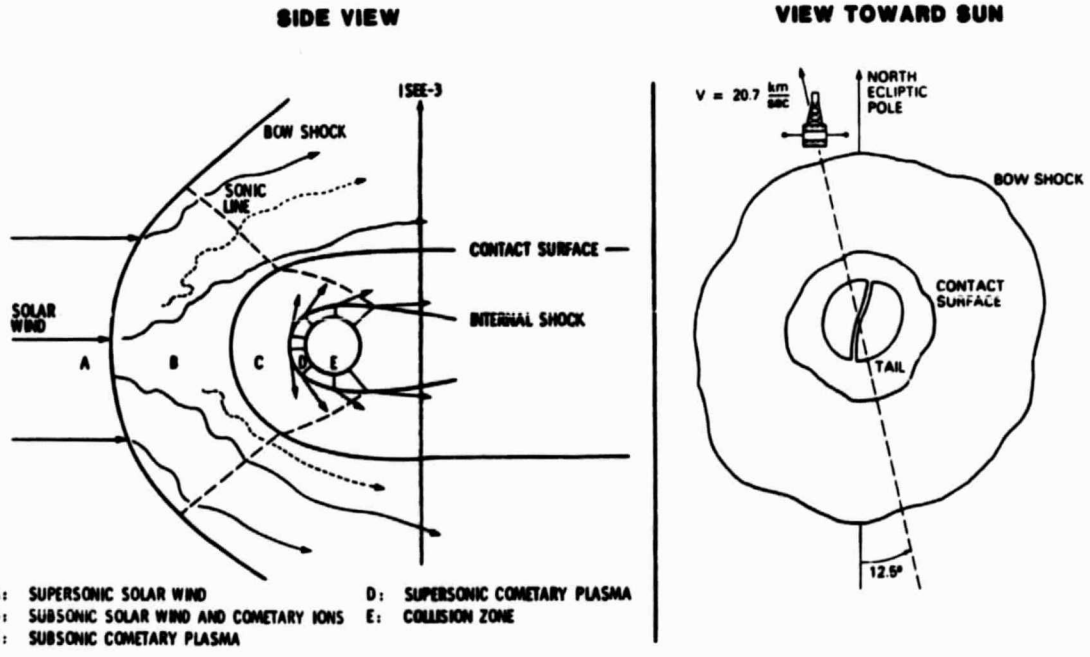


Figure 3. Comet Intercept

In Table 1 the science payload of ISEE-3 is listed and the principal investigators are identified. For all but the four cosmic ray instruments (bottom), the functional measurements are described, and the anticipated encounter sample times and spatial resolution scales (for 1024 bit/sec telemetry rate and 21 km/sec flyby speed) are tabulated (the Ogilvie instrument will be configured to operate in its most rapid scan mode). This table indicates that ISEE-3 has an excellent science capability for study of the solar wind-comet interaction, and we proceed to illustrate this capability by showing in Figure 4 some simultaneous ISEE-3 measurements obtained during a 30-hour interval on November 11-12, 1978, when an interplanetary shock swept past the spacecraft. These interplanetary measurements resemble those that will be obtained in the foreshock, near the shock, and downstream.

TABLE 1: ISEE-3 SCIENCE PAYLOAD

| Investigation | Principal Investigator | 1024 BPS Sampling Period (sec) | Spatial Resolution (km) |
|---|---|---|---|
| PLASMA ELECTRONS<br>5 eV to 1.0 keV | S. J. Bame | 24 sec | 500 km |
| MAGNETIC FIELD<br>± 4 gamma up to ± 1.4 Gauss; 0-3 Hz | E. J. Smith | 1/3 sec | 7 km |
| PLASMA WAVES<br>E-Field: 16 channels; 18 Hz to 100 kHz<br>B-Field: 11 channels; 0.3 Hz to 1 kHz | F. L. Scarf | 1 sec | 21 km |
| RADIO WAVES<br>E-Field: 24 channels; 30 kHz to 2 MHz | J. L. Steinberg | 112 sec | 2,400 km |
| PLASMA IONS<br>Velocity: 20-200 km/sec; M/Q: 4-50 | K. W. Ogilvie | 1,200 sec | 25,000 km |
| ENERGETIC PROTONS<br>30 keV to 1.4 MeV | R. J. Hynds | 32 sec | 660 km |
| ENERGETIC ION COMPOSITION<br>30 keV/Q < E/Q < 600 keV/Q | D. Hovestadt | 120 sec | 2,500 km |
| X RAYS AND ELECTRONS<br>Electrons: > 200 keV<br>X Rays: 5-1250 keV | K. A. Anderson | 1 sec | 21 km |
| HIGH ENERGY COSMIC RAYS | E. C. Stone | | |
| HIGH ENERGY COSMIC RAYS | H. H. Heckman | | |
| MEDIUM ENERGY COSMIC RAYS | T. von Rosenvinge | | |
| COSMIC RAY ELECTRONS | P. Meyer | | |

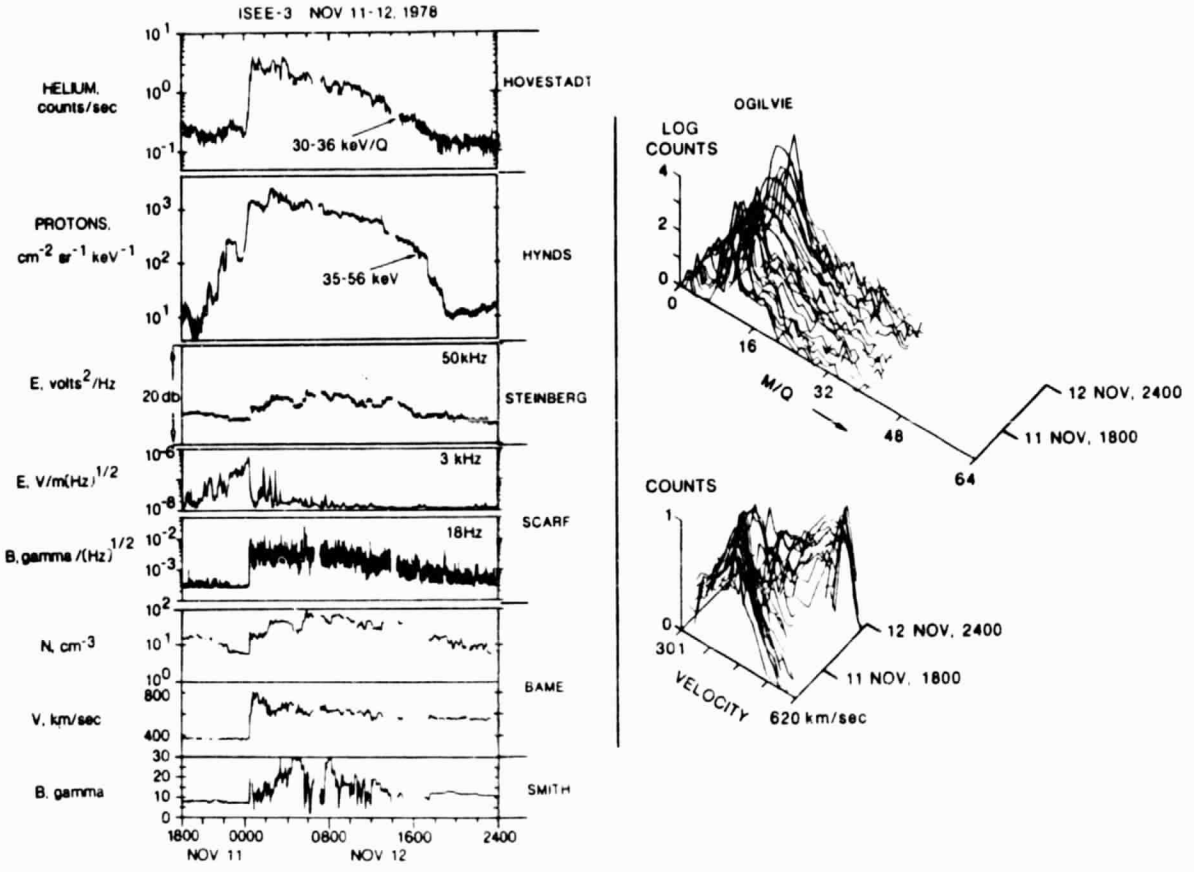


Figure 4. ISEE-3 Measurements During Passage of an Interplanetary Shock

The magnetic field profile in the bottom panel of Figure 4 shows that the interplanetary shock arrived at ISEE-3 at 0028 on November 12, and that the extensive downstream region of disturbance was characterized by the presence of intense low-frequency magnetic turbulence. The velocity and density panels from the plasma electron instrument also indicate passage of a strong shock with post-shock flow disturbances, and the 18 Hz panel from the plasma wave instrument shows that the region had large-amplitude magnetic noise that we identify as whistler mode waves. Other significant post-shock characteristics are the elevated 50 kHz noise levels from the radio mapping investigation and the very large enhancements in the fluxes of energetic protons and helium ions. In Figure 4 there is also clear evidence of a foreshock region with high amplitudes for the ion acoustic waves (3 kHz E-field) and a pre-shock build-up for the 30 keV protons suggesting local acceleration. The ion mass spectrometer profiles on the right side of Figure 4 illustrate the large variations in flow speed and composition over the two-day interval; at this time the instrument was clearly able to resolve changes in the populations of $^3He^{++}$, $^4He^{++}$, $O^{7+}$, $O^{6+}$, $^4He^+$, and Fe ions.

The relevance of these interplanetary plasma physics measurements for the Giacobini-Zinner encounter can be understood by considering the right side of Figure 5. Here we depict the anticipated magnetic field and plasma density profiles by sketching possible variations of the electron plasma frequency, $f_p^-$ [=(9$\sqrt{N}$) kHz, with N in $cm^{-3}$], the electron cyclotron frequency, $f_c^-$ [=(28 B) Hz, with B in gamma], and related ion and hybrid characteristic frequencies. Many models of the solar wind-comet interaction suggest a shock-to-plasma sheet-to-shock distance of 2-4 million kilometers for the downstream trajectory shown in Figure 2, and this would mean that the first half passage from the "shock region" to the center of the plasma sheet might take from 13-26 hours at a speed of 21.7 km/sec. Thus, the total traversal across the tail is expected to occupy at least a full day. Moreover, the extensive foreshock contains comet-related energetic ions, electrons, and enhanced turbulence levels for mhd and plasma waves, so that the total time for passage through the comet interaction region may well involve several days (The Space Science Board of the US National Academy of Sciences suggested that local measurements of the comet interaction be made over a distance of $10^7$ km, implying coverage for five days at the ISEE-3 encounter speed.

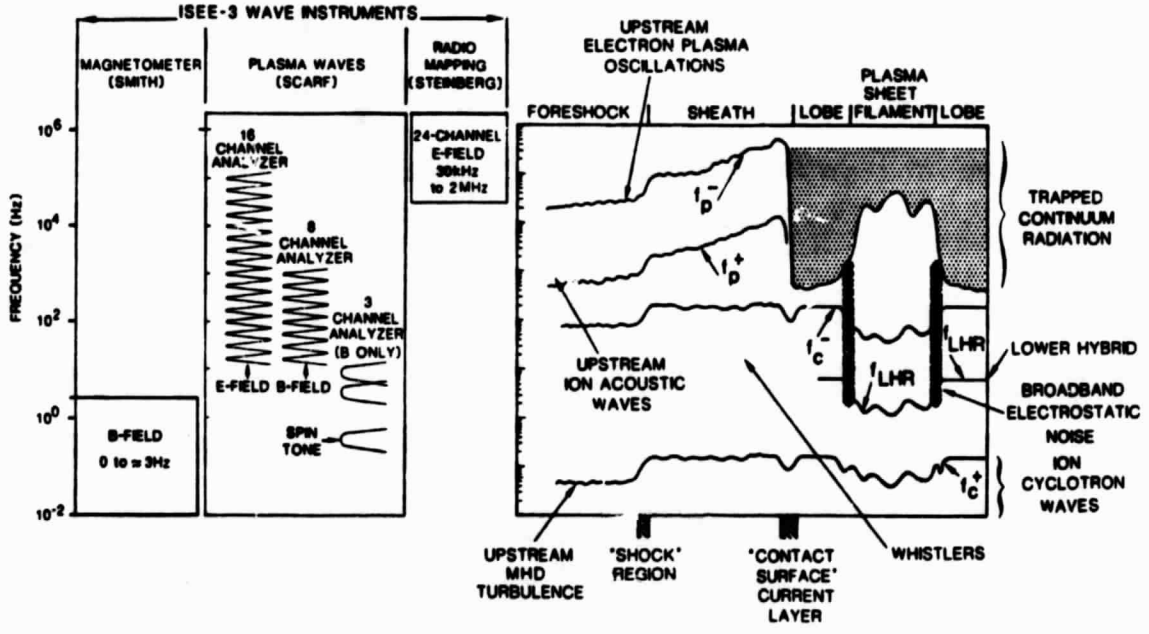


Figure 5. ISEE-3 Wave Coverage (Left Side) and Anticipated Variation of Characteristic Wave Frequencies (Right Side)

The labels on the right side of Figure 5 designate wave phenomena that must be studied during the comet flyby because (a) these measurements yield information on very significant local wave-particle interactions

(e.g., upstream waves; bow shock and ionosheath turbulence; current-driven plasma oscillations near the contact surface and the plasma sheet boundaries), or (b) because these measurements provide unique diagnostic information (e.g., detection of trapped continuum radiation in the tails of Earth and Jupiter yields absolute plasma density profiles; detection of upper hybrid emissions behind Titan yields similar absolute density information). In addition, the very-low-frequency ion and hybrid mode waves may be related to processes that develop continuously near the tail boundary region (plasma mantle) or intermittently during substorm-like tail disruptions. Our experience in studying plasma physics phenomena behind Earth, Jupiter, and Titan suggests that comprehensive wave coverage is needed, and the panels on the right side of Figure 5 show that the ISEE-3 payload will indeed provide such coverage over the range from DC to 2 MHz.

The expected science return from the ISEE-3 encounter with Comet Giacobini-Zinner is summarized in Table 2. As noted above, ISEE-3 has no remote sensing or imaging capability and no way to analyze physical or chemical characteristics of dust (although the plasma wave instrument may be able to provide dust impact data just as the Voyager 2 instrument provided similar information during the crossing of Saturn's G-ring). However, as shown in Table 2, the ISEE-3 instruments will yield comprehensive information on the dynamical plasma processes that control the solar wind interaction with an active short-period comet.

TABLE 2: EXPECTED SCIENCE RETURN - ISEE-3 TO GIACOBINI-ZINNER

- PHYSICS OF THE COMETARY BOW SHOCK
  - EVALUATE SHOCK LOCATION, STRENGTH, STRUCTURE, AND RELATED PARTICLE ACCELERATION;
  - DETERMINE CHARACTERISTICS OF UPSTREAM IONIZATION AND MASS LOADING;
  - DETERMINE EXTENT OF THE FORESHOCK.
- PHYSICS OF THE IONOSHEATH AND CONTACT SURFACE
  - DETERMINE THE NATURE OF THE INTERACTION BETWEEN THE INTERPLANETARY MAGNETIC FIELD AND THE COMETARY PLASMA;
  - DETERMINE LOCATION, THICKNESS, AND MICROSTRUCTURE OF THE INNER BOUNDARY (CONTACT SURFACE);
  - EVALUATE SHEATH IONIZATION PHENOMENA AND TURBULENCE CHARACTERISTICS;
  - EVALUATE ELECTRON DISTRIBUTION FUNCTIONS; SEARCH FOR ELECTRON PEAKS THAT MIGHT RELATE TO IONIZATION OF PARENT MOLECULES.
- PHYSICS OF THE COMET TAIL
  - DETERMINE CONFIGURATION OF THE MAGNETIC TAIL AND CONTENT OF THE PLASMA SHEET FILAMENTS;
  - EVALUATE CURRENTS, WAVE-PARTICLE INTERACTIONS AND ACCELERATION PROCESSES IN THE TAIL;
  - EVALUATE IONIC COMPOSITION, ENERGETIC PARTICLE SPECTRA, AND ELECTRON HEAT FLUX;
  - SEARCH FOR PLASMA MANTLE REGIONS, CROSS-TAIL E-FIELD ACCELERATION PROCESSES, AND SUBSTORM-LIKE PHENOMENA.

The encounter of ISEE-3 with Giacobini-Zinner creates opportunities for coordinated measurements that will enhance the overall scientific yield from the many 1985-86 comet investigations now planned. Conditions for observing Giacobini-Zinner from Earth will be excellent during 1985. The bottom part of Figure 6 has one of the 1959 pictures of the comet, and the top of Figure 6 shows the most relevant parameters related to Earth-based viewing of the comet along with the corresponding information for Halley. For an observer located at a latitude of 35N, Giacobini-Zinner can be viewed for four or more hours throughout 1985 and, in particular, at the time of the encounter. The predicted brightness (apparent total magnitude) will exceed that of Halley until October-November and will reach 8th magnitude at encounter.

The phasing of Giacobini-Zinner relative to Halley is such that viewing of the two comets tends to be mutually complementary. Giacobini-Zinner will be available for viewing during the dark hours for several months prior to Halley and for a month or so around the time of Halley perihelion passage which occurs in daylight.

There will also be post-encounter opportunities for ISEE-3 to make particle and field observations in the solar wind upstream of Halley while Earth-based or space observations of Halley are being made. Figure 2 (above) shows the location of Halley during two intervals of closest approach to the Halley-sun line. The first of these "radial" lineups would occur on 31 October 1985 before Halley reaches perihelion, when the view of Halley from Earth will be excellent. At that time, the radial separation will be 0.9 AU and fast streams, sector boundaries and other solar wind phenomena would be expected to reach Halley about 4 days later. The second lineup would occur 31 March 1986 after the Halley perihelion passage. This line-up will have a separation distance of 0.2 AU, and earlier in March 1986, as the other spacecraft encounter Halley's comet, ISEE-3 should be able to provide excellent upstream information on corotating solar wind streams and transients.

## Acknowledgments

We wish to thank our ISEE-3 colleagues, S. Bame, J. Fainberg, G. Gloeckler, D. Hovestadt, R. Hynds, F. Ipavich, K. Ogilvie, J.S. Steinberg and K.P. Wenzel for providing information about the November 11, 12 interplanetary event. The work at TRW was supported by NASA under contracts NASW-3690 and NAS5-20682. The work at JPL represents one aspect of research carried out by JPL for NASA under contract NAS7-100.

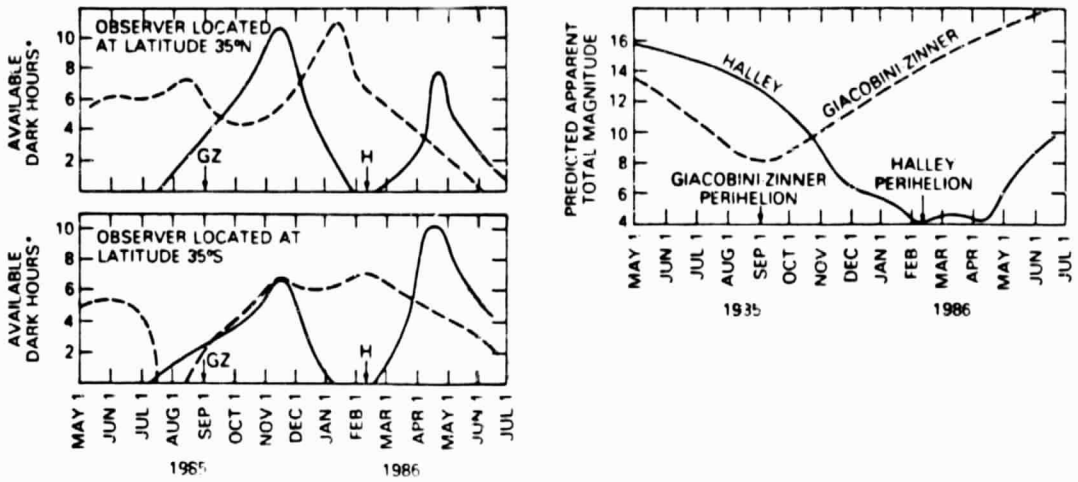


*AVAILABLE DARK HOURS – IS DEFINED AS THE TIME INTERVAL DURING WHICH THE SUN IS BELOW THE LOCAL HORIZON BY AT LEAST 18 DEGREES AND THE COMET IS SIMULTANEOUSLY ABOVE THE LOCAL HORIZON

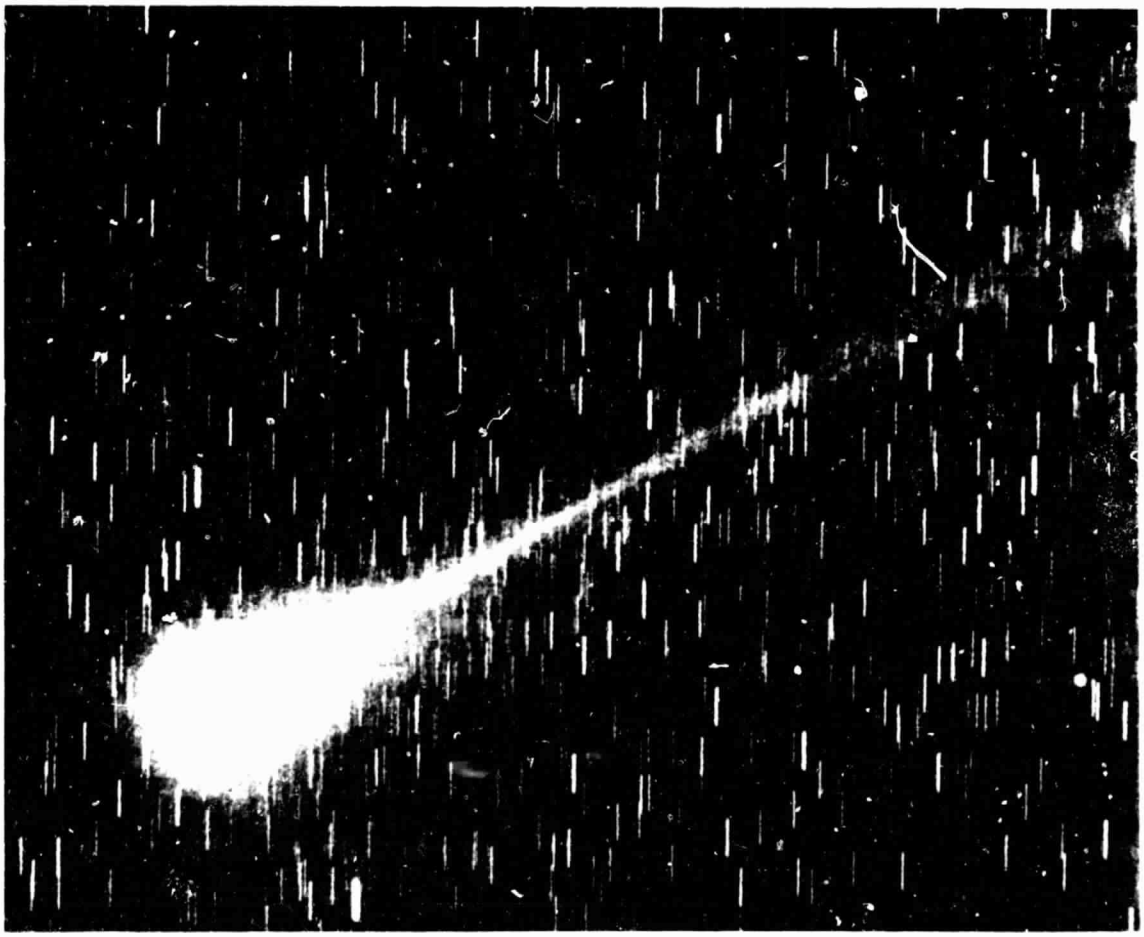

Figure 6. Top: 1985-86 Observing Conditions for Comets Halley and Giacobini-Zinner. Bottom: 1959 Photograph of Comet Giacobini-Zinner.

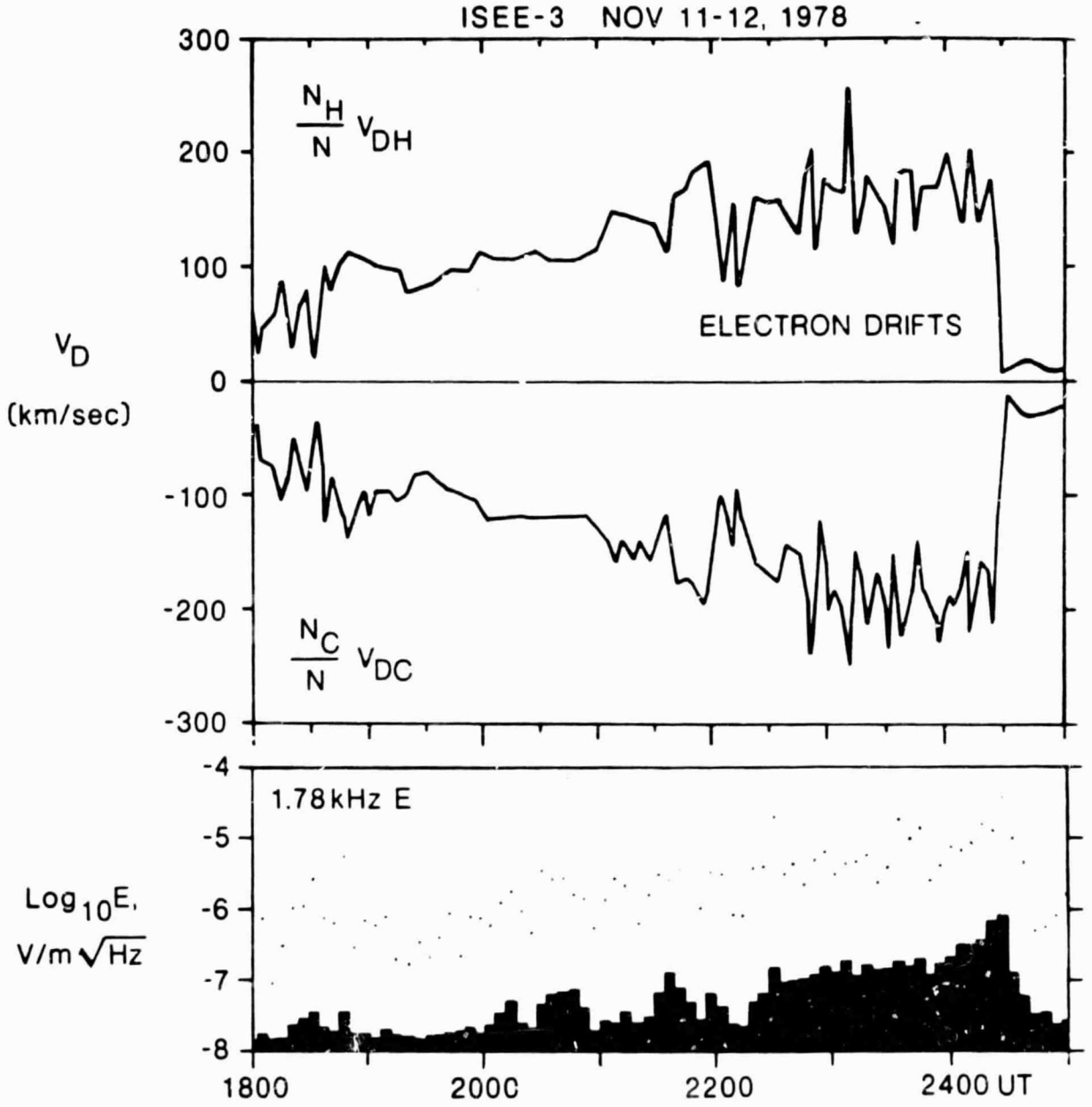


Figure 18

D4



# THE INTERPLANETARY SHOCK EVENT OF NOVEMBER 11/12 1978 - A COMPREHENSIVE TEST OF ACCELERATION THEORY

K.-P. Wenzel, T.R. Sanderson, P. van Nes
Space Science Department of ESA, ESTEC, Noordwijk, The Netherlands
C.F. Kennel, F.L. Scarf, F.V. Coroniti
TRW Space and Technology Group, Redondo Beach, California 90278
C.T. Russell
University of California, Los Angeles, California 90024
G.K. Parks
University of Washington, Seattle, Washington 98195
E.J. Smith
Jet Propulsion Lab., California Inst. of Technology, Pasadena, 91109
W.C. Feldman
Los Alamos Scientific Laboratory, Los Alamos, New Mexico 87545

## ABSTRACT

A comprehensive study of the November 11/12, 1978 shock event based on energetic particle, solar wind, magnetic field and wave data from the ISEE-3, -1 and -2 spacecraft has been undertaken both from the energetic particle and the collisionless shock point of view. The energy density of 10-50 keV protons accelerated by the shock is found to be equivalent to the upstream magnetic field energy density. The observations are in quantitative agreement with Lee's (1983) self-consistent theory for the excitation of hydromagnetic waves and the acceleration of ions upstream of interplanetary shocks.

## 1. Introduction

We present selected results of a comprehensive study of the quasi-parallel interplanetary shock event of November 11/12, 1978 from both the collisionless shock and energetic particle points of view using magnetic field, plasma, MHD wave and energetic ion measurements on ISEE-3 ($\sim$200 $R_E$ upstream from the Earth's bow shock) and ISEE-1/2 (upstream, but close to the bow shock) (Kennel et al., 1983). Specifically we compare the observations with quantitative predictions of current theories of particle acceleration by quasi-parallel shocks. Several papers have addressed the November 11/12 shock event (Reinhard et al., 1981; Kennel et al., 1982; Scholer et al., 1983; Tsurutani et al., 1983; Lee, 1983).

## 2. Event Overview

Figure 1 presents selected ISEE-3 energetic ion, plasma wave, solar wind and interplanetary magnetic field (IMF) data for the period 1800 UT on Nov. 11, 1978 to 2400 UT on Nov. 12. The shock encounters ISEE-3 at 0028 UT on Nov. 12. In the upstream period the 35-56 keV proton and the 3 kHz ion acoustic wave intensities increased and the solar wind density decreased, all three with superimposed fine structure, until the shock. The IMF magnitude and solar wind speed remained virtually constant at 7.5 nT and 375 km $s^{-1}$, respectively. At the shock the ion acoustic wave amplitude maximised and then suddenly dropped. The 35-56 keV proton flux rose by a factor of 10 in the last half hour before the shock passage to

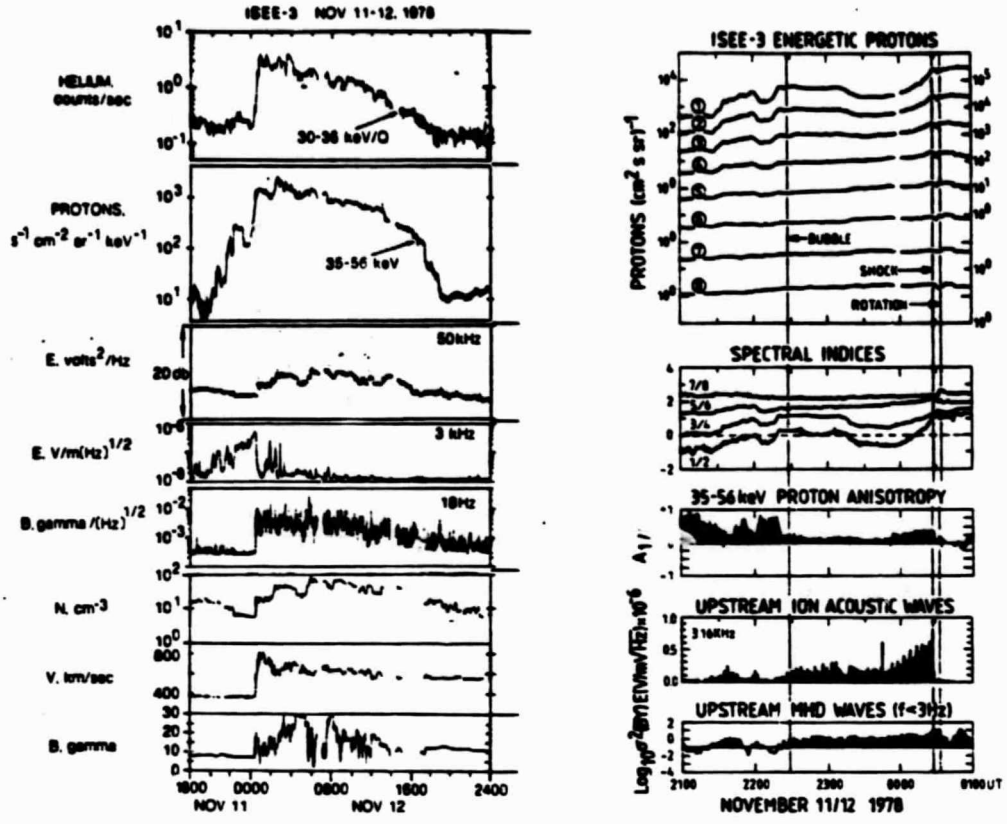


Fig. 1. (left) 30-hr period of selected ISEE-3 data around the interplanetary shock encountered at 0028 UT on Nov. 12, 1978. N is the solar wind pseudo-density taken from the data pool.

Fig. 2. (right) Time evolution for the period 2100 UT to 0100 UT of ISEE-3 energetic proton fluxes in 8 particle channels between 35 and 1600 keV ((1) 35-56 keV; (2) 56-91 keV; (3) 91-147 keV; (4) 147-237 keV, etc.); ratio of differential fluxes in successive energy channels; first-order parallel anisotropy amplitudes of 35-56 keV proton distribution in solar wind frame; spectral density of 3.16 kHz ion acoustic waves; variance in the 0.01 - 3 Hz IMF Y-component.

a first maximum at the shock, reached a second peak about 0240 UT, commenced a slow decline and dropped suddenly near 1715 UT coincident with the arrival of the flare ejecta at ISEE-3.

Figure 2 compares intensities, spectral indices and the anisotropies of the 35-1600 keV protons with ion acoustic and <3 Hz MHD wave amplitudes in the ISEE-3 upstream region. This entire region was free from effects associated with the bow shock. Detailed analysis of the solar wind electron observations, which exhibited strong bidirectional streaming, provides strong evidence that ISEE-3 entered a closed magnetic loop ("bubble") at 2230 UT that intersected the approaching interplanetary shock at both ends. Inside this upstream bubble the ion acoustic and MHD wave amplitudes are intense and nearly constant till ~0000 UT. The low energy ($\lesssim$ 200 keV) proton channels respond significantly to the

arrival of the bubble. On entering it the first-order proton anisotropy goes essentially to zero, indicating an isotropic distribution. In the last half hour prior to the shock encounter the ion acoustic wave amplitude increases, strongly correlated with the steep rise of the low-energy proton intensity and the start of significant field-aligned streaming in the solar wind frame from the direction of the approaching shock. The <3 Hz MHD wave amplitude remains nearly constant.

## 3. Shock Structure and Wave Activity

Detailed analysis of the IMF and solar wind data from ISEE-3 and -1 using four different techniques (Kennel et al., 1983) resulted in the shock normal angle $\Theta_{BN} = 40^{\circ}$, a fast Mach number $M_F = 2.6$, a jump of field strength of 2.2. We note that these parameters are for the local plasma subshock and do not take into account the effects of energetic ions.

We suggest that energetic ions must play a significant role in the shock structure. The measured 35-56 keV proton flux of the shock is $3 \times 10^4$ p/cm$^2$ s sr. The corresponding number and energy densities are $\sim 10^{-3}$ p cm$^{-3}$ and $0.7 \times 10^{-10}$ ergs cm$^{-3}$, respectively. This energetic proton energy density, probably even an under-estimate, is about 1/3 of the energy density of the upstream magnetic field, $2 \times 10^{-10}$ erg cm$^{-3}$. Extrapolating the observed proton spectrum down to 10 keV results in an increase of the particle energy density by a factor 4.

Upstream waves are continuously present to unusually large distances from the shock. Emissions at 1900 UT on Nov. 11 imply that the scale of the upstream wave region corresponds to $\sim$0.04 AU (Tsurutani et al., 1983). This region of enchanced upstream wave activity coincides with the extended region of the energetic protons (Fig. 1). Figure 3 shows 8 minutes of high-resolution magnetic field data surrounding the ISEE-3 (top) and ISEE-1 (bottom) shock encounters. Large amplitude (6 nT p-p) slightly compressional waves with $\sim$7-s periods are apparent just ahead of the shock.

The region between the shock and a strong IMF rotation contains extremely large ($\sim$20 nT p-p) transverse magnetic field fluctuations, with wavelengths ($\sim$3 to 20 s periods) comparable with the thermal ion Larmor radius in the shock-heated plasma and therefore consistent with the resonant firehose instability. The upstream and downstream waves near the shock propagate essentially parallel to the local magnetic field.

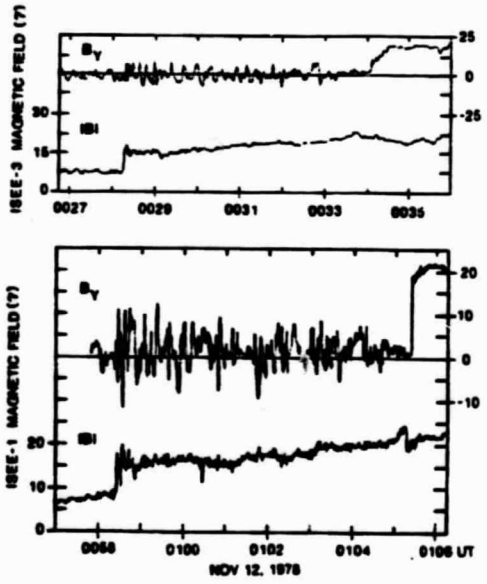


Fig. 3. IMF Y-component and magnitude around the ISEE-3 (0028:20 UT) and ISEE-1 (0058:30 UT) shock encounters. Both magnitude profiles are essentially identical.

## 4. Comparison of Observations with Theory

Lee (1983) recently presented a self-consistent theory for the excitation of hydromagnetic waves and the

acceleration of ions upstream of interplanetary shocks by first-order Fermi processes. We compare several facets of our observations with the predictions made by the equilibrium theory.

a) The measured proton distribution transformed into the solar wind frame shows field-aligned streaming away from the shock with an amplitude of $\sim$0.35 for the 35-56 keV protons in the $\sim$100 $R_E$ wide upstream region adjacent to the shock. In the near-shock downstream region we observe isotropy. If we transform our observations into a frame moving with the shock velocity, we find isotropy in the near-shock upstream region. These results agree with the prediction of Lee (1983) and the observations of Scholer et al. (1983). Farther upstream (2230-0000 UT) we also observe isotropy in the solar wind frame.

b) The energy spectrum can be fitted neither up nor downstream by a single exponent power law over the full 35-1600 keV range. For $E \lesssim 250$ keV the differential proton spectrum has a spectral index of $\gamma = 1.1$ at the shock and hardens with increasing upstream distance from the shock, in agreement with theory. Farther upstream, inside the bubble, the spectrum turns over, as calculated by Lee. In the downstream region ($\gtrsim$ 20 min. postshock) we find over the full energy range an excellent fit of the differential energy spectrum $dJ/dE \sim v^{-2}\, e^{-v/v_0}$ where $v_0 = 4.9 \times 10^8$ cm $s^{-1}$ in agreement with the calculations of Forman (1981).

c) We measure for 35-56 keV protons an e-folding distance of $3.3 \times 10^{10}$ cm in the shock frame ($V_{sh} \approx 700$ km $s^{-1}$) in the last 10 min. upstream of the shock. This is in fair agreement with the value which we calculate from Lee's theory as $L_s = 1.2 \times 10^{10}$ cm using the shock ($\Theta_{BN} = 40^\circ$, $n_{up} = 3.1$ cm $^{-3}$) and particle parameters ($f_p(30\ \text{keV},0) = 3.3 \times 10^{-29}$ $cm^{-6}$ $s^3$, $\gamma = 1.1$) of this study. The observed scale length increases, as predicted, with energy.

d) Lee (1983) predicts that upstream of the shock ion cyclotron waves should be generated by resonant cyclotron interactions with the energetic particle distribution. He estimates that the rms amplitude of the ion-excited waves at the shock front, normalised to that of the upstream field, is about 0.13. We find from ISEE-3 $(\delta B)_{rms}/B = 0.14 - 0.16$, in excellent agreement with theory.

## 5. Acknowledgements

R.R. Anderson (Univ. of Iowa), F. Mozer and M. Cameron (Univ. of California at Berkeley) have contributed to the comprehensive study.

## References

Forman, M.A. (1981), Adv. Space Res. 1, No. 3, 97.
Kennel, C.F. et al. (1982), J. Geophys. Res. 87, 17.
Kennel, C.F. et al., TRW Preprint (1983).
Lee, M.A., to appear in J. Geophys. Res. (1983).
Reinhard, R. et al. (1981), Proc. 17th Int. Cosmic Ray Conf., Paris, 10, 122.
Scholer, M. et al. (1983), J. Geophys. Res. 88, 1977.
Tsurutani, B.T. et al., to appear in J. Geophys. Res. (1983).

D5



Rouett DRAFT

# PLASMA AND ENERGETIC PARTICLE STRUCTURE OF A COLLISIONLESS QUASI-PARALLEL SHOCK

by

C. F. Kennel, F. L. Scarf, F. V. Coroniti
TRW Space and Technology Group
Redondo Beach, California 90278

C. T. Russell
Institute of Geophysics and Planetary Physics
University of California at Los Angeles
Los Angeles, California 90024

E. J. Smith
Jet Propulsion Laboratory
California Institute of Technology
Pasadena, California 91109

K. P. Wenzel, R. Reinhard, T. R. Sanderson
European Space Research and Technology Centre
Noordwijk, The Netherlands

W. C. Feldman
Los Alamos National Laboratory
Los Alamos, New Mexico 87545

G. K. Parks
Geophysics Program
University of Washington
Seattle, Washington 98195

F. S. Mozer
Space Sciences Laboratory
University of California at Berkeley
Berkeley, California 94720

R. R. Anderson
Department of Physics and Astronomy
University of Iowa
Iowa City, Iowa 52242

February 1983

Bldg R-1, Rm 1176
TRW Space and Technology Group
One Space Park
Redondo Beach, California 90278
(213) 536-2015

## Abstract

We study the quasi-parallel interplanetary shock of November 11-12, 1978 from both the collisionless shock and energetic particle points of view, using measurements of the interplanetary magnetic and electric fields, solar wind electrons, plasma and MHD waves, and intermediate and high-energy ions obtained on ISEE-1, -2, and -3. We will characterize the interplanetary environment through which the shock was propagating when it encountered the three spacecraft, document as completely as possible the observations of this shock, and test current theories of quasi-parallel shock structure and particle acceleration. These observations tend to confirm present self-consistent theories of first-order Fermi-acceleration by shocks and of collisionless shock dissipation involving firehose instability. 10-50 keV protons accelerated by the shock achieved a $\beta$ of order unity just upstream of the shock and, next to the solar wind energy flux, $\rho v^3/2$, were the most significant dynamical parameter characterizing the upstream flow. The 5 keV "seed" or "upstream" protons were highly anisotropic and may have been accelerated by the ion cyclotron electron heat flux instability. The shock was propagating in a closed magnetic loop when it encountered ISEE-1, -2, and -3.

# 1. INTRODUCTION

## 1.1 Introductory Remarks

The shock of November 11-12, 1978 has been characterized as "the granddaddy of all quasi-parallel interplanetaries" (J. T. Gosling, private communication, 1982). Whether or not this is apt, the shock has attracted considerable interest. The facts that it was high-speed (600-700 km/sec) and quasi-parallel were enough to single it out for attention. It was the first interplanetary shock for which an extended region of ion acoustic turbulence, essentially identical to that upstream of the bow shock, was found (Kennel et al., 1982). The region of ion acoustic disturbance ahead of it proved to be surprisingly large -- large enough to be of interest to cosmic ray acceleration theories -- and immediately raised the question of whether other signatures of the earth's foreshock would be found equally far upstream of it. In the meantime, the energetic particle community was also looking into the November 11-12, 1978 shock, for it was one of the strongest ESP particle acceleration events observed in the intermediate energy range, ~10 keV - 2 MeV (Reinhard et al., 1981). The number of papers concerned with the November 11-12, 1978 shock, wholly or in part, is increasing rapidly (Russell et al., 1982; Tsurutani et al., 1983; Scholer et al., 1983; Lee, 1983) and shows no signs of early abatement.

In view of the manifest experimental and theoretical interest in the November 11-12, 1978 shock, we believe a synoptic survey of the observations of this shock is now in order. This paper assembles ISEE-1, -2, and -3 observations of the interplanetary magnetic and electric fields, plasma, plasma waves, and intermediate and high-energy ions from 1800 UT on November 11,

1978 to 2400 UT on November 12, 1978, a period which includes the passage over the three spacecraft of a large region of upstream interplanetary disturbance, the shock, multiple neutral sheet crossings downstream, and, finally, the piston. We will collect enough information to begin to examine, for the first time, a quasi-parallel shock from the points of view of both its collisionless shock structure and of its interaction with energetic particles. For this shock, we will see that the two approaches cannot be separated.

Our objectives in this paper are three-fold: First, to characterize the interplanetary environment through which the shock was propagating when it encountered ISEE-1, -2, and -3; second, to document as completely as possible the observations of the shock; and, third, using this documentation, to test at least the conceptual outlines and, where possible, the quantitative predictions of current theories of quasi-parallel shock structure and particle acceleration. Because of its objectives, this paper will be long, and its structure will be complex. Section 1.2 lists the instruments whose data we use. Chapter 2, in which we summarize the observational and theoretical context from which this study has emerged, introduces the questions upon which our observations have a bearing. Chapter 3 characterizes the gross properties of the November 11-12, 1978 shock event in terms of eight energetic particle and plasma diagnostics recorded during a 30-hour period containing the shock. In Chapter 4, we present ISEE-1 and -3 measurements of the shock and the shock normal solution emerging from these measurements. Chapter 4 also characterizes the events that occurred in the first two to three hours after shock encounter. Chapter 5 focuses on ISEE-3 measurements taken during the 6-hour period prior to shock encounter, and Chapter 6 summarizes the corresponding ISEE-1 data.

Chapter 7 presents some experimental data bearing upon the ion acoustic turbulence observed upstream of the shock and on the possible existence of the ion cyclotron electron heat flux instability upstream of the shock. Chapter 8 compares the theoretical predictions discussed in Section 1.2 with our observations, and Chapter 9 closes with a few brief remarks.

## 1.2 Instruments

Table 1 lists the instruments whose data we have assembled for this study. These instruments and their capabilities have been described in a special issue of the IEEE Transactions on Geoscience Electronics (Vol. GE-16, No. 3, July, 1978) and in subsequent scientific publications by members of the individual scientific teams. The second column in Table 1 lists the first author and the page number in Geoscience Electronics of the article that describes each instrument.

This paper also makes use of data on α-particle count rates, obtained by the ISEE-3 Nuclear and Ionic Charge Distribution Particle Experiment (Hovestadt et al., p. 166, 1978), and on 50 kHz electric field voltages obtained by the ISEE-3 3-Dimensional Radio Mapping Experiment (Knoll et al., p. 199, 1978), which were communicated to us privately.

In most cases, the data assembled here are survey data presented in standard display formats developed by each experimental team in the course of their research, and the data analyses were not optimized particularly for the study of the November 11-12, 1978 shock. In several instances, the individual experimental teams are presently working on refined analyses of the data for this and other interplanetary shock events, which they will publish separately.

TABLE 1. INSTRUMENTS

ISEE-3

| Instrument | Reference |
|---|---|
| Solar Wind Plasma | Bame et al. (p. 160) |
| Low-Energy Protons | Balogh et al. (p. 176) |
| Plasma Waves | Scarf et al. (p. 191) |
| Vector Helium Magnetometer | Frandsen et al. (p. 195) |

ISEE-2

| Instrument | Reference |
|---|---|
| Fluxgate Magnetometer | Russell (p. 239) |
| Energetic Particles | Anderson et al. (p. 213) |

ISEE-1

| Instrument | Reference |
|---|---|
| Fluxgate Magnetometer | Russell (p. 239) |
| Energetic Particles | Anderson et al. (p. 213) |
| Plasma Waves | Gurnett et al. (p. 225) |
| DC and Low-Frequency Electric Fields | Mozer et al. (p. 258) |

## 2. OBSERVATIONAL AND THEORETICAL BACKGROUND

### 2.1 Introductory Remarks

In recent years, the space and astrophysical plasma communities have been occupied with different aspects of three general questions:

- Why are quasi-parallel ($Q_{\parallel}$) and quasi-perpendicular ($Q_{\perp}$) collisionless shocks so different?
- How do collisionless shocks accelerate particles to high energies?
- How does energetic particle acceleration affect shock structure?

It is gradually becoming clear that all three questions are interrelated, and we will have to consider all three to interpret the data we have assembled for the interplanetary shock event of November 11-12, 1978. We might also add a fourth question to the above list which data on shocks in the solar system alone cannot answer: To what extent can the knowledge gained from solar system shock studies be successfully applied to the study of cosmic ray acceleration by astrophysical shocks?

## 2.2 $Q_{||}$ and $Q_{\perp}$ Shock Structure

Bow shock studies have revealed a profound difference between $Q_{||}$ and $Q_{\perp}$ shocks (Formisano, 1977; Greenstadt and Fredricks, 1979). The shock normal angle $\theta_{Bn}$ separates the two types; $Q_{\perp}$ shocks have $\theta_{Bn} \gtrsim 45°$-$55°$, and *vice versa* for $Q_{||}$ shocks. Quasi-perpendicular shocks appear to be about an ion Larmor radius thick (Leroy *et al.*, 1982; Livesey *et al.*, 1982), as measured by jumps in both the magnetic field strength and plasma density. On the other hand, in $Q_{||}$ shocks, the magnetic field undergoes a much broader and more disorderly transition whose spatial scale is difficult to determine from bow-shock measurements. It is not known whether there is a thin density jump embedded within the broad region of large-scale magnetic turbulence that characterizes $Q_{||}$ shocks.

The facts that $Q_{||}$ shocks allow significant access upstream of particles that have interacted with the shock, while $Q_{\perp}$ shocks do not, appear to be the primary observational distinction between the two. As early as 1968, we knew that an element of solar wind flow could have foreknowledge of an impending bow-shock crossing if it were connected magnetically to the bow-shock surface. The connected region of upstream disturbance has come to be known as the foreshock. The interplanetary field line that is instantaneously tangent to the bow-shock surface defines the leading edge of the foreshock; at the point of tangency, the shock normal angle $\theta_{Bn}$ is 90°. Near the point of tangency, the locally $Q_{\perp}$ shock evidently accelerates electrons (Anderson, 1968, 1969; Anderson *et al.*, 1981) and ions (Gosling *et al.*, 1978; Greenstadt *et al.*, 1981) into focused beams which escape upstream along field lines. When they are observed upstream, the electron and ion beams may be traced kinematically back to the shock. Although they both are generated where the shock is locally

$Q_\perp$, the electron beam is encountered upstream of the ion beam. The escaping electron and ion distributions become progressively more diffuse downstream of their beam leading edges, on field lines that connect to a bow shock that is more and more $Q_\parallel$ (Anderson et al., 1979; Gosling et al., 1978; Greenstadt et al., 1980).

The superthermal particles in the foreshock generate a rich spectrum of magnetohydrodynamic and plasma waves. Escaping electrons generate electron plasma waves (Scarf et al., 1971; Anderson et al., 1981), low-frequency (~ 1 Hz) whistler waves (Sentman et al 1982), and higher-frequency whistlers (Fairfield, 1974). Ion acoustic waves are closely associated with superthermal ions and electrons in the foreshock (Scarf et al., 1971; Rodriguez and Gurnett, 1975; Anderson et al., 1981). The measured ion beam (Gary, 1981) and diffuse ion (Sentman et al., 1981b) distributions are unstable to hydromagnetic waves, which achieve large amplitudes in the diffuse proton zone (Paschmann et al., 1979; Greenstadt et al., 1980; Hoppe et al., 1981).

The impressive clarification of foreshock phenomenology cited above has not improved our fundamental understanding of the difference between $Q_\perp$ and $Q_\parallel$ shocks because of an ambiguity inherent in the interpretation of foreshock measurements. It has been argued that many, perhaps most, of the upstream ions come from the ion foreshock beam (Bame et al., 1981). As such beam ions propagate upstream, they destabilize low-frequency electromagnetic waves which subsequently scatter and decelerate them. The decelerated ions and the waves are blown downstream by the solar wind to fill the entire foreshock with waves and superthermal ions. The waves are ultimately blown back into the quasi-parallel zone of the shock surface, possibly accounting for the disordered magnetic structure of $Q_\parallel$ shocks. In this interpretation, the $Q_\parallel$

bow-shock structure we observe is an artifact of the small radius of curvature of the bow shock. Indeed, the foreshock has a spatial scale that equals or exceeds the bow shock's curvature radius. On the other hand, one can argue that superthermal ions ought to escape naturally from plane $Q_{||}$ shocks (Edmiston et al., 1982). In this case, some of the foreshock phenomena we observe might be inherent to $Q_{||}$ shock structure. Indeed, the superthermal ions have an an energy density comparable with that of the interplanetary field, and, more significantly, the solar wind is decelerated and deflected when it enters the foreshock (Bonifazi et al., 1980) by an amount compatible with the momentum flux carried by shock-escaping ions (Sentman et al., 1981a), suggesting that part of the shock transition is accomplished in the foreshock.

Although it is not possible to ascertain the true extent of $Q_{||}$ shocks from bow-shock data, one is more likely to succeed with interplanetary shocks, whose radii of curvature are 250-2500 times that of the bow shock. To ascertain whether $Q_{||}$ interplanetary shocks have foreshocks, one should begin by comparing measurements made at equal distances upstream of interplanetary shocks and the bow shock. This implies searching for foreshock signatures a few minutes before an interplanetary shock encounter, when the high-speed shock is a few earth radii from the spacecraft. At present, the search for interplanetary foreshock phenomena is incomplete. However, Russell and Hoppe (1982) and Tsurutani et al. (1983) have found hydromagnetic waves, whose amplitudes and frequencies are similar to those in the earth's foreshock, a few earth radii ahead of $Q_{||}$ interplanetary shocks. Moreover, Kennel et al. (1982) found that the amplitude and spectrum of ion acoustic waves a few $R_E$ ahead of interplanetary shocks are remarkably similar to those in the earth's foreshock. Thus, at least two features characteristic of the earth's foreshock also occur

upstream of $Q_{||}$ interplanetary shocks.

The ion acoustic waves were observed to extend several hundred earth radii ahead of $Q_{||}$ interplanetary shocks, the first indication that their foreshocks might be very much larger than is possible to infer from bow-shock studies (Kennel et al., 1982). It is of obvious interest to inquire whether other phenomena characteristic of the earth's foreshock also occur far upstream of interplanetary $Q_{||}$ shocks. However, it would be difficult to relate a burst of superthermal ions, or an outbreak of magnetic turbulence, that occurs several hours before an interplanetary shock encounter, to the shock, unless one could also associate it with the ensemble of phenomena characteristic of the earth's foreshock. Thus, case studies of interplanetary shocks are called for. This paper reports the results of one such study. About three hours before the November 11-12, 1978 quasi-parallel shock passed over ISEE-3, ion acoustic turbulence began to increase in intensity, at first irregularly and then steadily until the shock was encountered (Kennel et al., 1982). One objective of this paper will be to document, with as many plasma diagnostics as possible, the extended region of disturbance upstream of this shock.

Let us now briefly survey the development of our theoretical ideas concerning the structure of quasi-parallel shocks. It has been popular to separate the structure into a local shock layer, whose thickness scales as the Larmor radius of a thermal ion, and a more extended region, of as yet undetermined thickness, in which part of the shock dissipation required by the Rankine-Hugoniot conditions is accomplished. It is in the extended foreshock that the processes thought responsible for energetic particle acceleration occur. In other words, the overall $Q_{||}$ shock consists of a foreshock and a plasma subshock. In general, laboratory and space plasma theoreticians have

concentrated on the subshock and the near foreshock, and cosmic ray and astrophysical plasma theorists have focused on the foreshock and neglected subshock structure.

Parker (1961) was the first to recognize implicitly the role of escaping ions in the dynamics of $Q_{||}$ shocks, when he argued that parallel ion beams would be firehose unstable and thereby produce large-amplitude Alfvén turbulence that accomplishes the shock transition on a scale of many ion Larmor radii. Moiseev and Sagdeev (1963) developed a model in which upstream ions could be reflected from an electrostatic potential structure at low sonic Mach numbers; at sonic Mach numbers exceeding 1.6, the steady potential structure would no longer exist. Moiseev and Sagdeev (1963) then argued that turbulent heating would produce a firehose unstable turbulent anisotropy if the upstream plasma $\beta$ were sufficiently high. This point of view was subsequently taken up by Kennel and Sagdeev (1967) and Kennel and Petschek (1968), who developed a theory of low Mach number firehose shocks in high $\beta$ plasmas. Auer and Volk's (1973) numerical simulation subsequently confirmed the general outlines of firehose shock theory. These models of the shock failed to recognize the importance of Parker's (1961) suggestion and did not include the effects of escaping upstream ions. Kennel (1981) suggested that a fusion of the ion heat-flux and anisotropy firehose models might be promising.

The above models considered only the long wavelength limit of the firehose instability, where it is non-resonant. On the other hand, the same mode is resonant for wavelengths near the thermal ion Larmor radius, or when the plasma $\beta$ is less than unity (Kennel and Scarf, 1968). Recent work on resonant anisotropy instability has focused on the foreshock and not on the

subshock. Gary (1981) and Sentman et al. (1981) showed that the ions escaping from the terrestrial subshock are unstable to the resonant instability and, if the conditions are appropriate, to the non-resonant instability as well. It is generally believed that this instability is responsible for the large-amplitude upstream waves in the earth's foreshock. Lee (1982) has developed a self-consistent theory for the decay of an ion beam escaping from a parallel subshock due to resonant quasi-linear scattering by low-frequency electromagnetic waves and the subsequent energization of ions by scattering and shock compression. In this theory, the physics of the escaping superthermal ions and cosmic ray acceleration are both consequences of turbulence generated by pitch-angle anisotropies.

Until recently, there was no evidence for MHD waves well upstream of interplanetary shocks. However, Russell et al. (1982) and Tsurutani et al. (1983) have recently found them upstream of quasi-parallel shocks. Lee (1983) extended his self-consistent theory to the interplanetary case and applied it to the November 11-12, 1978 shock. Starting with Scholer et al's (1983) measured 30 keV/Q ion intensity, he was able to account for their particle measurements at higher energy and to predict a wave amplitude and spectrum that we will compare with observation in this paper.

Numerical simulations have contributed substantially to quasi-parallel shock theory. Because of the limitations of spatial scale, numerical simulations treat only the subshock. Biskamp and Weller (1972) proposed an electrostatic, rather than electromagnetic, ion beam instability as the dissipation mechanism for the strong quasi-parallel shock they simulated. Forslund and Friedberg (1971) and Forslund et al. (1980) found that the $Q_{||}$ shock produces a large-amplitude standing whistler which decays into an ion acoustic wave and another

whistler, and proposed that the ion wave accomplishes the ion heating in the quasi-parallel shock. Recent 2-D simulations (Quest et al., 1983) confirm that large-amplitude whistler turbulence on the ion inertial scale length is generated in the shock. They also find that intense fluxes of ions are reflected upstream. Kan and Swift (1983) have simulated $Q_{||}$ shocks in one spatial dimension. They find that a whistler wave train standing upstream of the shock resonantly scatters the incoming thermal ions, and that non-resonant firehose modes are created downstream.

In summary, nearly all theories of $Q_{||}$ shock structure agree that large-amplitude magnetic turbulence, with frequencies that span the range from well below to somewhat above the ion cyclotron frequency, is central to the dissipation in the plasma subshock and to the dynamics of the foreshock ahead of it.

## 2.3 Shock Acceleration of Energetic Particles

Until recently, most theories of cosmic ray acceleration have concentrated on elucidating how single particles can attain high energy by single or multiple encounters with collisionless shocks which are considered to be infinitely thin and whose plasma structure is therefore assumed to be relatively unimportant. Looked at in this fashion, shocks can accelerate particles in several ways. Ions whose Larmor radius exceeds the shock thickness conserve their gyrophase averaged magnetic moment (E. N. Parker, unpublished manuscript, 1958; Chen and Armstrong, 1972; Shebanskii, 1972; Pesses, 1979; Teresawa, 1979a,b). Such ions approaching the shock from upstream would therefore be either reflected from or transmitted through the jump in magnetic field at the shock, depending upon their pitch angle. Reflected ions grad-B drfit parallel to the flow electric field, and they thereby acquire energy more efficiently the more quasi-perpendicular the shock. However, since multiple reflections are needed to account for the observed acceleration by interplanetary shocks (Pesses, 1979), reflected ions would have to scatter from upstream MHD turbulence back towards the shock. They then can be either re-reflected or retransmitted at their next encounter with the shock. Re-reflected particles can repeat the above cycle, and some can reach high energy.

Energetic particles that are transmitted through the shock can be scattered by downstream magnetic turbulence back towards the shock. Such particles are subject to first-order Fermi-acceleration by multiple reflections between upstream and downstream waves that convect approximately with the local flow speed. The shock then serves primarily to decelerate the flow so that the scattering centers appear to converge toward one another

in the shock frame. In the test particle limit, this mechanism does not take intc account the momentum transfer between cosmic rays and the plasma. The integral spectrum calculated for non-relativistic particles Fermi-accelerated by infinite plane shocks depends only upon the ratio of upstream and downstream flow speeds (Krimsky, 1977; Axford et al., 1977; Bell, 1978a,b; Blandford and Ostriker, 1978). Because the particle spectral index calculated for strong shocks is close to the observed galactic cosmic ray index, supernova shocks are promising candidates to accelerate galactic cosmic rays.

For the solar system, the theory of first-order Fermi-acceleration has been applied to the diffuse ions upstream of the bow shock (Eichler, 1981; Teresawa, 1981; Lee et al., 1981; Forman, 1981; Ellison, 1981; Lee, 1982), and to the so-called ESP events associated with interplanetary shocks, in which energetic ions are observed to increase well before the shock encounter (Scholer and Morfill, 1975; Scholer et al., 1983; Lee, 1983). Lee's (1982) theory predicts the energy spectra of different species reported by Ipavich et al., (1981a,b) and the rough spectrum and amplitude of the low-frequency waves observed upstream of the bow shock by Hoppe et al. (1981) and others. The observed spectrum of bow-shock diffuse particles cuts off above about 100 keV, which may be explained by the finite extent of the bow shock. Either a given magnetic field line remains connected to the region where the bow shock is strong for a finite time, or the particles diffuse across the magnetic field onto field lines which no longer interact with the shock. Either effect limits the number of shock crossings a particle can have and, therefore, the energy to which it can be accelerated.

The field line connection time is much larger for interplanetary shocks than for the bow shock, so the first-order Fermi mechanism will have longer

to operate. According to the simplest theory, the energetic ion fluxes should increase exponentially approaching the shock, maximize at the shock, and hold approximately constant downstream -- features characteristic of ESP events. The accelerated ions upstream should be essentially isotropic in the shock frame and isotropic in the solar wind frame. Until very recently, there have been relatively few measurements of moderate energy ions in ESP events in the energy range (10's of keV) that bridges the low-energy plasma and "seed" particles (see below) and high-energy cosmic rays. A recent study of 30-150 keV/Q protons and alphas in three ESP events (Scholer et al., 1983) finds that the observed particle energy and angular distributions and spatial profiles are consistent with first-order Fermi-acceleration theory. One of Scholer et al's (1983) three events is the shock of November 11-12, 1978, and we will discuss Scholer et al's results for this shock in due course.

## 2.4 Relation of Shock Structure and Particle Acceleration

Most theories of particle acceleration by shocks treat the cosmic rays as test particles. E. N. Parker was one of the first to realize that cosmic rays had sufficient energy density to contribute to shock structure. Wentzel (1971) and Axford et al. (1977) included cosmic rays as a second fluid in the shock Rankine-Hugoniot relations. Cosmic rays and plasma were assumed to have different dissipation mechanisms, whose scale length is much larger for the cosmic rays than for the plasma. In these models, energetic particles are presumed to reside upstream prior to shock passage; the cosmic ray flux, a free parameter, is conserved across the shock, and if it is large enough, it can create a shock entirely in cosmic rays without a subshock in the thermal plasma. Such multiple-fluid shock models have been extended by Drury and Volk (1981) and Axford et al. (1982), who modeled the plasma hydrodynamically. It appears that interplanetary shocks should have both a cosmic ray foreshock and a plasma subshock for the range of sonic Mach numbers and particle intensities encountered in the solar system. An extension of these theories to magnetohydrodynamics (Hada and Kennel, 1983) confirms this conclusion. The shocks identified in the interplanetary medium should thus be considered as subshocks, and part of the shock transition should be accomplished across a very much more extended cosmic ray foreshock, an effect already observed in the terrestrial foreshock. Since the November 11-12, 1978 shock did have a pre-existing upstream energetic particle flux that was contained in a closed magnetic field region, it will be used to test the quantitative predictions of the above two-fluid models of shocks.

## 2.5 Toward a Unified View of Shock Structure and First-Order Fermi-Acceleration

Three more interrelated questions must be answered before we arrive at a theory that, among other things, computes the cosmic ray intensity and spectrum as a function of shock parameters:

- Under what circumstances is the Fermi-acceleration scenario realized in practice?
- How do particles that are originally part of the thermal plasma reach the energy threshold where Fermi-acceleration begins to operate?
- To what extent is the turbulence that scatters thermal plasma in the subshock and energetic plasma in the foreshock similar in character?

Recent research has made the answer to the first of the above questions clear. Only quasi-parallel shocks have extended regions of MHD turbulence both upstream and downstream, and this fact is related to the ease with which not only energetic cosmic rays, but also particles on the tail of the thermal distribution, can free stream across the shock.

An answer to the second question, the so-called "seed particle problem", is urgently needed because it will ultimately tell us the efficiency with which shocks can convert flow energy into cosmic ray energy. One should not rely on a pre-existing flux of cosmic rays upstream, and it is generally believed that at least quasi-parallel shocks self-consistently generate their own characteristic spectrum of cosmic rays. Eichler (1979) and Ellison (1981) have developed a model in which both thermal and energetic ions interact with waves in essentially the same way to produce a spatial diffusion length that is proportional to the ion Larmor radius. Such a diffusion model is capable

of producing a high-energy tail with striking efficiency. Observationally, it is clear that the seed particles were once thermal ions that have interacted once with the shock on their way to participating in the Fermi process. In the case of the bow shock, these are the few keV, so-called "upstream" or "superthermal" ions that were reflected from (Bame et al., 1980) or transmitted through (Edmiston et al., 1982) the shock. There have been few studies of the few keV analog of upstream particles from interplanetary shocks.

Nearly all theories of seed particles, cosmic ray acceleration, and, to a lesser extent, shock structure overlook the possible role of electrons and electron heat fluxes, not only in regulating the potential drop across the shock, but in participating in instabilities that subsequently energize or scatter ions. We will present evidence that an important interaction with the electron heat flux occurred in the foreshock far upstream of the shock of November 11-12, 1978.

Existing research suggests that it may be possible to accomplish the entire quasi-parallel foreshock-subshock transition with low-frequency electromagnetic waves as the dominant scattering mechanism. Ellison's (1981) Monte Carlo simulation was based upon this presumption. The theories cited above for the resonant scattering of upstream particles (Lee, 1982, 1983) and the thermalization of the plasma (Parker, 1961; Kennel and Sagdeev, 1967; Kennel and Petschek, 1968; Auer and Volk, 1973) all invoke long-wavelength electromagnetic waves destabilized by pitch-angle anisotropy. Even the thermalization of incoming plasma ions by standing whistlers found in numerical simulations (Quest et al., 1983; Kan and Swift, 1983) is a variation on the same theme. However, the role, if any, of short-wavelength electrostatic turbulence in quasi-parallel shock structure has not been defined experimentally or considered theoretically with any cogency.

## 3. INTRODUCTORY VIEW OF NOVEMBER 11-12, 1978 SHOCK

Figure 1 presents selected ISEE-3 data for the period 1800 UT on November 11, 1978 to 2400 UT on November 12, 1978. The shock encountered ISEE-3 at 0028 UT on November 12, 1978. The data shown are, starting at the top panel and working downwards, 30-36 keV/Q α-particle count rates (M. Scholer, private communication, 1982), 35-56 keV proton intensities, 50 kHz electric field voltages (J. L. Steinberg, private communication, 1982), 3 kHz electric field spectral amplitudes, 17.8 Hz magnetic field spectral amplitudes, the solar wind speed and density (Bame et al., 1981), and the interplanetary magnetic field magnitude.

During the entire period from 1800 UT until the shock, the interplanetary field magnitude and solar wind speed remained virtually constant at 7γ and 370 km-s$^{-1}$, respectively. Variable fluxes of energetic protons streaming along magnetic field lines away from the earth indicate that ISEE-3 had been magnetically connected to the earth's bow shock prior to 1725 UT on November 11. During the variable proton event and until 1840 UT, the superthermal electron fluxes were also highly variable, with their heat flux alternately toward and away from earth, suggesting that the period 1725-1840 UT was one of complex, variable connection to the bow shock. We will concentrate on the more orderly data after 1840 UT, where we will argue there was no evidence of a bow-shock connection.

The solar wind density maximized, and the 35-56 keV proton intensity and 3.16 kHz electric field amplitude minimized, at about 1920 UT. Thereafter, the 35-56 keV proton intensity and the 3.16 kHz electric field amplitudes increased, and the solar wind density decreased, all three with superposed fine structure, until the shock. The five-hour, more or less steady increase

in the energetic proton intensity prior to the shock identifies this as an ESP event.

It is particularly important to note the sudden drop in solar wind density at 2230 UT, which is coincident with sudden increases to plateaus in the 35-56 keV proton and 3.16 kHz ion acoustic wave intensities. According to Kennel et al. (1982), the electric field amplitudes between 1 and 10 kHz jumped near 2230 UT. Note that the 50 kHz electric field voltage diminished slightly at 2230 UT. The count rate of 30-36 keV/Q Helium ions reached a small secondary maximum after 2230 UT. A number of other measurements, to be presented later, will indicate that the state of the solar wind after 2230 UT was distinctly different from the one preceding 2230 UT.

The 35-56 keV proton intensity increased by a factor 10 in the last half-hour before the shock passed over ISEE-3. If this energetic proton front co-moved with the shock, which had a speed of about 700 km-$s^{-1}$, its exponential scale length was about 50 $R_E$. The measured 35-56 keV proton intensity was about $3 \times 10^4$ p-$cm^{-2}$-$s^{-1}$-$sr^{-1}$ just prior to the shock encounter. The corresponding 35-56 keV proton number and energies were about $10^{-3}$ p-$cm^{-3}$ and 0.7 ergs-$cm^{-3}$, respectively. This energy density is probably an underestimate, because the measured spectrum was quite hard, but even it is about 1/3 the energy density of the magnetic field upstream, $2 \times 10^{-10}$ ergs-$cm^{-3}$. Extrapolating the observed $E^{-1}$ differential proton spectrum from 35 keV to 10 keV would increase the energetic proton energy density by a factor 3.6. The fact that the energetic proton energy density was comparable to that of the plasma and magnetic field upstream of the shock suggests that energetic protons played a significant role in the overall structure of the shock.

The 3.16 kHz ion acoustic wave amplitudes maximized at the shock and then

dropped suddenly. The amplitude of 17.8 Hz whistler mode magnetic turbulence, which was near threshold upstream, increased suddenly and gradually returned to threshold 18 hours later. The amplitudes of 0.1 - 1 kHz electric fields (not shown), which were also near threshold upstream, jumped suddenly at the shock and persisted for many hours downstream (Kennel et al., 1982). The 50 kHz electric field voltage jumped at the shock and only returned to the preshock level after 1600 UT. Persistent enhancements of broadband low-frequency turbulence, 0.1 - 1 kHz electric field turbulence, and electric field noise above the plasma frequency (some tens of kHz in the downstream region), are characteristic features of the flow downstream of interplanetary shocks (Kennel et al., 1982; Hoang et al., 1980). Grigorieva and Slysh (1970), Meyer-Vernet (1979), and Hoang et al. (1980) interpret the high-frequency electric field continuum as due to enhanced thermal electron plasma wave fluctuations.

The count rate of 30-36 keV/Q Helium ions, which had hovered slightly above threshold at the shock, jumped by a factor 40 at the shock and gradually returned to threshold over the next 18 hours. The 35-56 keV proton intensity rose to $10^3$ $cm^{-2}$-$s^{-1}$-$sr^{-1}$-$keV^{-1}$ at the shock. Note the secondary peak, which is the absolute maximum, about two hours behind the shock. This peak appears to be associated with a local minimum in the post-shock solar wind speed and, possibly, with two magnetic neutral sheets which passed over ISEE-3 about when the 35-56 proton intensity maximized. After the maximum, the 35-56 keV proton flux remained more or less constant until about 1300 UT on November 12, at which time it commenced a more rapid decline and dropped suddenly near 1715 UT.

The flare ejecta arrived at about 1715 UT, at which time the solar wind proton temperature decreased, and the electron temperature diminished to

$4 \times 10^{6}$° K, and the thermal plasma was enriched in α-particles (Bame et al., 1981). This general behavior persisted until about 0200 UT on the next day, November 13, 1978. Strong bi-directional electron streaming observed at energies exceeding 80 eV was coincident with the arrival of the flare ejecta at ISEE-3 (Bame et al., 1981). The energetic protons, E > 35 keV, also exhibited bi-directional streaming at this time (Sanderson et al., 1981). Bame et al. (1981) argued that their data were best explained if the local interplanetary magnetic field were part of either a magnetic bottle rooted at the sun or a disconnected loop propagating outward. We will suggest that the shock propagated over several magnetic bubbles before it arrived at ISEE-3, since several magnetic neutral regions were detected in the post-shock flow, and was in another bubble when it encountered ISEE-3. The low time resolution interplanetary field data shown in Figure 1 has a number of depressions in magnetic field strength downstream of the shock, many of which, higher resolution data will indicate, were neutral sheet crossings.

## 4. SHOCK GEOMETRY AND DOWNSTREAM MAGNETIC STRUCTURE

### 4.1 Upstream Interplanetary Field

This paper will concentrate on the period 1800-0028 UT, when ISEE-3 was upstream of the oncoming shock, the 35-56 keV proton intensity increased by a factor 200, and, as we shall see, there was considerable activity in solar wind electrons, ion acoustic waves, and low-frequency magnetohydrodynamic waves. The average properties of the interplanetary magnetic field (IMF), however, remained relatively constant. The magnetic field strength at ISEE-3 was about 7$\gamma$ from 1800 UT on November 11, and was directed about 20° south of the ecliptic after 1840, until the shock. The IMF was approximately contained in the $(B_X,B_Z)$ plane that is perpendicular to the ecliptic and contains the sun. The average IMF measured at ISEE-1 had roughly the same magnitude, and was approximately parallel to that at ISEE-3 from 1820 UT, when ISEE-1 exited the earth's bow shock, until its 0058 UT interplanetary shock encounter.

The stability of the IMF prior to shock encounter provided Greenstadt et al. (1982) with a good opportunity to reconstruct the magnetic field lines near ISEE-3 from a time-series of individual vector measurements for the period after 2200 UT until the interplanetary shock encounter. They concluded that the field lines at ISEE-3 passed about 60 $R_E$ north of the ecliptic at earth during the entire time period, suggesting that ISEE-3 was not magnetically connected to the earth's bow shock. We note that the IMF lacked a significant "gardenhose" component throughout the interval after 1840 UT that ISEE-3 was able to observe the region upstream of the interplanetary shock without confusion from effects associated with the earth's bow shock.

## 4.2 Shock Encounter

Figure 2 shows eight minutes of high-resolution magnetic field data surrounding the ISEE-3 (top panel) and ISEE-1 (bottom panel) shock encounters at 0028 and 0058 UT, respectively. The magnitude of the magnetic field, $|B|$, jumps at the shock by the same factor of 2.2 at each spacecraft. The ISEE-3 upstream and downstream plasma number densities are $n_1 \approx 3$ cm$^{-3}$, $n_2 \approx 10$ cm$^{-3}$, and the corresponding flow speeds and proton temperatures are $V_1 = 375$ km-s$^{-1}$, $V_2 = 575$ km-s$^{-1}$, and $T_{p_1} = 3\times10^{4\circ}$ K, $T_{p_2} = 10^{6\circ}$ K, respectively (Bame et al., 1981). From the ISEE-3 data presented in this paper, we find the magnetic field strengths are $B_1 = 7.5\gamma$, $B_2 = 16.5\gamma$; the magnetic field components will be presented in Figure 5. The average electron temperatures, summing over core and halo components, were $T_{e_1} = 2.5\times10^{5\circ}$ K and $T_{e_2} = 4.5\times10^{5\circ}$ K. Since halo electrons may free stream through the shock, it may be more appropriate to consider the core electron temperatures, which were $T_{c_1} \approx 1.2\times10^{5\circ}$ K and $T_{c_2} \approx 2.5\times10^{5\circ}$ K. The solar wind accelerated downstream of the shock and reached a peak speed approaching 800 km-s$^{-1}$ one-half to one hour after the shock encounter.

If this interplanetary shock originated in a 2N flare observed near the central meridian of the sun at 0100 UT on November 10, 1978, the average shock velocity was 880 km-s$^{-1}$ (Reinhard et al., 1981). The 30-minute delay between the ISEE-3 and ISEE-1 shock encounters indicates that the shock speed was about 700 km-s$^{-1}$ near the earth.

We have calculated shock normals using four different techniques: (1) Using coplanarity across the shock at ISEE-1; (2) using coplanarity at ISEE-3; (3) using three-dimensional solar wind data in the mixed mode method of Abraham-Schrauner and Yun (1976); and (4) taking the cross-product of the field jumps observed at ISEE-1 and -3 in various combinations (the double

delta B technique). The results using method (3) using 2-dimensional data, which were reported by Kennel et al. (1982), will be amended here. The shock solutions from these four techniques are presented in Table 2. The first column in Table 2 shows the components of the shock normal $\vec{n}$ in GSM coordinates; the second column shows the components of the magnetic field vector $\vec{B}$; and the third column shows the shock normal $\theta_{Bn} = \cos^{-1} \vec{n}\cdot\vec{B}/|B|$. The double delta B row contains three entries in the last two columns, corresponding to various estimates of the upstream magnetic field at ISEE-1 and -3.

All four techniques give similar shock normals and indicate that $\theta_{Bn}$ was roughly 40°. Using method (3), we have determined that the component of the shock velocity normal to the shock was 609 km-s$^{-1}$. For the upstream parameters in the first paragraph of this section, the ratio $\beta_e$, of the electron pressure, based upon the average electron temperature, to the magnetic pressure was 0.54. The thermal proton $\beta_p$ was about 0.065. For a total upstream $\beta_e + \beta_p$ of 0.55, solution of the Rankine-Hugoniot relations indicates that a fast Mach number $M_F$ of 2.6 is necessary to give a jump in field strength of 3.2 in the shock plane and a jump of 2.2 in the total field, approximately what was observed. Thus, the interplanetary shock of November 12, 1978 was of moderate strength, with $\theta_{BN}$ near the $Q_{\parallel} - Q_{\perp}$ transition (Greenstadt and Fredricks, 1979).

The shock normal and Rankine-Hugoniot solutions in this paper and, to our knowledge, all others in the literature to date do not take into account the effects of energetic ions, whose $\beta$ was close to unity and possibly exceeded that of the plasma just upstream of the November 12, 1978 shock. These solutions are, strictly speaking, for the local subshock. The full Rankine-Hugoniot conditions should be taken between the points about a half-hour upstream where the energetic protons began to increase rapidly in intensity and a point well downstream of the subshock.

Figures 3a and 3b sketch the geometry of the shock at the moment it passed over ISEE-3 at 0028 UT on November 12, 1978. We used the method (3) shock normal solution discussed above and ISEE-1 and -3 interplanetary field data. Taken by itself, the X-Y projection (Figure 3b) might suggest that both ISEE-1 and ISEE-3 could have been connected simultaneously to the interplanetary shock and the bow shock, because the $B_Y$-component was nearly zero. However, the X-Z projection (Figure 3a) suggests that the IMF had a southward component that would cause the ISEE-3 field line to miss the bow shock in the absence of significant field line curvature between ISEE-3 and the bow shock, as Greenstadt et al. (1982) argued. The fact that the simultaneously-measured ISEE-1 and -3 magnetic fields were more or less parallel suggests that such curvature was indeed absent at the time of ISEE-3 encounter. The fields at ISEE-1 and -3 were approximately parallel from at least 2100 UT on November 11, 1978 until the shock was encountered at each spacecraft. A time projection of the ISEE-3 magnetic field line indicates that it missed the bow shock throughout this period (Greenstadt et al., 1982); however, it is likely that ISEE-1 was connected to both shocks. The uniformity of the IMF indicates that the structure in the interplanetary field had a spatial scale exceeding the 200 $R_E$ that separate ISEE-1 and ISEE-3.

TABLE 2

| Technique | Normal | | | Upstream B(γ) | | | $\theta_{BN}$ |
|---|---|---|---|---|---|---|---|
| | $n_X$ | $n_Y$ | $n_Z$ | $B_X$ | $B_Y$ | $B_Z$ | |
| ISEE-1 Co-planarity | -.966, | .043, | -.256 | 6.13, | 0.31, | -3.05 | 41.6 |
| ISEE-3 Co-planarity | -.942, | .298, | -.152 | 5.97, | -1.07, | -2.82 | 34.9 |
| ISEE-3 Mixed Mode | -.966, | .073, | -.247 | 6.40, | -0.99, | -3.23 | 41.0 |
| Double Delta B | -.954, | .104, | -.279 | 6.13, | 0.31, | -3.05 | 43.5° |
| | | | | 5.97, | -1.07, | -2.82 | 41.3° |
| | | | | 6.40, | -0.99, | -3.23 | 42.8° |

## 4.3 Properties of MHD Waves Near the Shock

Tsurutani et al. (1983) have studied the polarizations of the magnetic field oscillations measured by ISEE-3 in association with the November 11-12, 1978 shock event. We summarize their conclusions here. Large-amplitude compressional waves with about 7-second periods are apparent just ahead of the shock in the top panel of Figure 2. The waves between 0026:20 and 0027 UT were found to be elliptically polarized. A minimum variance analysis showed that the angle $\theta_{KB}$ between the wave propagation vector $\hat{K}$ and the local average magnetic field direction $\hat{B}$ was 7°. The $B_Y$-component in the top panel of Figure 2 revealed shorter-period (3 sec) waves of even larger amplitude just downstream of the shock. The waves measured between 0028:19 and 0028:30 UT were right-hand elliptically polarized with $\theta_{KB}$ = 12°. 20-second quasi-periodic waves occur in the interval 0029:20 - 0031 UT; these waves were non-compressive, predominantly right-hand elliptically polarized with $\theta_{KB}$ = 5°. Thus, in all three cases, the waves near the shock propagated essentially parallel to the local magnetic field.

## 4.4 Rotational Discontinuity

As Figure 2 shows, the shock initiated a period of intense magnetic oscillations that was terminated by a strong rotational discontinuity six to seven minutes later observed at both spacecraft. The discontinuity rotated the average IMF from the X-Z plane configuration that had prevailed for the previous six hours to an "anti-gardenhose" configuration in the X-Y plane.

Figure 4 shows two components of the electric field and three components of the IMF measured at ISEE-1 between 0050 UT and 0115 UT, a period which contains the shock at 0058 UT and the rotational discontinuity at 0105 UT. These electric field components are accurate to about ± 1 mV/m, and the third component may be estimated assuming $\vec{E}\cdot\vec{B} = 0$. We have verified that these electric fields are consistent with the solar wind speed measured upstream of the shock. The general anticorrelation of $E_Y$ and $B_Z$ is consistent with an MHD flow in the -X direction, and a strong rotation of the electric field is apparent at the magnetic discontinuity. Note the partial re-entry into the state upstream of the rotational discontinuity at about 0108 UT.

The large-amplitude magnetic oscillations in Figure 2, which Figure 4 shows were essentially linearly polarized, were concentrated between the shock and the rotational discontinuity.

## 4.5 Downstream Neutral Regions

ISEE-3 and ISEE-1 each encountered a succession of magnetic neutral sheets downstream of the shock. Figure 5 shows the first of these, which followed 26 and 24 minutes after the shock passed over ISEE-3 and -1, respectively. The top four panels show three components and the magnitude of the IMF measured at ISEE-3, and the bottom panel shows the IMF magnitude at ISEE-1. The IMF magnitude reached a minimum of less than 1$\gamma$ at about 0054:20 at ISEE-3 and a minimum of about 2.5$\gamma$ at 0122:20 at ISEE-1. The 28-minute delay between the neutral sheet encounters is roughly consistent with the solar wind travel time between ISEE-3 and -1. The ISEE-1 neutral sheet encounter differed in one significant way from its ISEE-3 counterpart. The second panel down in Figure 5 indicates that at ISEE-3, the $B_Y$-component of the IMF changed sign, whereas at ISEE-1 our data (not shown) indicate that $B_Y$ dipped to zero and recovered back to its original positive value during the neutral sheet crossing.

Figure 6 shows the magnitude of the IMF for the next three partial neutral sheet encounters by ISEE-3, near 0114 UT, 0207 UT, and 0229 UT on November 12, 1978.

In summary, the interplanetary magnetic field was unusually configured during the entire November 11-12, 1978 shock event. From 1800 UT on November 11, six and one-half hours upstream of the shock until many hours downstream, the IMF acted as though it were not connected to the sun. The IMF was in the X-Z plane throughout the upstream period; a rotational discontinuity that followed the shock did create a non-zero $B_Y$, but it rotated the IMF into an anti-gardenhose sense, with both $B_X$ and $B_Y$ positive. These observations may have a simple explanation, for if ISEE-1 and -3 were near the general field reversal of the solar wind, one might expect neutral sheet dissipation to disconnect the IMF

from the sun, and there would be no reason for the disconnected field lines to be in the gardenhose configuration. The succession of neutral sheets that passed over ISEE-1 and -3 following the shock support this view and have an interesting implication. ISEE-3 and -1 may have detected a train of X and O-type neutral regions in the field reversal layer. The magnetic field surrounding an O-type neutral region will be essentially closed. Bame et al. (1981) associated one such closed region with the driver of the November 12, 1978 shock. The shock had evidently passed over several others before arriving at ISEE-3, as the succession of neutral sheets suggests. Furthermore, we will argue here that the shock was in the process of devouring another closed magnetic loop, which ISEE-3 and -1 entered two hours and one hour before their shock encounters, respectively.

## 5. UPSTREAM REGION: ISEE-3

Figure 7 shows model electron parameters derived from measurements made by the LANL/MPI solar wind electron detector for the period 1800 UT on November 11 to 0100 on November 12. These model parameters are defined, and their significance discussed, by Feldman et al. (1982). The top panel of Figure 7 shows the electron heat flux parallel to the magnetic field, the bulk of which is carried by "halo" electrons with energies of tens of eV. With the exception of a short interval near 1830 UT, this heat flux was directed away from the sun. The middle panel shows electron densities for the same time period; the upper curve shows the total density, and the bottom curve shows the density of the superthermal halo population. The bottom panel shows model electron temperatures, with the halo temperatures at the top, the core at the bottom, and the density-weighted average temperature inbetween. The temperatures have been shaded to indicate the thermal anisotropy; the top of each shaded graph is the parallel temperature, and the bottom is the perpendicular.

ISEE-3 was connected to the earth's bow shock for several hours prior to 1840 UT. The last portion of this period of connection is evident in the top panel of Figure 7, which shows that the heat flux fluctuated violently. The electron diagnostics became much more regular after 1840 UT and never fluctuated so violently again until the 0028 UT shock encounter. The total density (top curve, middle panel) rose to a local maximum of about 15 $cm^{-3}$ at 1930 UT, where Figure 1 indicates the 35-56 keV proton flux minimized, and settled to a plateau. The density dropped suddenly at 2100 UT, recovered somewhat, and then resumed its decline, which ended in a sudden drop at about 2220 UT. The density was constant from then until the shock encounter. The halo electron parallel temperature rose steadily from 2130 to 2230 UT and held more or less constant

until the shock. The core electron temperature rose gradually and then more rapidly between 2130 and 2230 UT; it, too, held constant from about 2230 UT until the shock encounter. The electron heat flux, which had been more or less constant since 1900 UT, diminished between 2200 and 2230 UT, and then remained constant until the shock.

The solar wind electron parameters displayed in Figure 7 all indicate that the solar wind entered a new state after 2230, in which the electron density and net heat flux were lower, and the electron temperature was higher, than before 2200 UT. Figure 8 displays refined halo electron parameters that help to diagnose the transition between these two states. The top panel shows the halo drift speed parallel to the magnetic field -- the first parallel velocity moment of the entire halo distribution. The halo drift speed was between 1500-2000 km/sec, directed away from the sun, between 1840 and 2100 UT; it dropped to less than 1000 km/sec and held roughly constant between 2230 UT and the shock at 0028 UT. To help define the source of the halo electrons, we consider the properties of those electrons streaming along the magnetic field toward and away from the sun separately. The partial density and parallel speed moments of the "away" and "toward" semi-distribution functions are displayed in the middle and bottom panels of Figure 8. The density of "away" electrons (top curve of middle panel) did <u>not</u> decrease, but increased somewhat, as the new solar wind region moved over ISEE-3. In addition, the "away" drift speed (top curve of bottom panel) also increased, so that the thermal flux carried by electrons streaming away from the sun was about a factor 2 larger after 2230 UT than before. On the other hand, the partial density and speed of the electrons streaming toward the sun (bottom curves of the middle and bottom panels), which were small prior to 2200 UT, both rose abruptly beginning about 2200 UT to values more nearly comparable with those of

the away electrons which remained constant between 2230 UT and the shock. The net heat flux and mean halo drift (top panels of Figures 7 and 8, respectively) did not decrease because the halo electrons streaming away from the sun and the oncoming interplanetary shock diminished in intensity, but because a new component of electrons streaming toward the sun was present after 2230 UT, and the halo electron distribution was more symmetrical.

Figure 9 diagnoses the transition between the two solar wind states identified above with higher time resolution. Its top panel shows the 35-56 keV proton flux between 2200 and 2300 UT; the middle panel displays the first parallel velocity moment of the 35-56 keV proton angular distribution, and the bottom panel presents the electric field spectral density of 3.16 kHz ion acoustic waves. Prior to 2220 UT, the 35-56 keV protons streaming velocity was directed away from the sun, and after 2230 UT, it was essentially zero, by which time the ion acoustic waves had increased in intensity. The 35-56 keV ions remained isotropic until about 2400 UT, at which time a significant streaming anisotropy away from the sun developed and increased until the shock encounter. The ion acoustic waves also increased in intensity between 2400 UT and the shock (see Figure 10). In contrast to the halo electrons, the 35-56 keV protons did not exhibit a bi-directional streaming, but tended toward isotropy between 2230 and 2400 UT.

The fluxes of halo electrons streaming toward the sun detected after 2230 UT can be interpreted in at least two ways. ISEE-3 could have been magnetically connected to the earth's bow shock after 2230 UT and thus have detected bow-shock electrons, or ISEE-3 could have entered a closed magnetic loop at 2230 UT that intersected the interplanetary shock at both ends. In the second case, one might expect ISEE-3 to detect stronger fluxes streaming away from the point of nearer connection and weaker fluxes appearing to stream toward the sun that were generated at the point of further connection and followed a long path around the closed

field to reach ISEE-3. Although electron data alone might not distinguish between these two alternatives, we believe the balance of evidence favors the second. The data from the period before 1840 UT, when ISEE-3 was definitely sporadically connected to earth, differed in internal character from that after 2230 UT. The electron heat flux parameters fluctuated violently, and the heat flux intermittently reversed sign, prior to 1840 UT; the > 35 keV protons also had a streaming anisotropy away from earth prior to 1725 UT. On the other hand, the electron parameters were stable, and a sunward proton anisotropy was absent, after 2230 UT. We will present further arguments supporting the magnetic loop hypothesis later.

Figure 10 shows four hours of 3.16 kHz electric field data (top panel) and the rms average (.01-3 Hz) interplanetary field fluctuation amplitude surrounding the ISEE-3 shock encounter (bottom two panels). Shown are the Y and Z-components of the rms fluctuation amplitude; we have shaded the periods when the squared rms deviation exceeded 0.1 to guide the eye. The 3.16 kHz electric field and the low-frequency magnetic field fluctuations appear to track one another; bursts of ion acoustic noise near 2140 UT and 2200 UT were accompanied by bursts of hydromagnetic waves. There is a definite change of character after about 2230 UT, which we have denoted by a vertical line connecting all three panels; the times of the shock, field rotation, and first neutral sheet encounter are indicated in similar fashion. After 2230 UT, the ion acoustic and magneto-hydrodynamic wave amplitudes remained intense and nearly constant until 2400 UT. The ion acoustic amplitudes increased between 2400 UT and the shock encounter, during which time the 35-56 keV protons increased in intensity and again had a significant streaming anisotropy away from the oncoming shock. The rms interplanetary field amplitudes, at best, increased only slightly during this last half hour before shock encounter.

We have made a rough determination of the frequency dependencies of the polarization and amplitude of the MHD turbulence that was observed during the last 16 minutes prior to shock encounter. Figure 11 presents our results for the period 0012-0028 UT (solid line), and also for the shorter period 0025:30-0027 UT, immediately upstream of the shock. All the data have binned into factor 2 intervals of spacecraft frame frequency. Starting from the top, the panels in Figure 11 present the frequency dependencies of (1) the angle $\theta_{KB}$ between the wave propagation vector, $\vec{K}$, and the IMF, $\vec{B}$; (2) the ellipticity and sense of rotation of the polarization in the spacecraft frame; (3) the percent polarization; and (4) the total rms amplitude $<(\delta\vec{B}\cdot\delta\vec{B})^{\frac{1}{2}}>$ and the rms compressional amplitude $<(\delta B^2_T)^{\frac{1}{2}}>$, both normalized to the interplanetary field magnitude. The proton gyrofrequency based upon the measured magnetic field strength of ~ 7.5$\gamma$ was roughly 0.12 Hz; the maximum Doppler-shift frequency $KV/2\pi$ for $KR_I = 1$, where $R_I$ is the thermal proton Larmor radius based upon the measured upstream proton temperature, $7p_1 = 3\times10^{4\circ}$ K, and flow speed, 370 km-s$^{-1}$, was roughly 1.5 Hz.

Figure 11 indicates that the total rms amplitude was concentrated between 0.01 and 0.16 Hz and reached a peak normalized amplitude of 0.16 between 0.02 and 0.08 Hz. Thus, the MHD turbulence had frequencies below the local proton cyclotron frequency and, since the power diminished above 0.16 Hz, wavelengths that were considerably larger than the thermal ion Larmor radius. The waves propagated at about 20° to the magnetic field between 0.01 and 0.16 Hz, and, in keeping with this fact, their rms compressional power was much smaller than their total rms power in this frequency band. The waves were weakly, predominantly left hand elliptically polarized in the spacecraft frame.

Figure 12 compares the properties of 35-1600 keV protons (top two panels) with the fluctuating $B_Z$-component of the .01-3 Hz interplanetary field from 2100 UT on November 11 to 0100 UT on November 12, 1978. The arrivals of the bubble, the shock, and the rotational discontinuity at ISEE-3 are indicated by the vertical lines that connect all three panels. The top panel shows proton intensities for eight channels, labeled as follows: 1 (35-56 keV), 2 (56-91), 3 (91-147), 4 (147-237), 5 (237-383), 6 (383-619), 7 (619-1000), and 8 (1000-1600 keV). The middle panel shows the effective energy power law spectral index obtained from the ratios of the differential energy fluxes in channels 1 and 2 (bottom trace), 3 and 4 (second from bottom), 5 and 6 (second from top), and 7 and 8 (top). The proton intensities increased upstream of the shock at all energies. Even the 1-1.6 MeV proton intensities increased by a factor 3 during the 4½ hours prior to shock encounter. However, only the lowest energy channels, 1, 2, and 3, responded significantly to the arrival of the bubble. The proton intensities in channels 1, 2, and 3, which dipped about 2200 UT, rose prior to 2230 UT and reached a plateau inside the bubble. They diminished somewhat near 2320 UT and then began their rapid rise as the shock approached. The intensification was most pronounced at the lowest energy. The approach of a shock which is accelerating protons is evident in the spectral index plots in the middle panel. The spectral index determined from the lowest-energy channels actually turned negative, indicating that the peak of the energy distribution was above 56 keV, at 2320, before rising to its post-shock value of about 1.3. Scholer et al. (1983) have shown that the energetic proton e-folding distance was roughly proportional to the square root of the particle energy upstream of the November 12, 1978 shock, so that the negative spectral index in Figure 12 may signify the prior arrival of a diffusion front at energies above 56 keV.

## 6. UPSTREAM REGION: ISEE-1

Figure 13 displays the Swept-Frequency-Receiver (SFR) plasma wave electric field measurements made on ISEE-1 between 1800 UT on November 11, 1978 and 0200 UT on November 12, 1978. ISEE-1 entered the solar wind at approximately 1840 UT, at which point the intense low-frequency waves ($f < 2$ kHz) characteristic of the magnetosheath diminished in intensity. As it crossed the bow shock, ISEE-1 began to detect 40-50 kHz electron plasma oscillations which persisted without significant interruption until the interplanetary shock encounter at 0058 UT. The frequency of the electron plasma waves decreased throughout this period, in keeping with the general decline of electron density found after 1930 UT by ISEE-3. However, the more rapid decline in density that began abruptly at 2100 UT at ISEE-3 appears to have been delayed by an hour or more at ISEE-1. These plasma waves, which were probably generated by energetic electrons escaping from the bow shock (Anderson, 1968; Anderson et al., 1979; Feldman et al., 1982), were not detected at ISEE-3. Thus, while ISEE-1 may well have been connected to the earth's bow shock prior to the interplanetary shock encounter, these results again suggest that ISEE-3 was not.

The 500 Hz - 5 kHz ion acoustic amplitudes at ISEE-1 increased at about 2300 UT, approximately two hours before shock encounter. If they had been generated by particles escaping from the earth's bow shock, one might have expected them to have been present between the bow shock exit and the interplanetary shock encounter, for the average IMF did not change its direction significantly during most of this period. In fact, ion acoustic waves were much less intense between 2000 UT and 2300 UT, suggesting that the increase in intensity after 2300 UT was related to the approach of the interplanetary shock.

Let us suppose that ISEE-3 entered a closed magnetic bubble at 2300 UT.

The leading edge of the bubble -- the separatrix between "open" and "closed" field lines -- should propagate at the solar wind speed ahead of the shock, ~ 370 km/sec. One would thus expect ISEE-1 to enter the bubble about an hour later than ISEE-3. Figure 14 compares the rms fluctuation amplitudes of the total ($B_T$) and Y-component ($B_Y$) of the interplanetary field measured at ISEE-1 and -3 aligned in time according to the shock encounter. The estimated times of arrival of the bubble at ISEE-1 and ISEE-3 are indicated by an arrow. While the hydromagnetic wave activity is sporadic prior to the bubble arrival at each spacecraft, the rms amplitudes increased at 2230 (ISEE-3) and 2330 (ISEE-1) and remained enhanced until the shock encounters.

Figure 15 presents ISEE-1 data for the period 2200-0200 UT that diagnoses further the arrival of the bubble at ISEE-1. The top two panels show 1 kHz and 1.78 kHz electric field amplitudes; the middle panel shows the rms $B_Z$ interplanetary field amplitude; and the bottom panels show the fluxes of 2 and 6 keV protons measured along the spin axis of the ISEE-1 spacecraft. Prior to 2330 UT, sporadic bursts of 2 and 6 keV protons, magnetohydrodynamic waves, and ion acoustic waves accompany one another. The change in solar wind state at 2330 UT is strikingly apparent in the proton fluxes, which increase abruptly and remain enhanced -- albeit with violent fluctuations -- until the shock encounter.

The onset of the magnetic turbulence appears to have been rather sudden at the times of bubble arrival at ISEE-1 and -3. Figure 16 compares high resolution measurements of the interplanetary field for 12 minutes surrounding 2230 UT at ISEE-3 (top curves in each panel) and 2325 UT at ISEE-1 (bottom curves in each panel). The ISEE-3 amplitude scales are to the left of each panel, and the ISEE-1 are to the right. A clear onset is apparent in each data set; the waves appear to have 15 to 20-second periods and to be largely transversely polarized, similar to the hydromagnetic waves upstream of the

earth's bow shock. Since such magnetohydrodynamic waves propagate within about 100 km/sec of the solar wind speed, the sudden onsets of wave turbulence suggest that the waves, and the particles responsible for their generation, were already present in the bubble before it moved over each spacecraft. Figure 15 seems to support this conclusion.

## 7. ORIGIN OF UPSTREAM ELECTROSTATIC WAVES

Figure 17 presents ISEE-1 (bottom two panels) and ISEE-2 (top two panels) 6 keV proton fluxes and the Z-component of the IMF for the period 2324-2336 UT surrounding the passage of the closed magnetic field bubble over the two spacecraft. The 6 keV proton fluxes exhibited factor 100 modulations whose time scales were comparable with the periods of the hydromagnetic waves. A similar modulation was observed at 2 keV. The five vertical lines, which have been drawn in to guide the eye, indicate that the 6 keV proton fluxes peaked when $B_Z$ approached zero. The proton detectors are sensitive to a narrow cone of particle arrival angles centered along the spin axes of the two spacecraft, which in turn are very nearly perpendicular to the $(B_X,B_Y)$ plane. Therefore, when $B_Z$ neared zero, 90° pitch-angle protons were being detected. We therefore conclude that the 2 and 6 keV protons were highly anisotropic, with a strong peak near 90° pitch angle. Similar modulations of the 6 keV proton flux were detected sporadically but continually from the entry of ISEE-1 and -2 into the bubble near 2330 UT until the shock encounter at 0058 UT.

ISEE-2 was about 4000 km upstream of ISEE-1 at the time the measurements displayed in Figure 17 were taken. The ISEE-1 and -2 data were offset by 12 seconds -- about the solar wind travel time between the two spacecraft, based on a speed of 370 km/sec -- to show the correspondence between the peaks in proton flux and $B_Z$ at ISEE-1 and -2. These data suggest that the anisotropic 6 keV protons and hydromagnetic waves were convected downstream at about the solar wind speed between the two spacecraft.

The very strong electron heat flux in the region upstream of the shock (Figure 7), which is carried by halo electrons, would lead to a strong electrical

current unless the core electrons also had a net drift relative to the ions that neutralizes the heat current. The top two panels in Figure 18 plot the measured model parameters $(N_H/N)V_{DH}$ and $(N_C/N)V_{DC}$, where $V_{DH}$ and $V_{DC}$ are the halo and core drift velocities parallel to the magnetic field, respectively. The extent to which the two panels are mirror-symmetric indicates the degree of current neutrality. We note that the cold electrons drifted with respect to the ions with a speed of about 200 km/sec between 2230 UT and the shock.

The bottom panel shows 328-sec average 1.78 kHz electric fields (bar graph), and the peak amplitudes (individual points) detected during each 328-second interval. The 1.78 kHz ion acoustic waves were similar to those at 3.16 kHz (Figure 10) upstream of the shock. We have enough data to ask whether these waves were due to the ion acoustic heat flux instability (Forslund, 1970). For the measured core electron temperature (Figure 7) and Bame et al's (1981) reported temperatures, the calculations of Kindel and Kennel (1971) indicate that a core electron drift of 200 km/sec will be stable to ion acoustic waves. We conclude, therefore, that the upstream ion acoustic waves may have been thermal fluctuations that were enhanced when the core electron drift increased. On the other hand, a drift of 200 km/sec is close to the instability threshold of electrostatic ion cyclotron waves. This suggests that the highly anisotropic 6 keV protons in Figure 17 may have been generated by a solar wind analog of the process that accelerates auroral ions perpendicular to the magnetic field to form "conic" distributions (Okuda and Ashour-Abdalla, 1982; Ashour-Abdalla and Okuda, 1982). We also note that the 200 km-$s^{-1}$ drift also exceeds the Alfvén speed, which was about 100 km-$s^{-1}$, so that the electromagnetic ion cyclotron wave might also be unstable to the electron heat flux (Forslund, 1970).

# 8. OBSERVATIONAL TESTS OF THEORY

## 8.1 Introductory Remarks

In this chapter, we use the data we have assembled to test some of the theoretical predictions discussed in Section 1.2. In Section 8.2 we compare the properties of the energetic particles upstream of the November 11-12, 1978 shock with theory. We discuss the electromagnetic waves upstream of the shock in Section 8.3. In Section 8.4, we briefly consider the question of the energetic particle effects on shock structure, and in Section 8.5 we compare observations and theory of the state downstream of the plasma shock.

## 8.2 Energetic Particles Upstream

The theory of first-order Fermi acceleration makes the following broad predictions about the behavior of ions whose energies exceed a certain threshold of about 10 keV:

- The energetic proton distribution upstream should increase essentially exponentially leading up to the shock. The exponential scale length can be calculated using a self-consistent model of the generation of MHD waves by the energetic particles.
- The energetic protons upstream should be essentially isotropic in the frame of the shock. The anisotropy in the solar wind frame provides the free energy for wave growth.
- The energetic proton momentum distribution should be a power law whose spectral index $\beta$ is given by $\beta^{-1} = 1/3(1 - V_2/V_1)$, where $V_1$ and $V_2$ are the solar wind velocity components perpendicular to the shock plane upstream and downstream, respectively.
- The power law should prevail between a lower limit momentum, determined by shock injection processes, and an upper limit, set by the condition that the momentum diffusion time be less than the shock connection time.

The four points above have been considered in detail by Lee (1983) and Scholer *et al.* (1983) for the shock of November 11-12, 1978. We will paraphrase Lee's (1983) discussion of them so that the reader may have a more complete perspective on the physics of this shock.

Scholer *et al.* (1983) found that protons upstream between 15-150 keV increased exponentially with a scale length that depends upon the square root of the particle energy. Lee (1983) derives the following expression for the

scale length at the shock:

$$L_s = \frac{\beta(\beta-2)\, B^2 \cos\theta_{BN}}{24\pi^3\, V_A |\Omega_p| M_p^4} \left[f_p(30\ \text{keV})\right]^{-1} (V_{30})^{-3} \left(\frac{V}{V_{30}}\right)^{\beta-3}, \qquad (8.1)$$

where $\beta$ is the momentum spectral index, $V_A$ is the Alfven speed, $\Omega_p$ is the proton cyclotron frequency, $M_p$ is the proton mass, $f_p(E)$ is the omnidirectional proton momentum distribution function at the energy E, and $V_{30} = 2.4\times10^8$ cm-s$^{-1}$ is the speed of a 30 keV proton. According to Scholer et al. (1983), $\beta = 4.1$ and $f_p(30\ \text{keV}) = 3\times10^{-24}$ s$^3$ cm$^{-6}$. Upstream of the shock, we find $B = 7.5\gamma$ and $N = 3$ cm$^{-3}$ (Bame et al., 1981), so that $V_A = 100$ km-s$^{-1}$. We choose $\theta_{BN} = 40°$, in keeping with the revised Rankine-Hugoniot solutions in Section 4.2. Substituting these values into (8.1), we obtain $L_s(30\ \text{keV}) = 1.2\times10^{10}$ cm, about a factor 2 smaller than the measured value, $L_s(30\ \text{keV}) = 2.6\times10^{10}$ cm (Scholer et al., 1983).

Scholer et al. (1983) did find that the upstream energetic proton distribution was approximately isotropic in the shock frame. We agree with this conclusion for the 30-minute period before the shock crossing to which Lee's (1983) theory primarily applies. The matter of the upstream and downstream proton spectra has been discussed by Sanderson et al. (1981) and Scholer et al. (1983), and the exact form of the distribution function may be subject to some revision. Scholer et al. (1983), in an attempt to close with theory, fit the momentum distribution with a power law of spectral index $\beta = 4.1$. Our measured compression of the components of the interplanetary field tangential to the shock, 3.2, agrees with the observed density compression of about 3 and implies $V_2/V_1 = 1/3.2$. Inserting this value into the theoretical expression above leads to $\beta = 4.36$, in excellent agreement with the observational estimate. Note that we used the compression ratio of the plasma subshock and not the (slightly)

larger ratio that would apply to the full plasma shock-energetic particle foreshock system.

By setting the characteristic acceleration time equal to the solar wind travel time from the sun, Lee (1983) finds that the power law spectrum should extend up to about 200 keV/nucleon, in rough agreement with observation.

## 8.3 MHD Waves Upstream

Lee's (1983) self-consistent theory makes the following predictions concerning the MHD waves upstream of a quasi-parallel shock:

- Electromagnetic ion cyclotron waves should be generated by resonant cyclotron interactions with the energetic particle distribution.
- The wave spectrum should peak at a frequency that resonates with the lowest energy particle that participates in the Fermi process and fall to the ambient solar wind background above that frequency.
- The waves upstream of interplanetary shocks should be more nearly unpolarized than those in the earth's foreshock.
- Given the energetic particle distribution at one energy at the shock, the spatial and spectral distribution of the wave amplitude may be determined self-consistently.

Lee's (1983) theory was restricted to electromagnetic waves that propagate parallel to the ambient magnetic field. However, Tsurutani *et al.* (1983) and we find that the waves near the November 11-12, 1978 shock did propagate almost parallel to the magnetic field. Moreover, the waves upstream of interplanetary shocks show a smaller polarization than those in the earth's foreshock.

Let us now estimate the frequency of the waves that resonate with an energetic proton whose velocity parallel to the magnetic field is $V_R$ in the solar wind frame. The cyclotron resonance condition is approximately $|V_R| \approx |\Omega_p/K_{||}|$, where $K_{||}$ is the parallel wave number. Since the phase velocity is much less than the solar wind speed, the frequency f observed

in the spacecraft frame will be bounded by

$$f \leq \frac{K_{\parallel} V}{2\pi} \approx f_{ci}(V/V_R), \qquad (8.2)$$

where V is the solar wind speed and $f_{ci}$ is the proton cyclotron frequency in Hz. For B = 7.5γ as observed, $f_{ci}$ = 0.12 Hz. The lowest-energy particle that can escape upstream of the shock will have a speed of about $V_{SH} \approx 700$ km-s$^{-1}$ in the spacecraft frame. It seems reasonable to assume that the shock injects particles at about twice this speed, 1400 km-s$^{-1}$, corresponding to 10 keV energy in the spacecraft frame, since the observed particle spatial profiles are smooth above 10 keV (see Scholer et al., 1983, and our Figure 12), whereas they are much more irregular below 10 keV (Figure 15). For V = 350 km-s$^{-1}$, $V_R$ is 1150 km-s$^{-1}$, and (8.2) indicates that the turbulent magnetic field spectrum should peak near $f \approx f_{ci}/3 \approx 0.04$ Hz, or correspondingly down to a wave period of 25 seconds. Figures 14 and 16 reveal considerable power at about 25-second periods when the closed magnetic field bubble sweeps over ISEE-1, -2, and -3, and this general behavior persists until the shock. Figure 10 indicated that the spectrum peaked between 0.02 and 0.08 Hz, near the shock. We note that the 0.01-3 Hz magnetic field variances in Figures 9, 10, 12, and 13 captured the peak of the wave-spectrum, though they do not contain the wave power at periods exceeding 100 seconds produced by protons above 160 keV energy.

Lee (1983) has estimated the rms amplitude of ion-excited waves at the shock front, normalized to that of the upstream interplanetary field, to be about 0.18. Referring to the ISEE-3 measurements (which are less likely to be contaminated by bow-shock effects) in Figure 11, we find that $|\delta B|_{rms}/B$ was about 0.14-0.16, in excellent agreement with theory. We

note that the MHD wave amplitudes do not increase monotonically approaching the shock, as theory suggests, but appear to fill the entire closed region more or less uniformly. Further analysis of the data and extension of the magnetic field rms amplitude data to lower frequencies will be needed to ascertain whether this observation really conflicts with the theory, which did not visualize the closed magnetic confinement geometry in which the November 11-12, 1978 shock was found.

## 8.4 Effects of Energetic Ions Upon Shock Structure

The November 11-12, 1978 shock can be used to test two-fluid models of shock structure (Drury and Volk, 1981; Axford et al., 1982) because it satisfies the conditions of these theories. We presume that first-order Fermi-acceleration theory applies to the strong increase in energetic particle fluxes during the last half-hour before shock encounter (see Figure 12). This ramp had a scale small compared with that of the magnetic bubble, and so we can assume that the plasma subshock-energetic particle foreshock system was planar. However, significant energetic particle fluxes were contained by the closed field configuration upstream of the extended shock system. In a companion paper (Hada and Kennel, 1983), we will extend the above two-fluid shock theories to magnetohydrodynamics and compare the predicted energetic particle energy density at the shock with observations. We will find that the two-fluid magnetohydrodynamic theory overestimates the energetic particle pressure at the shock by a factor 2 - 3. Moreover, it is curious that the slight acceleration of the solar wind expected in such theories was not detected in the last half-hour before shock encounter.

## 8.5 Downstream Properties

The energetic particle distribution, according to theory, should not change at the shock, remain constant in space downstream, maintain the spectrum achieved at the shock, and be isotropic in the solar wind frame. Reinhard et al. (1981) and Scholer et al. (1983) have shown that the protons with 10's of keV energy were, in fact, isotropic in the solar wind frame downstream. Figures 1 and 12 indicate that the first three of these requirements were satisfied qualitatively by the November 11-12, 1978 shock (see, also, Reinhard et al., 1981). However, the particle intensity does respond to the passage of the rotational discontinuity seven minutes after the shock and maximizes about an hour downstream, and the spectrum softens somewhat well downstream of the shock.

Theories of $Q_{||}$ shock structure (Moiseev and Sagdeev, 1963; Kennel and Sagdeev, 1967; Auer and Volk, 1973) suggest that thermal anisotropy induced by shock compression should create a large-amplitude spectrum of downstream transverse electromagnetic waves by the resonant (or non-resonant) firehose instability. A numerical simulation by Kan and Swift (1983) indicates that firehose waves will be generated if the Alfvén Mach number of the shock exceeds about 2.5, a condition satisfied by the November 11-12, 1978 shock. Figure 2 reveals that large-amplitude waves ($\delta B_\gamma \sim 10\gamma$) existed between the shock and the field rotation seven minutes downstream. These appear to have about 10-sec periods and a polarization different from that of the waves upstream. Let us now estimate the wavelength of these waves. Let us assume that the observed frequency is given by $f = KV_2/(2\pi)$, where $V_2 \approx 650$ km/sec is the solar wind speed downstream of the shock. With $f \approx 0.1$ Hz, we find $K \approx 10^{-7}$ cm$^{-1}$. For the measured proton temperature of $1.0 \times 10^{6}$° K and a magnetic field of $16\gamma$,

the thermal proton Larmor radius $R_I$ is about $\sim 10^7$ cm, so that $KR_I \approx 1$. Thus, we conclude that the periods of the waves observed downstream are consistent with the resonant fireshose instability, whose growth rate peaks near $KR_I \approx 1$ (Kennel and Scarf, 1968).

## 8.6 Summary

The observations of the November 11-12, 1978 interplanetary shock discussed here by Lee (1983) and by Scholer et al. (1983) confirm the conceptual outlines of current theories of quasi-parallel shock structure and energetic particle structure. The spatial profiles, energy spectra, and angular anisotropies of the shock-associated energetic particles are in semi-quantitative accord with first-order Fermi-acceleration theory. The frequency and amplitudes of the low-frequency electromagnetic waves observed upstream of the shock again agree semi-quantitatively with a quasi-linear description of the resonant cyclotron interaction with energetic protons. Large-amplitude turbulence, whose wavelength is consistent with firehose instability, extended about 50 $R_E$ downstream of the shock.

It is not clear to what extent the observations of the November 11-12, 1978 shock are typical. First of all, even moderately strong quasi-parallel interplanetary shocks are relatively rare. Moreover, the November 11-12 shock appears to have been propagating in a closed magnetic field region when it encountered ISEE-1, -2, and -3. This certainly affected escape conditions for energetic particles. It does appear that at least the strongest part of the energetic proton shock was smaller than the magnetic confinement region, and so we used the data from the last half-hour before shock encounter to test theory. On the other hand, halo electrons probably had a longer scattering mean free path than energetic protons, and their distribution was quite different on open and closed field lines. Finally, the electron heat flux upstream of interplanetary shocks may be sensitive to shock parameters as well as geometry.

Certain aspects of the present study are incomplete. Not much is known about few kev "seed" particles upstream of interplanetary shocks, and although

we succeeded in detecting them, it requires very high time-resolution measurements to document how they emerge from the thermal distribution in the shock front. We suggested that these particles might have interacted with the electron heat flux via the ion cyclotron instability upstream of the November 11-12, 1978 shock, but we have no indication how common this effect might be. Our diagnosis of the turbulent state downstream of the shock lacks essential details, such as careful studies of the wave polarizations and thermal anisotropies. Such studies appear essential for quasi-parallel shocks, which, if they have extended regions of disturbance upstream, should also have them downstream.

Two aspects of the present study are puzzling. The MHD wave amplitudes did not build up in the last half-hour before the shock, when both the energetic particle fluxes and ion acoustic wave amplitudes increased significantly. The acceleration of the solar wind expected in the foreshock was not detected.

One question raised by the present study is unsettled: The role of the electrostatic and/or electromagnetic electron heat flux instabilities in the upstream region. Moreover, we note that our documentation of the wave modes present is incomplete. For example, we have not searched for the ~ 1 Hz waves that Sentman et al. (1983) find are due to energetic electrons escaping from the bow shock.

Clearly, the results of any case study have limited generalities. Given that shock structure depends sensitively on the shock parameters, and that quasi-parallel shocks are so thick that their properties can depend on their global configuration, systematic studies of many shocks are called for. We hope the results of this paper can usefully guide such studies.

## 9. CONCLUDING REMARKS

Although theoretical models of quasi-parallel shocks are over 20 years old, and although the suggestion that energetic particles are significant to shock structure is equally venerable, experimentalists could do little with these ideas until the past five years. The earth's foreshock had a complex phenomenology whose disorder had to be reduced before it could be fitted into a theoretical framework that had seemed peculiarly ill-adapted to bow-shock observations. Now, it is clear that quasi-parallel shocks have such an enormous spatial scale that interplanetary shocks are a better experimental arena to test theories of their structure. A coherent viewpoint is now emerging from the experimental and theoretical research of the past five years -- a viewpoint which this paper is based upon and largely substantiates. Only quasi-parallel shocks have the large regions of magnetohydrodynamic turbulence upstream and downstream that is an essential ingredient for first-order Fermi-acceleration of energetic particles. This fact is linked to the relative ease with which superthermal and energetic particles can stream through quasi-parallel shocks. It is clear that such particles generate the wave-fields that scatter them, and the outlines of a theory that will eventually predict the intensity and spectrum of shock-accelerated particles as a function of shock parameters are in view. That said, it is prudent to add two cautionary warnings. First, not much is known about the microstructure of quasi-parallel shocks, or even whether they have a microstructure. The current theoretical models are based on the interactions between particles and electromagnetic waves with wavelengths equal to or longer than a thermal ion Larmor radius. While it is conceivable that these physics could account both for the shock dissipation and energetic particle dissipation, it is not proven that it can

do so. Second, our experience with the earth's bow shock indicates that the shock structure is strongly parameter-dependent, and the picture of the large-scale quasi-parallel shock structure that has emerged from the two interplanetary shock studies completed to date might be misleading. It remains for future research to confirm, or to temper, our present enthusiasm.

Figure 1: Global View of the November 11-12, 1978 Shock Event

The eight panels in this figure show selected ISEE-3 data for the period 1800 UT on November 11, 1978, to 2400 UT on November 12, 1978. The top two panels present energetic ion measurements; the middle three, selected plasma wave observations; and the bottom three, the density, bulk velocity, and magnetic field in the solar wind. Several events are apparent in more than one diagnostic. For example, at 2230 UT, the solar wind plasma density drops, the 17.8 Hz whistler magnetic amplitudes and the 50 kHz thermal continuum amplitudes diminish; the 3.16 kHz ion acoustic electric field amplitudes increase, and the 35-56 keV proton intensity reaches a plateau. All these diagnostics indicate that the solar wind entered a new state after 2230 UT. The interplanetary shock, which encountered ISEE-3 at 0028 UT on November 12, is apparent in all the diagnostics. Note that the 35-56 keV proton intensity increased by more than an order of magnitude in the last half-hour before the shock encounter. The 35-56 keV proton intensity maximized approximately an hour downstream of the shock, in rough association with sporadic enhancements of the 50 kHz electron plasma wave continuum and a burst of ion acoustic waves. Note the sharp drop in 35-56 keV protor intensity at 1715 UT, which coincided with the arrival of the shock driver gas at ISEE-3 (Bame et al., 1981).

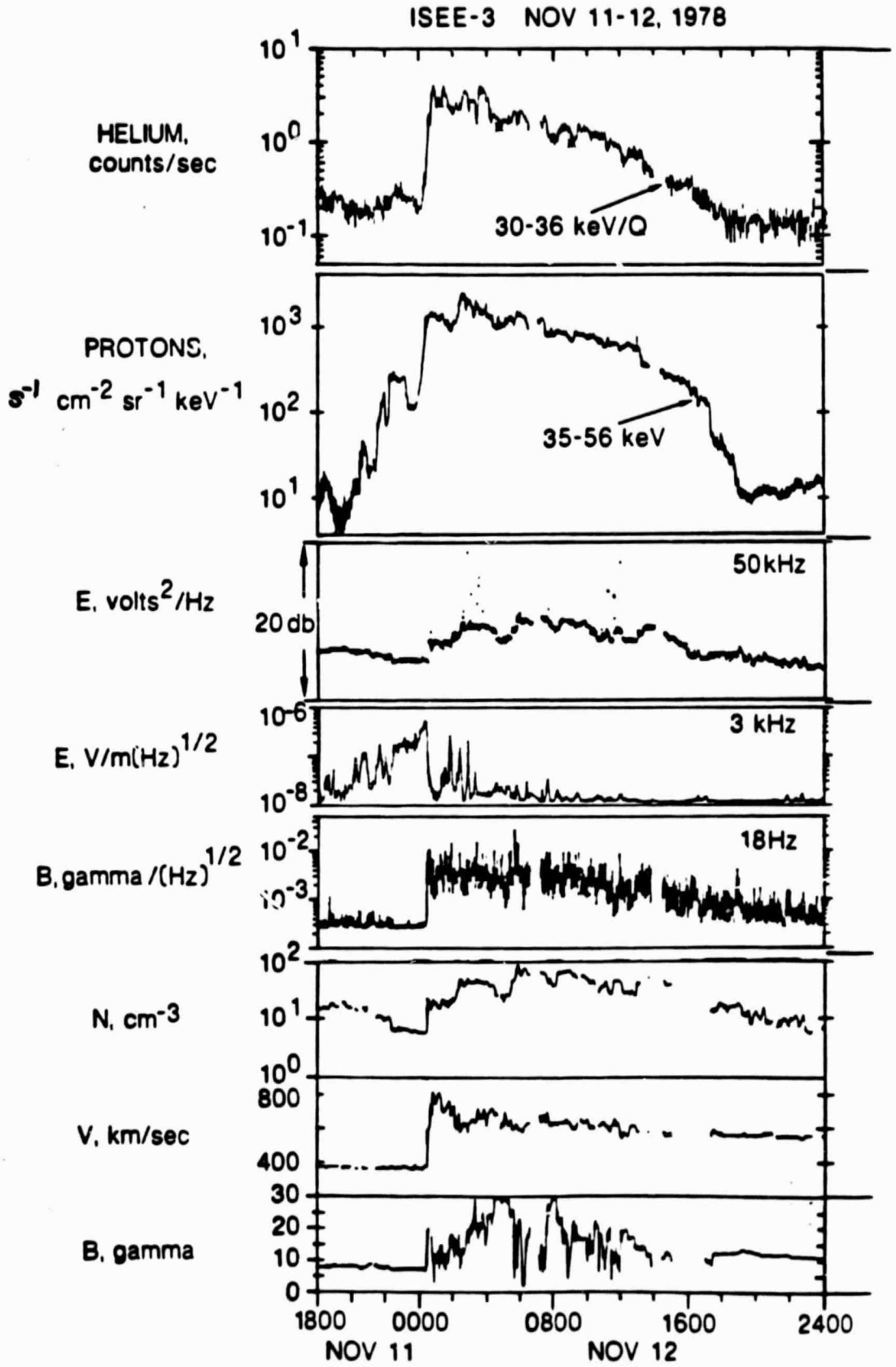


Figure 1

Figure 2: ISEE-1 and -3 Magnetic Field Measurements at Shock Encounter.

Shown here are the Y-component (GSM) and the magnitude of the magnetic field measured during and after the ISEE-1 and -3 shock encounters at 0058:30 UT and 0028:20 UT, respectively, on November 12, 1978. Note that the time scales are identical, but that the ISEE-1 and -3 vertical scales differ. The magnetic field magnitude profiles are essentially identical at each spacecraft. The shock compresses the field from 7.5 to 16.5$\gamma$: The shock is followed by a small overshoot in the magnetic field; after the overshoot, the field slowly increases until the strong rotation, which is apparent in the Y-component, is encountered at 0105:20 (ISEE-1) and 0034:10 (ISEE-3). The region between the shock and the rotation contains extremely large transverse magnetic field fluctuations which hardly affect the field magnitude. We will argue that these have wavelengths comparable with the thermal ion Larmor radius in the shock-heated plasma and are, therefore, consistent with the resonant firehose instability (Moiseev and Sagdeev, 1963; Kennel and Sagdeev, 1967; Kennel and Scarf, 1968).

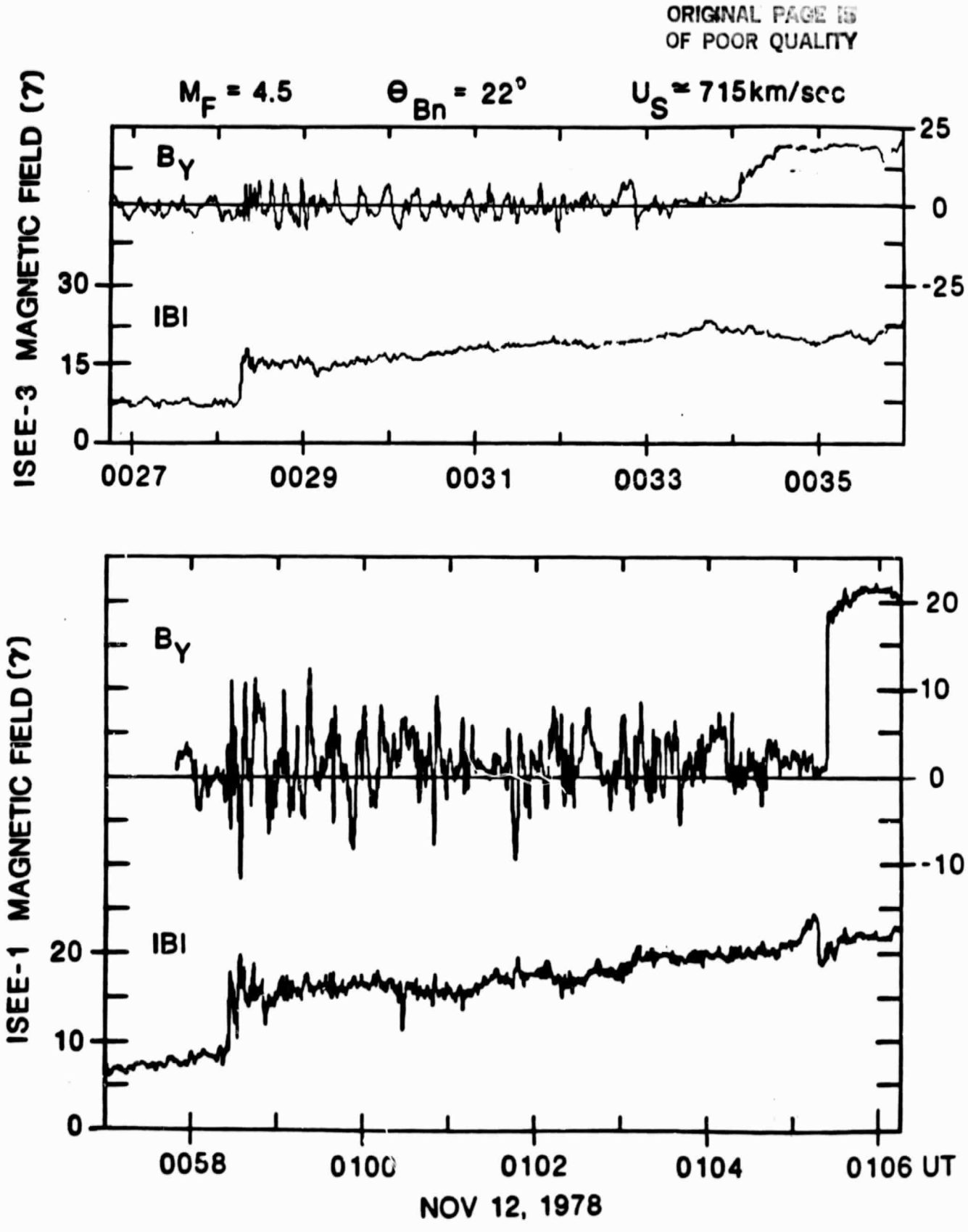


Figure 2

Figure 3a: Global Geometry of the Interplanetary Shock at the Time of the ISEE-3 Encounter: X-Z Plane

This figure sketches, approximately to scale, the relative positions of the terrestrial magnetosphere, ISEE-1, ISEE-2, ISEE-3, and the interplanetary shock at 0028 UT on November 12, 1978. Also shown are the magnetic field directions measured at ISEE-1 and -3 at that time, together with the post-shock magnetic field measured at ISEE-3. The shock normal $\hat{n}$ and the corresponding shock plane were taken from the Method 3 shock normal solution discussed in Section 3.2. The interplanetary field was essentially in the X-Z plane, and the shock normal angle $\theta_{BN}$ was roughly 40°. The fact that the magnetic fields measured at ISEE-1 and -3 were essentially parallel indicates that the IMF upstream of the shock was essentially uniform over the roughly 200 $R_E$ separating ISEE-1 and -3. A straight-line projection, as well as a more sophisticated time-projection (Greenstadt et al., 1982), of the ISEE-3 field line indicates that it was not connected to the bow shock. ISEE-1 and -2, on the other hand, were probably magnetically connected to both shocks.

Figure 3b. Global Geometry of the Interplanetary Shock at the Time of the ISEE-3 Encounter: X-Y Plane

This figure has the same format as Figure 3a. The magnetic field rotation apparent in the By-components of Figure 2, followed the shock at ISEE-3. If this rotational discontinuity co-moved with the post-shock flow (670 km-$s^{-1}$), it would have been approximately 40 $R_E$ downstream of the shock and is so sketched. We assumed that both the shock and the rotational discontinuity are planar in the absence of information to the contrary. Note that the rotation carries the IMF into an anti-gardenhose configuration.

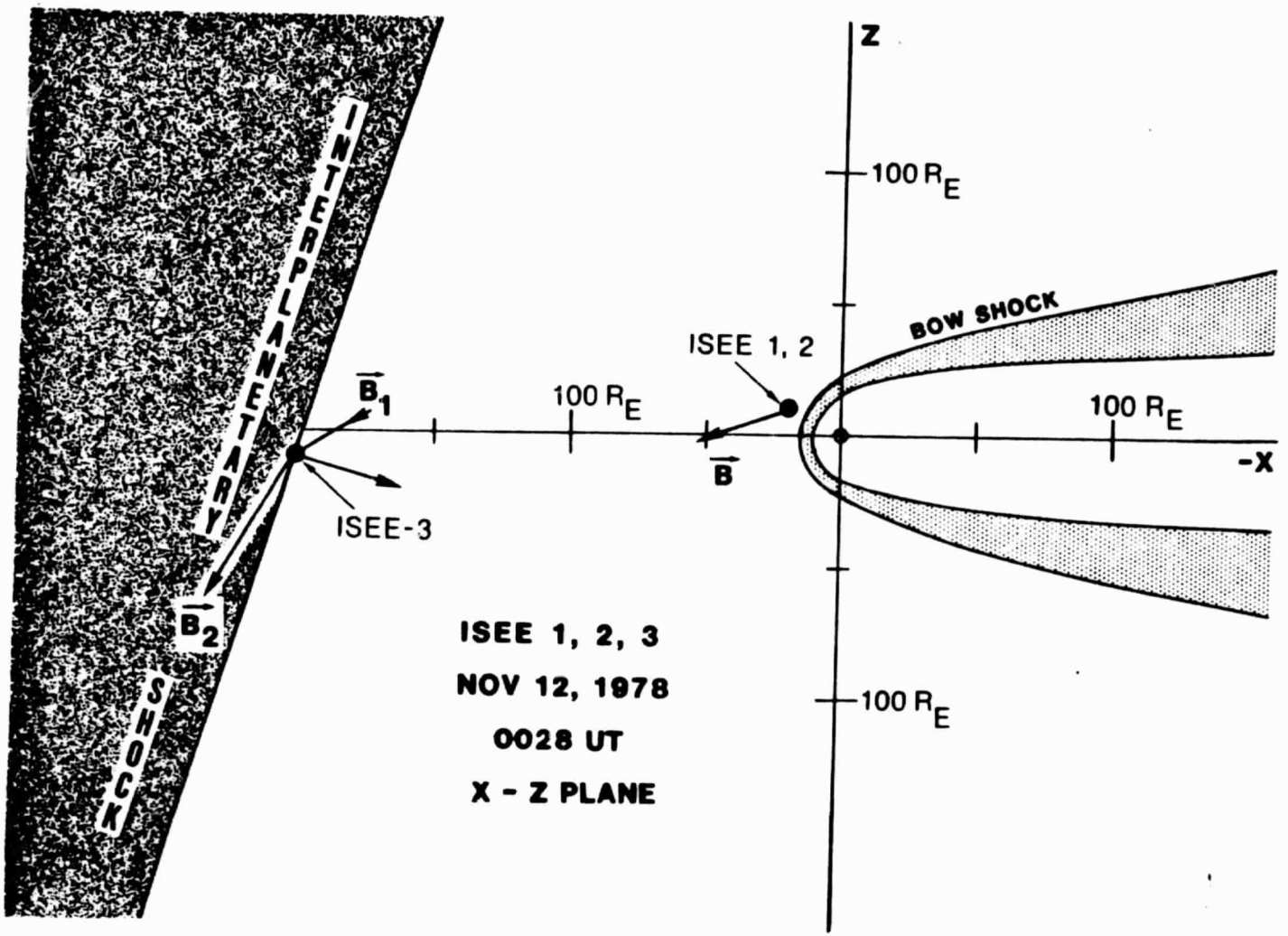




Figure 3a

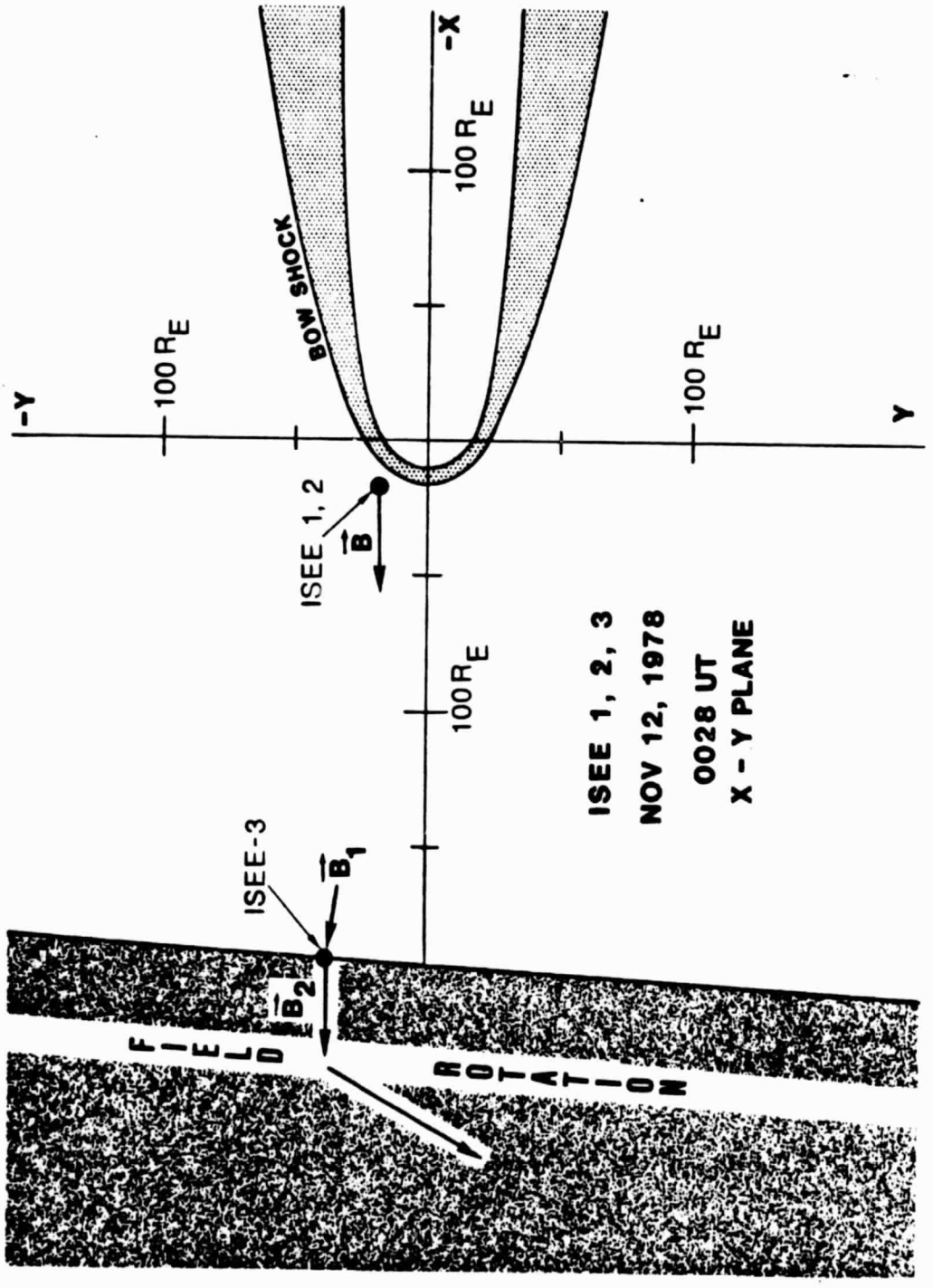


Figure 3b

Figure 4: Electric and Magnetic Fields Before and After ISEE-1 Shock Encounter

The top two panels show the X and Y-components of the interplanetary electric field, and the bottom three, the X, Y, and Z-components of the interplanetary magnetic field measured at ISEE-1 between 0050 and 0115 UT on November 12, 1978. The third component of the electric field, $E_Z$, can be estimated assuming $\vec{E} \cdot \vec{B} = 0$. The measured $\vec{E} \times \vec{B}$ drift upstream of the shock may be shown to be consistent with the measured solar wind velocity. The shock at 0058:30 is most apparent in $E_Y$ and $B_Z$. Note the gentle ramp in $E_X$ that leads the shock by about one minute. The rotational discontinuity at 0105:30 is manifested in $E_X$, $E_Y$, $B_Z$, and $B_Y$. Since $B_X$ changes only slightly near 0105:30, we infer that the rotational discontinuity was propagating in either the + or - X-direction. The large-amplitude magnetic turbulence in Figure 2 was restricted largely to the $B_Y$-component, suggesting that it was linearly polarized. This turbulence was confined to the region between the shock and the rotational discontinuity.

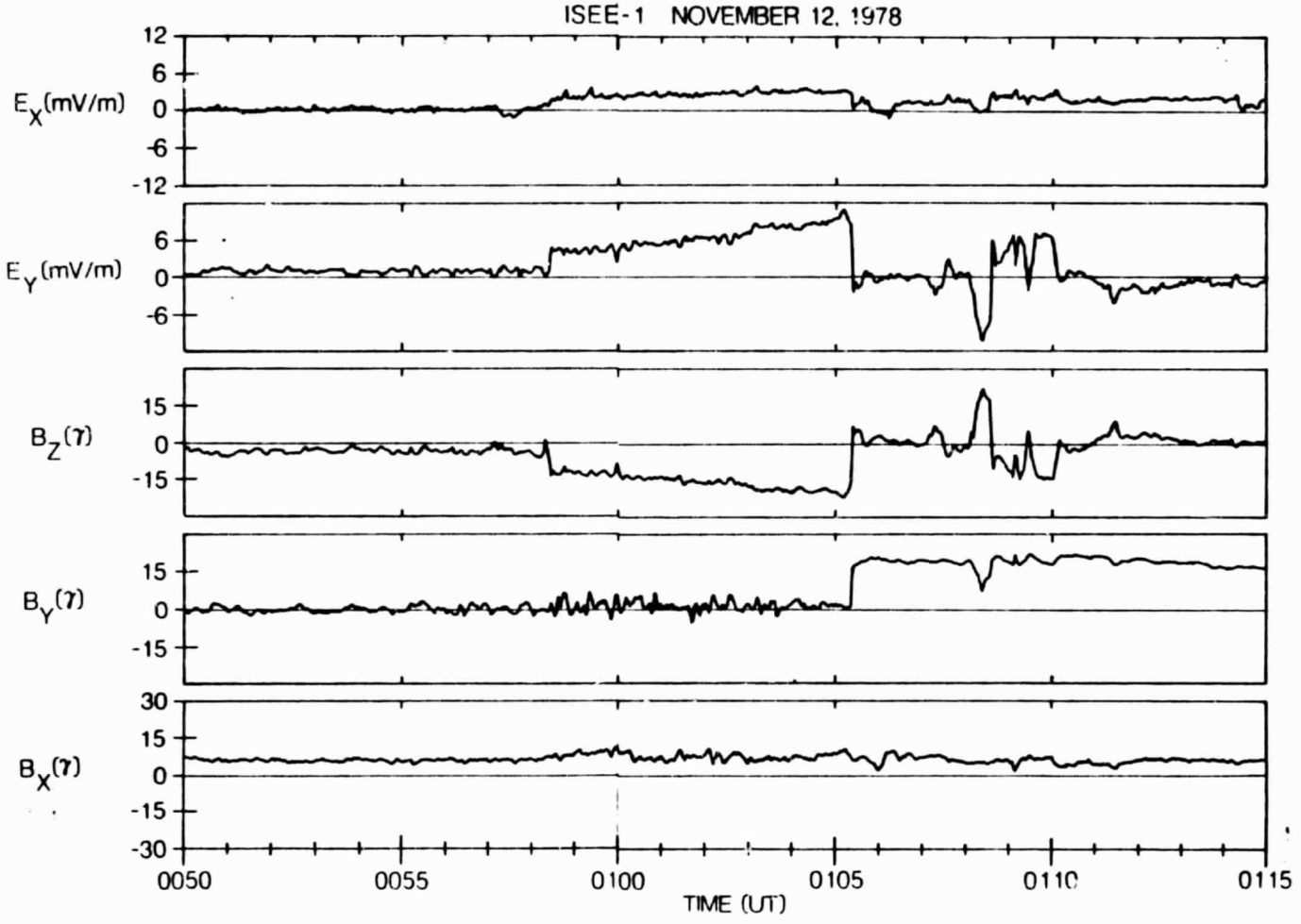


Figure 4

Figure 5: First Magnetic Neutral Sheet Encounter: ISEE-1 and -3

Both ISEE-1 and -3 encountered a magnetic neutral sheet approximately 26 minutes after their shock encounters. The top four panels show the ISEE-3 magnetic field magnitude and components, and the bottom panel shows the ISEE-1 magnitude, for the twelve minutes surrounding the neutral sheet encounters. Note that $B_X$ and $B_Y$ change sign at ISEE-3, while $B_Z$ remains small.

Figure 6: Next Three Magnetic Neutral Sheet Encounters: ISEE-3

These three panels show the magnitude of the IMF for twelve minutes surrounding the ISEE-3 magnetic neutral sheet encounters at 0114 UT, 0207 UT, and 0229 UT on November 12, 1978. The facts that the magnetic field was in the X-Z plane (Figures 3a,b) and multiple neutral sheets were encountered suggest that ISEE-1, -2, and -3 and the earth were in the general field reversal region of the solar wind during the shock event of November 11-12, 1978. Furthermore, we expect the IMF field topology was complex, with alternating regions of closed magnetic loops and "open" field lines. We will argue that the shock was in one such loop, which ISEE-3 entered at 2230 UT.

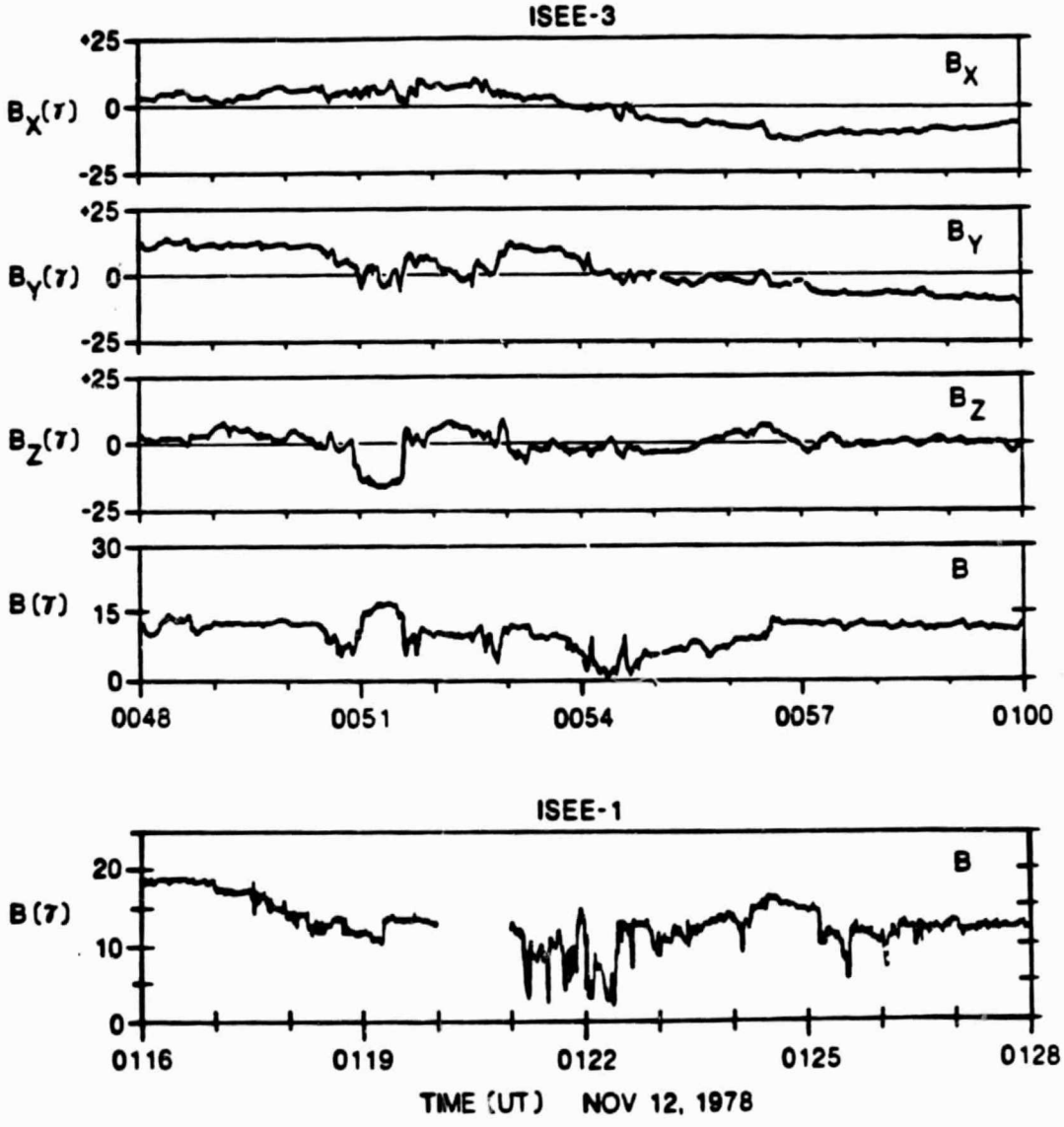


Figure 5

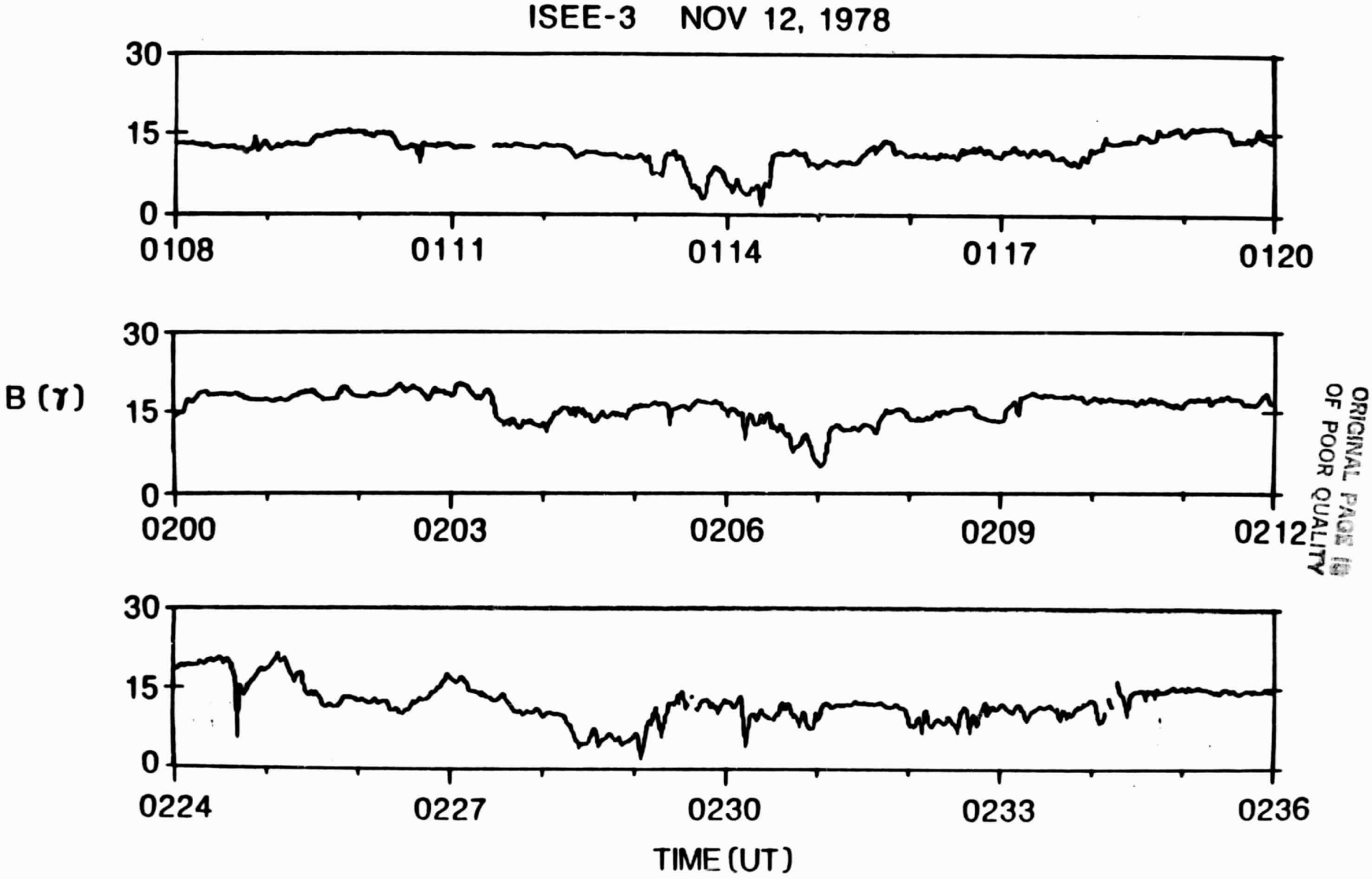




Figure 6

Figure 7: ISEE-3 Electron Model Parameters Upstream of the Shock

The ISEE-3 solar wind electron data are normally reduced, in survey mode, in terms of a model that fits the distribution by a sum of bi-Maxwellian, drifting core and halo distributions. Various moments of these models are then displayed as a function of time. The top panel in this figure shows the heat flux parallel to the magnetic field, the middle panel shows the total and halo component densities, and the bottom panel shows the halo (top pair of curves), the core (bottom pair), and the average (middle pair) electron temperatures. The thermal anisotropy may be estimated from the width of the shaded regions; the top of each region is the parallel temperature, and the bottom is the perpendicular.

Note that the heat flux, which was always away from the sun and the oncoming interplanetary shock, fluctuated violently before 1840 UT. The heat flux and the densities diminished, and the temperatures increased, at 2230 UT and then held constant until shock encounter. The solar wind electrons were clearly in a different state after 2230 UT.

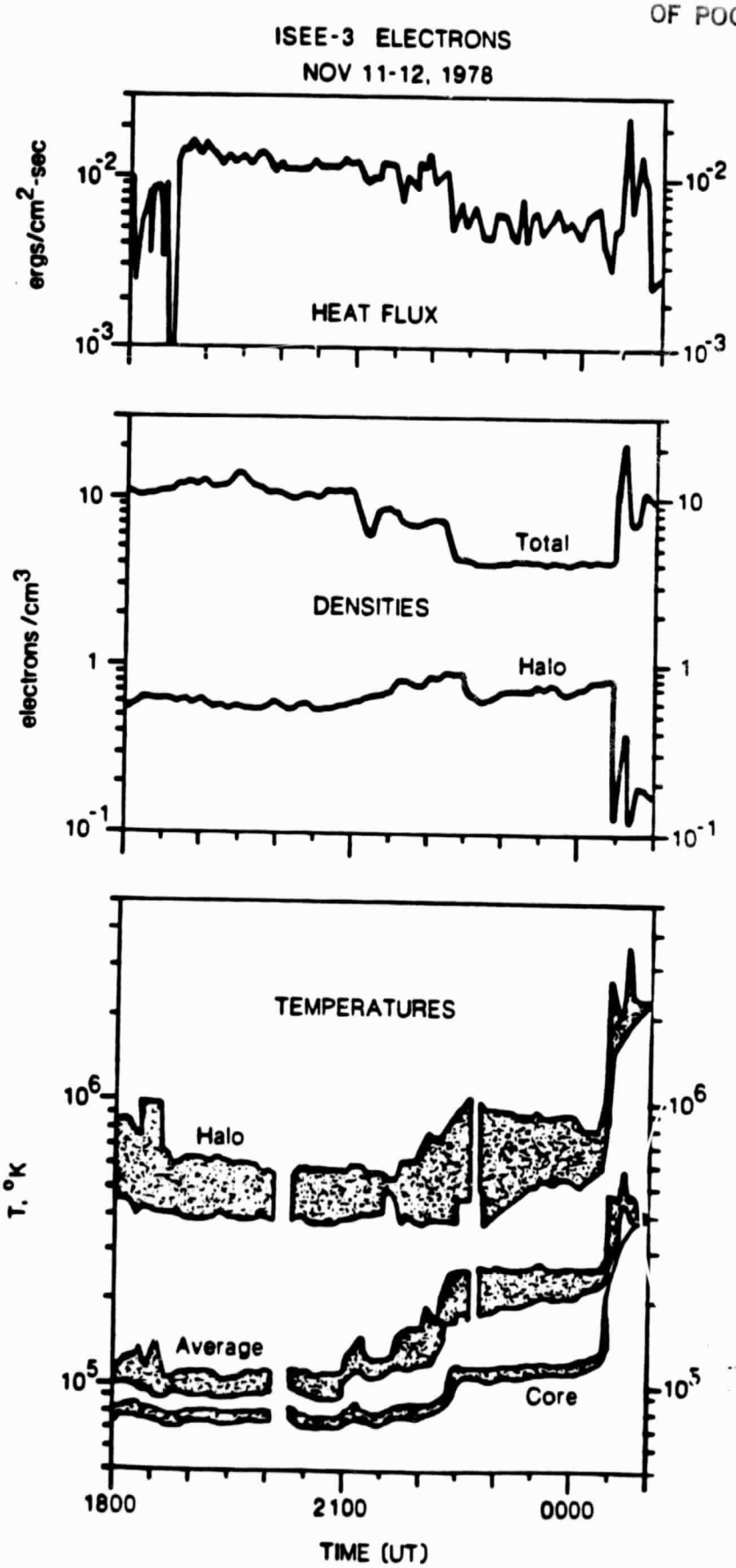


Figure 7

Figure 8: ISEE-3 Halo Electrons Upstream of the Shock

The top panel presents the parallel drift speed, relative to the solar wind ions, of the ISEE-3 model halo electron distribution. The middle and bottom panels present the partial densities and first moment drift velocities of the away ($V_{||} > 0$) and toward ($V_{||} < 0$) semi-distributions of halo electrons. The net halo drift (top panel) diminished near 2230 UT, not because the number of electrons streaming away from the shock declined, but because they were almost compensated by a new component of electrons streaming toward the shock. Since the ISEE-3 field line was not connected to the bow shock, the new "toward" halo electrons cannot have come from the bow shock. We believe that they, too, were generated at the interplanetary shock and streamed the long way around a closed magnetic loop to ISEE-3. This loop had a spatial scale of 800 $R_E$ or more.

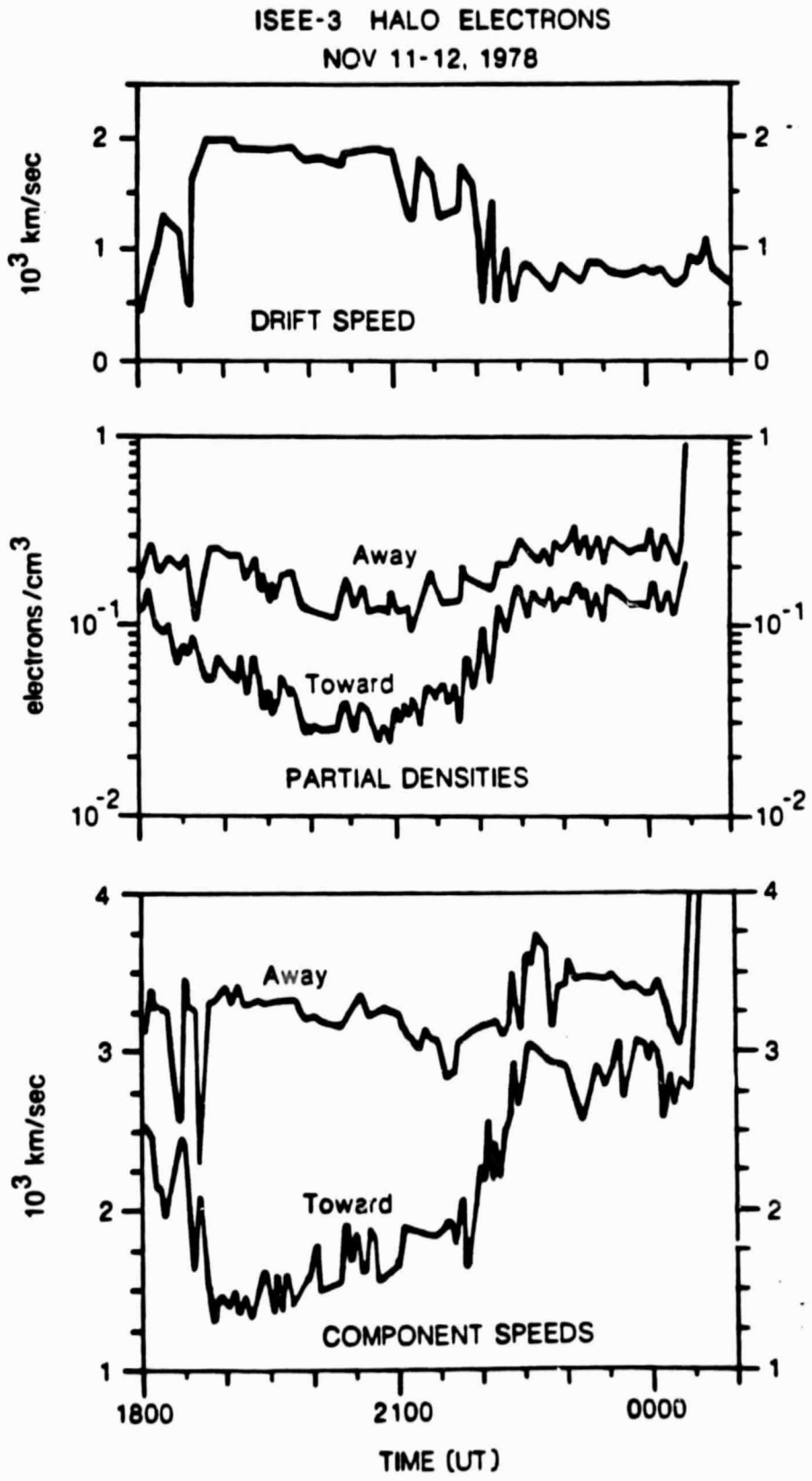


Figure 8

Figure 9: ISEE-3 Entry into the Closed Magnetic Loop

The increase in 3.16 kHz ion acoustic electric field amplitude at 2230 UT in Figure 1 evidently was associated with ISEE-3's passage into the closed magnetic loop. The bottom panel in this figure shows 1-min average 3.16 kHz electric field amplitudes on an expanded time scale. The averages clearly increase around 2230 UT. The top panel indicates that the 35-56 keV proton flux increased about a factor 3 upon entering the loop. The middle panel shows the first parallel anisotropy moment of the energetic protons. The protons become essentially isotropic upon entering the loop. Figure 1 indicates that there was sporadic activity in the ion acoustic amplitudes prior to 2230 UT; however, the intensities remained high after 2230 UT and increased toward shock encounter.

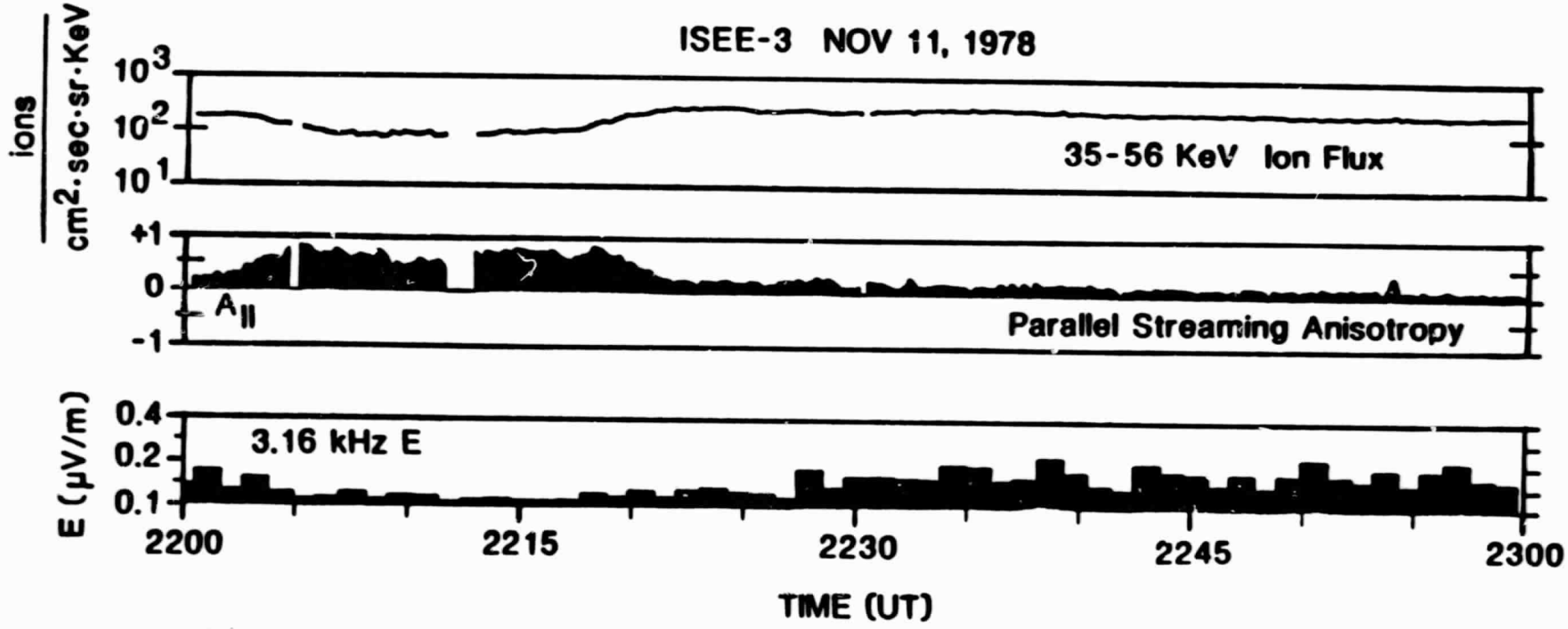


Figure 9

Figure 10: Upstream Ion Acoustic and MHD Waves: ISEE-3

The top panel shows the 3.16 kHz ion acoustic wave amplitudes, and the bottom two panels show the variances in the .01-3 Hz interplanetary $B_Y$ and $B_Z$ field components for the period 2100 UT on November 11 to 0100 UT on November 12, 1978. The times of magnetic bubble entry, and the encounters with the shock, field rotation, and the first neutral sheet are indicated by vertical lines. Bursts of ion acoustic and MHD wave activity accompany one another before bubble entry, and both ion and MHD waves are continuously enhanced within the bubble. Note that the 1-min average ion wave amplitudes increase significantly in the last half-hour before the shock, during which time the 35-56 keV proton intensity also increased, whereas the .01-3 Hz magnetic field amplitudes remained more or less constant.

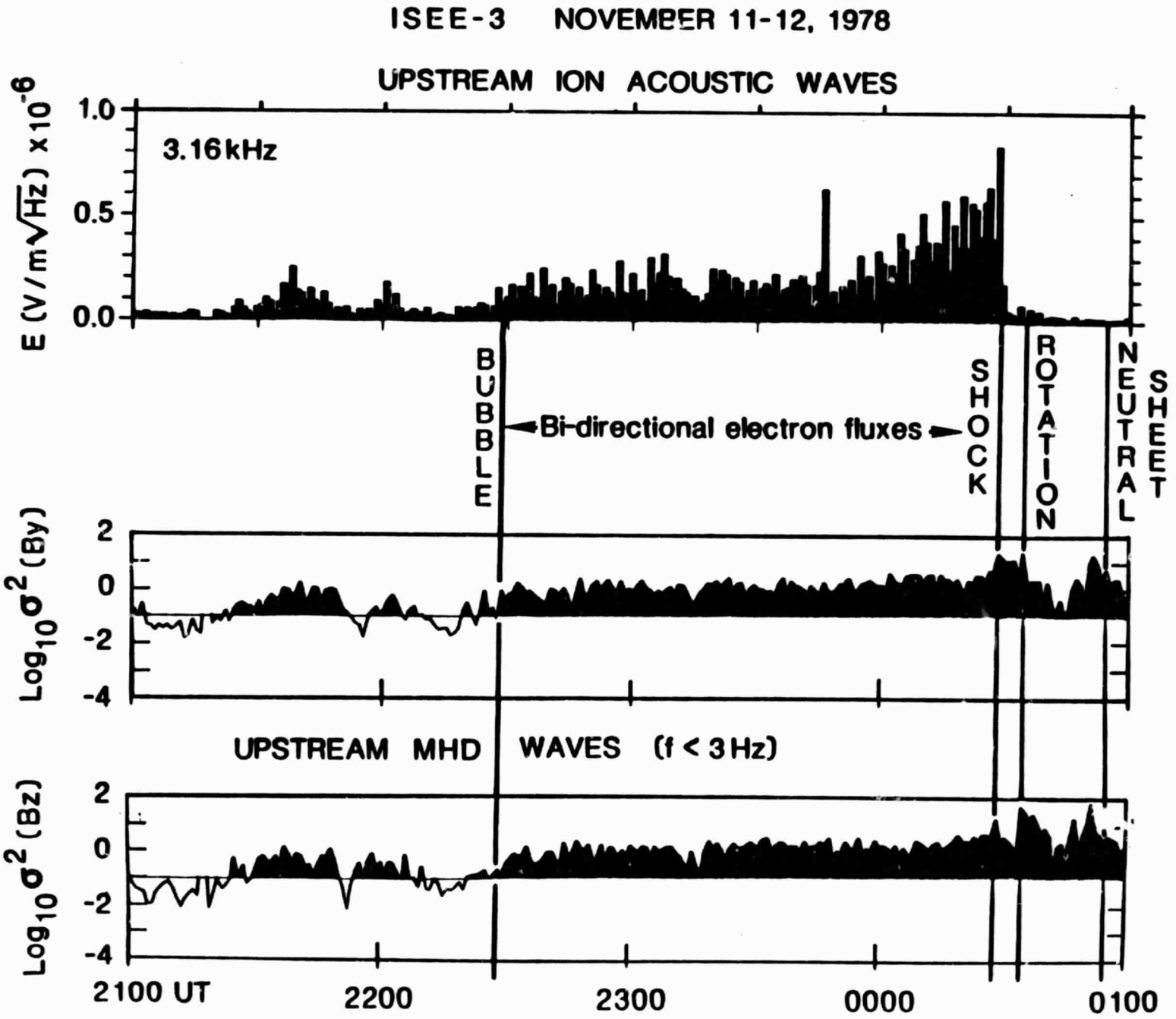


Figure 10

Figure 11: Frequency, Polarization, and Amplitude Characteristics of MHD Waves Measured Upstream of ISEE-3 Shock Encounter

Shown here are the wave normal angle $\theta_{KB}$, the ellipticity, the percent polarization, and the total rms and compressional amplitudes (normalized to the magnitude of the IMF) plotted against the frequency measured in the spacecraft frame. The spectral decomposition between .005 and 0.32 Hz for the period 0012-0028 UT on November 12, 1978 is plotted as a solid line. An indication of the spectral properties above 0.32 Hz is given by the dotted curves, which show data for the period 0025-0027:30 UT which ended approximately 40 seconds before shock encounter.

The total rms power was enhanced between 0.01 and 0.16 Hz; the proton cyclotron frequency was roughly 0.12 Hz. The absence of significant power near 1 Hz indicates that the wavelengths were longer than the thermal ion Larmor radius. Note that the waves were relatively weakly, elliptically polarized and propagated more or less parallel to the IMF ($\theta_{KB} \cong 20°$). The peak-normalized rms amplitude (0.16) will be compared with theoretical expectation in Chapter 8.

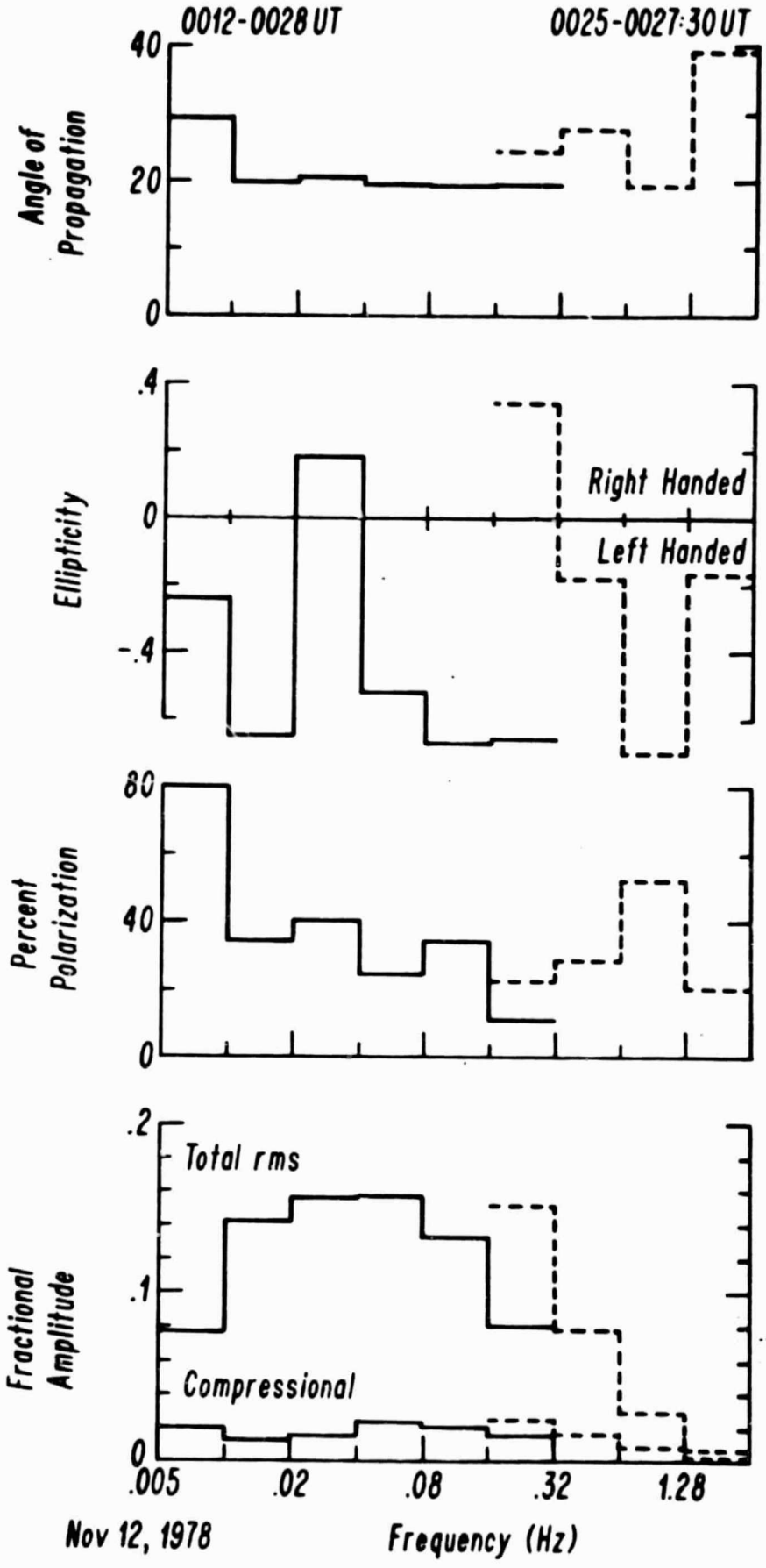


Figure 11

Figure 12: Energetic Protons and MHD Turbulence Upstream of the ISEE-3 Shock Encounter

The top panel shows the energetic proton fluxes in eight different energy channels; the middle panel, rough spectral indices formed from the ratios of the fluxes in adjacent energy channels; and the bottom panel, the variance in the Y-component of the IMF for the period 2100 UT to 0100 UT on November 11-12, 1978. The channel energies are as follows: (1) 35-56 keV; (2) 50-91 keV; (3) 91-147 keV; (4) 147-237 keV; (5) 237-383 keV; (6) 383-619 keV; (7) 619-1000 keV; and (8) 1000-1600 keV. The scales appropriate to the energy channels alternate: Channel 1 to the topmost left, channel 2 to the topmost right, and so on. The labels 1/2, 3/4, etc. in the middle panel refer to the energy spectral index inferred from the ratios of the fluxes measured in the first and second channels, third and fourth, and so on.

Note that the fluxes in channel 1 increased before bubble entry, plateaued, and then diminished near 2330 UT. The protons between 35 keV and 237 keV increased in intensity after 0000 UT and then held roughly constant after the shock. Protons at all measured energies responded to the rotational discontinuity. The fluxes of protons above 619 keV (channels 7 and 8) rose perceptibly as the shock approached, but did not change as the magnetic bubble passed over ISEE-3. The low-energy spectral indices diminished as the shock approached, and the 1/2 index even became negative, indicating the presence of high-energy particles diffusing to ISEE-3 from the oncoming shock.

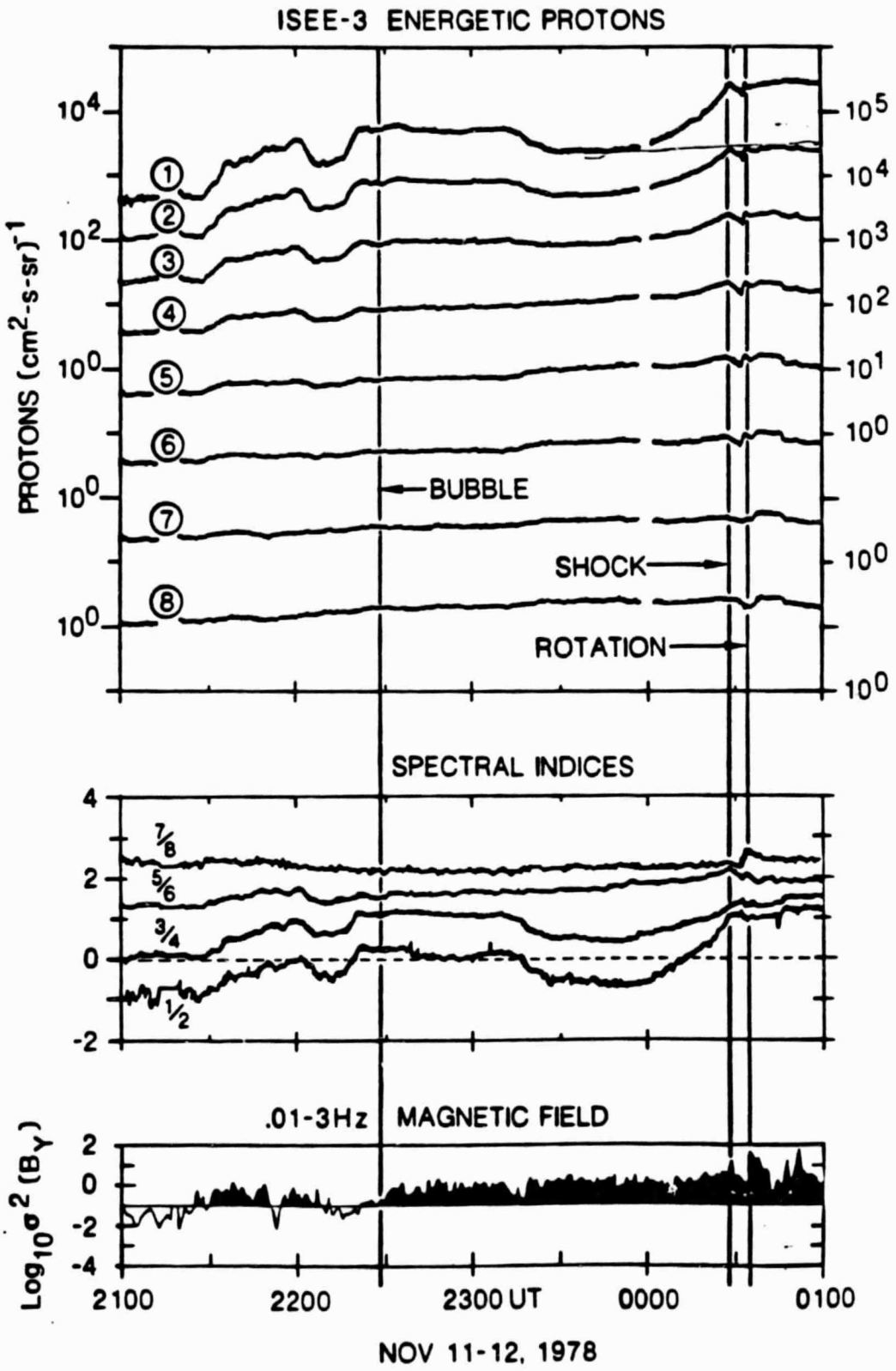


Figure 12

Figure 13: Plasma Wave Electric Fields Observed Upstream of the Interplanetary Shock and Bow Shock: ISEE-1

Presented here are swept frequency receiver (SFR) plasma wave electric field measurements made between 1800 UT and 0200 UT on November 11-12, 1978. ISEE-3 exited the bow shock at 1840 UT and immediately began to detect intense 40-50 kHz electron plasma waves which persisted, with a decrease in frequency consistent with the general decrease in density measured at ISEE-3 (Figure 1), until the interplanetary shock at 0058 UT. Such plasma waves were not detected at ISEE-3, which was not magnetically connected to the bow shock. The fact that the plasma waves at ISEE-1 were detected from bow-shock exit until interplanetary shock encounter suggests that ISEE-1 was connected to the bow shock, and probably also to the interplanetary shock, as Figures 3a,b suggest.

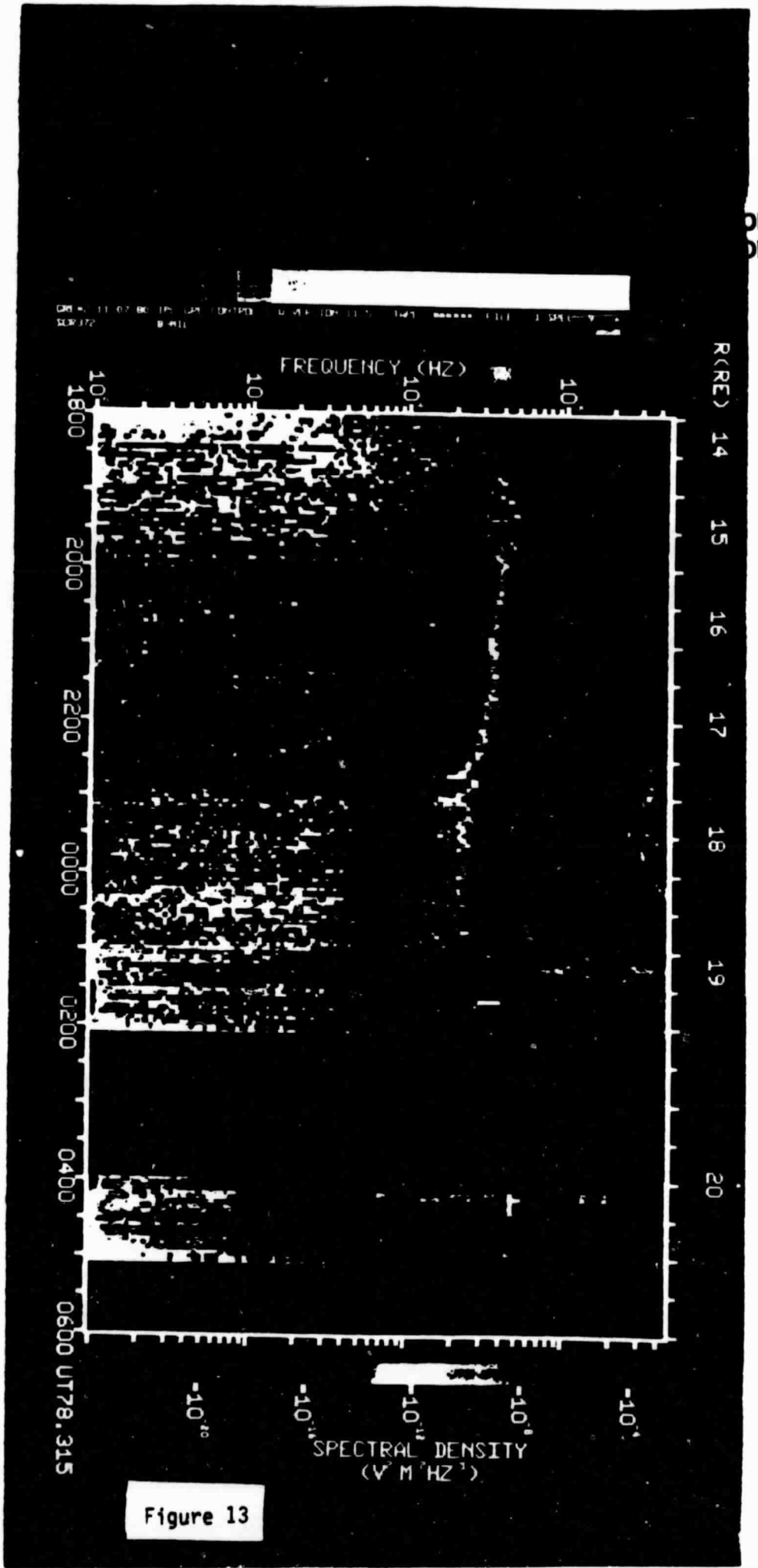


Figure 13

Figure 14: Comparison of Upstream MHD Waves Measured at ISEE-1 and -3

The top two panels show the RMS variances in the magnitude, $B_T$, and the Y-component, $B_Y$, of the interplanetary field at ISEE-3 for a 3½-hour period surrounding shock encounter. The bottom two panels show the same quantities measured at ISEE-1. We estimate that ISEE-3 entered a closed magnetic loop at 2228 UT on November 11; if the loop convected with the solar wind speed between ISEE-3 and -1, ISEE-1 would have entered it at about 2330 UT, as indicated. The variances at ISEE-1 do increase at that time. Note that the ISEE-1 magnitude variances are considerably larger than those at ISEE-3. This difference may be due in part to the fact that ISEE-1 may have detected upstream turbulence from both the interplanetary and bow shock.

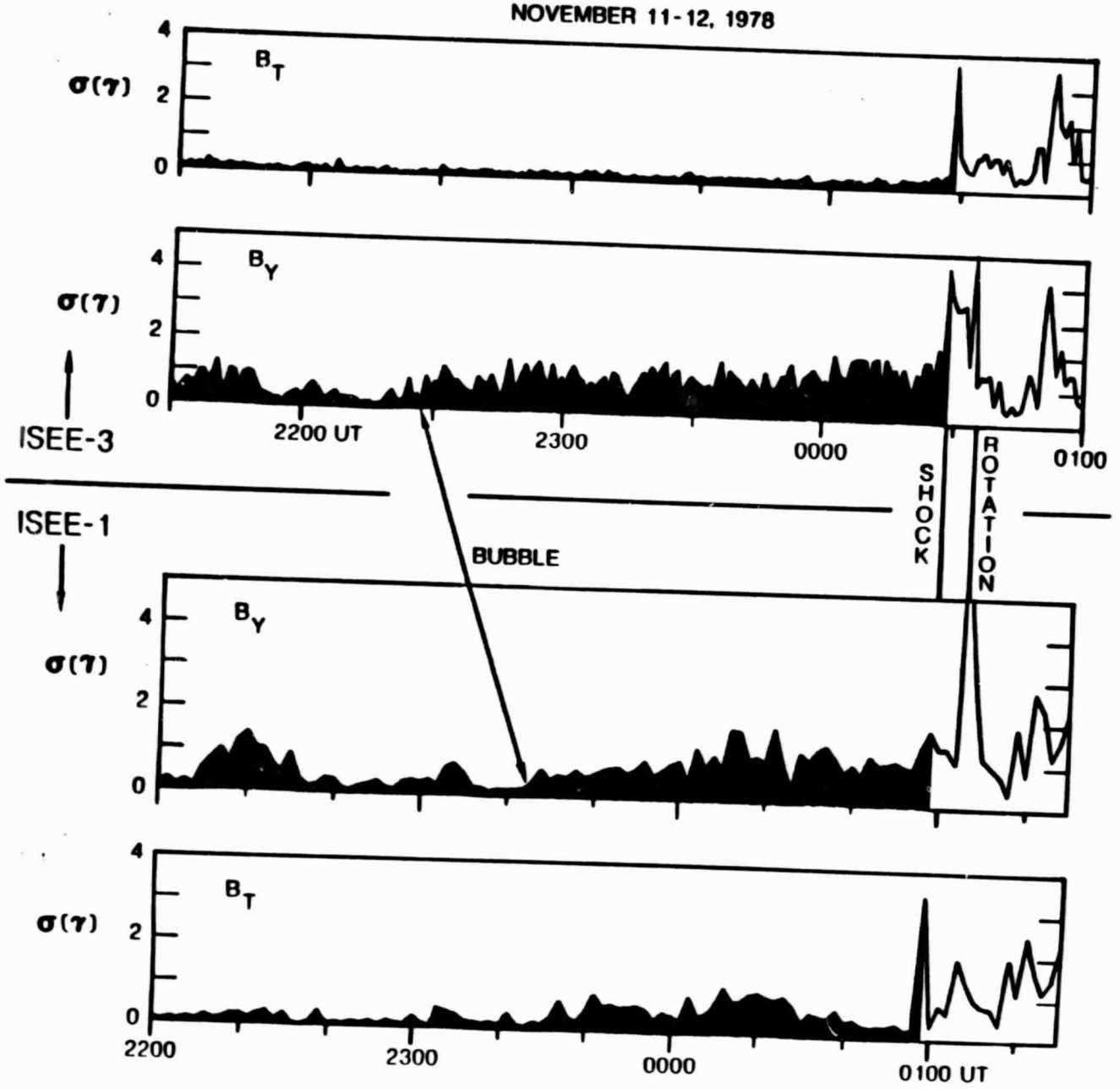


Figure 14

Figure 15: Bubble Entry and Shock Encounter: ISEE-1

The top two panels show 1 kHz and 1.78 kHz ion acoustic electric field amplitudes for the period 2200 UT - 0200 UT on November 11-12, 1978. The 1-min average amplitudes are indicated by solid shading, and the peak amplitudes detected during the averaging interval are connected by a thin line. Large peak-to-average amplitude ratios characterize solar wind ion acoustic turbulence. The middle panel shows the variances in the .01-3 Hz Z-component of the IMF, and the bottom two panels show the differential fluxes of 2 and 6 keV protons. Upstream of the bubble entry near 2330 UT, the activity in ion acoustic waves, MHD waves, and few keV protons tends to be correlated in time. Bubble entry is marked by a striking increase in the 6 keV proton differential flux.

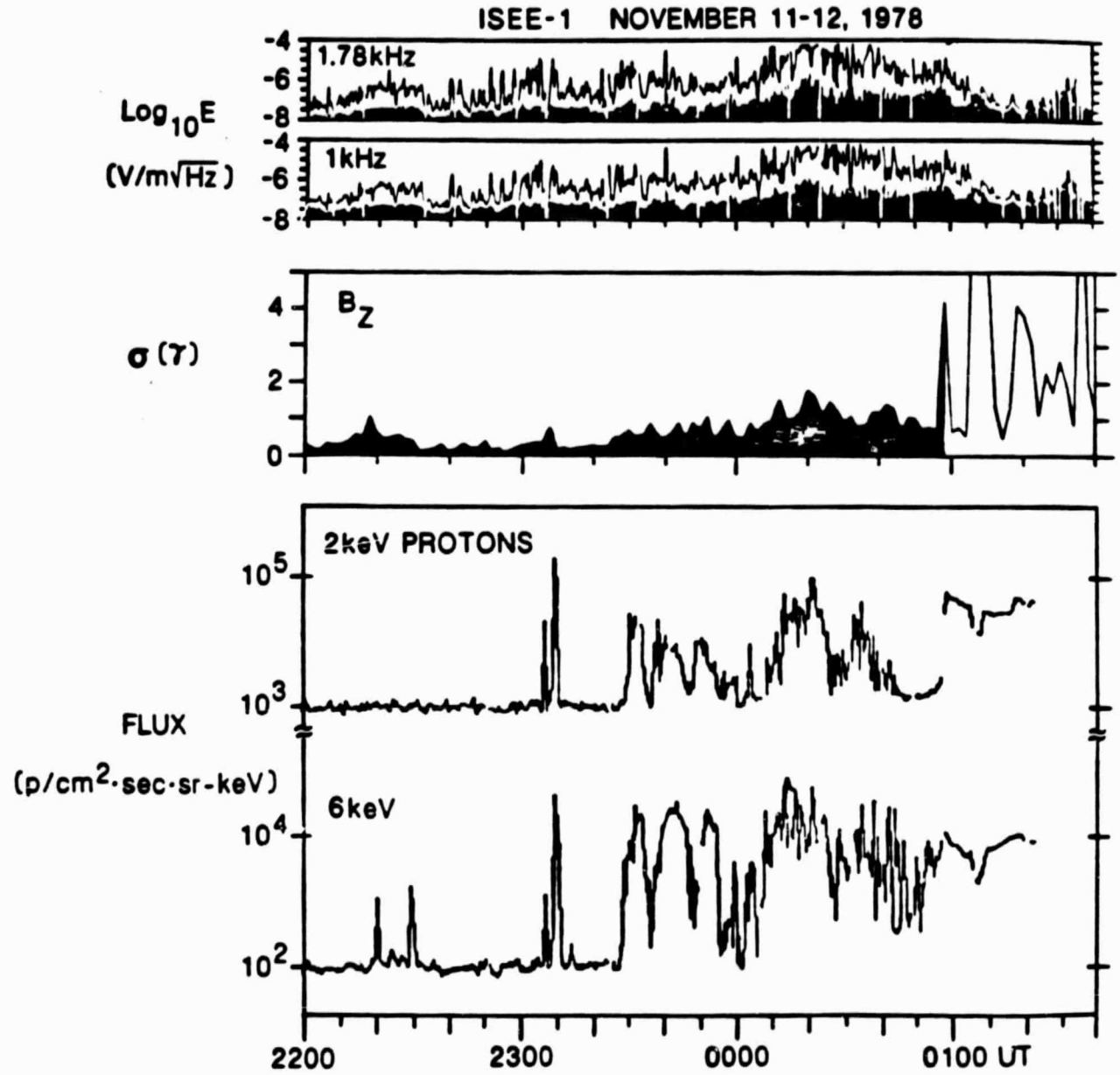


Figure 15

Figure 16: Character of Upstream MHD Waves at ISEE-3 and ISEE-1 Magnetic Bubble Entry

Although MHD wave activity occurred at ISEE-1 and -3 prior to bubble entry, it was continuously present afterward. This figure compares the MHD wave activity in all three vector components and in the magnitude of the magnetic field for a 12-minute period surrounding ISEE-3 bubble entry at 2228 UT, and the ISEE-1 entry at 2328 UT. ISEE-3 data is at the top of each panel, and ISEE-1 data is at the bottom. The ISEE-3 magnitude scale is at the left of each panel, and the ISEE-1 scale is at the right. The ISEE-3 time scale is at the top of the figure, and the ISEE-1 scale is at the bottom. It is clear that a significant enhancement of wave activity occurred at bubble entry and that the waves had the same general periodicity and character at both spacecraft. In particular, the magnitude and Y-component was noticeably less variable than were the Y and Z-components of the interplanetary field. The fact that large-amplitude oscillations commence within a few wave periods suggests that the waves were already present in the bubble before it swept over the spacecraft.

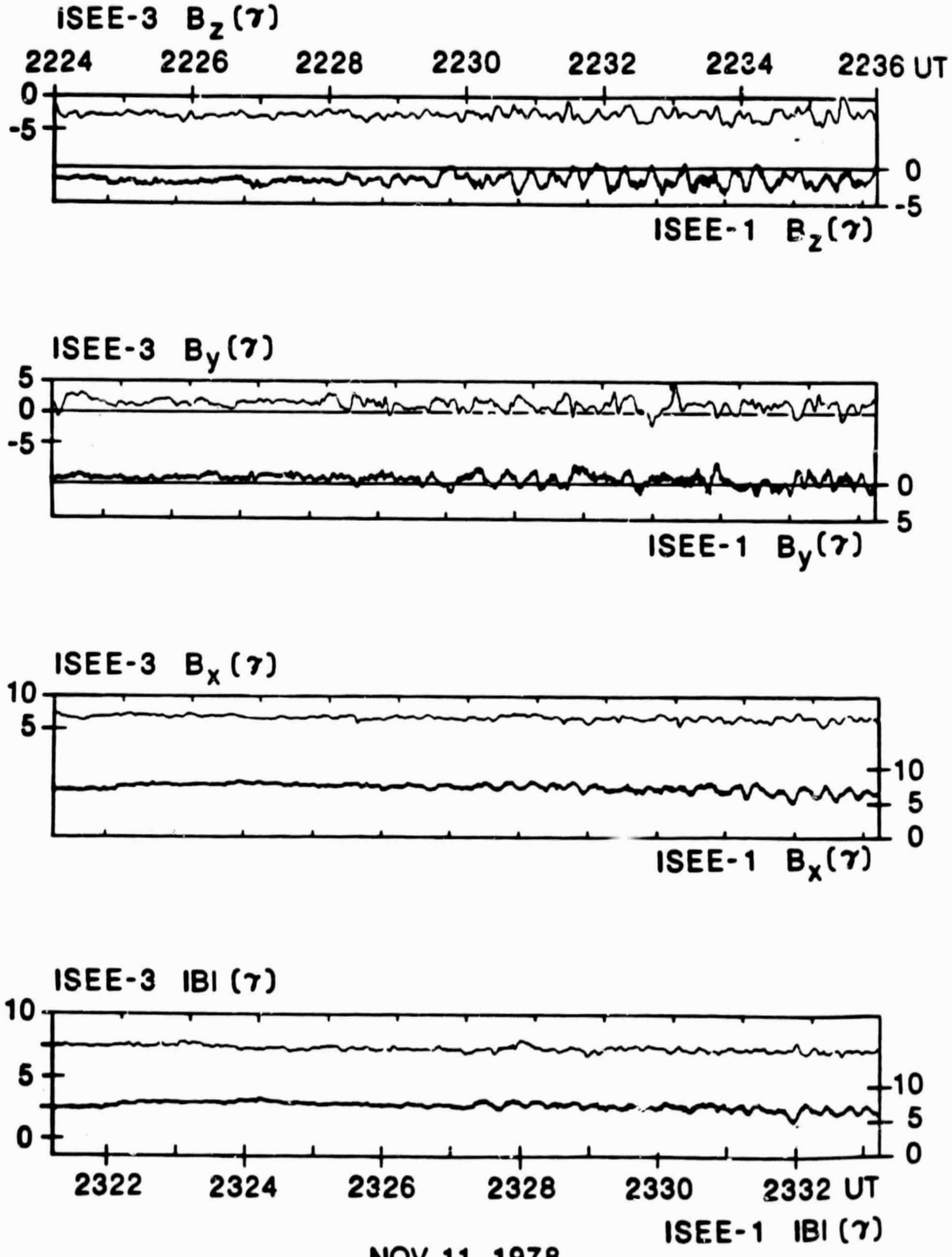


Figure 16

Figure 17: Modulated Few keV Protons at Bubble Entry: ISEE-1 and -2

This figure compares the 6 keV proton fluxes and the Z-component of the IMF measured at ISEE-1 and -2 for a 12-minute period surrounding bubble entry. Extremely large modulations of the proton fluxes accompany the MHD wave activity; the peak fluxes occur when $B_Z$ is closest to zero, as is indicated by the vertical lines. Since the 6 keV proton detector looks essentially along the Z-direction, the peaks correspond to 90° pitch angle protons. The 6 keV protons appear to be extremely anisotropic.

ISEE-2 was about 4000 km upstream of ISEE-1, corresponding to a 12-second delay at the solar wind speed. The ISEE-2 data has been offset relative to the ISEE-1 data by 12 seconds. The rough correspondence of the proton intensity peaks and magnetic field oscillations suggest that protons and waves were convected from ISEE-2 to ISEE-1.

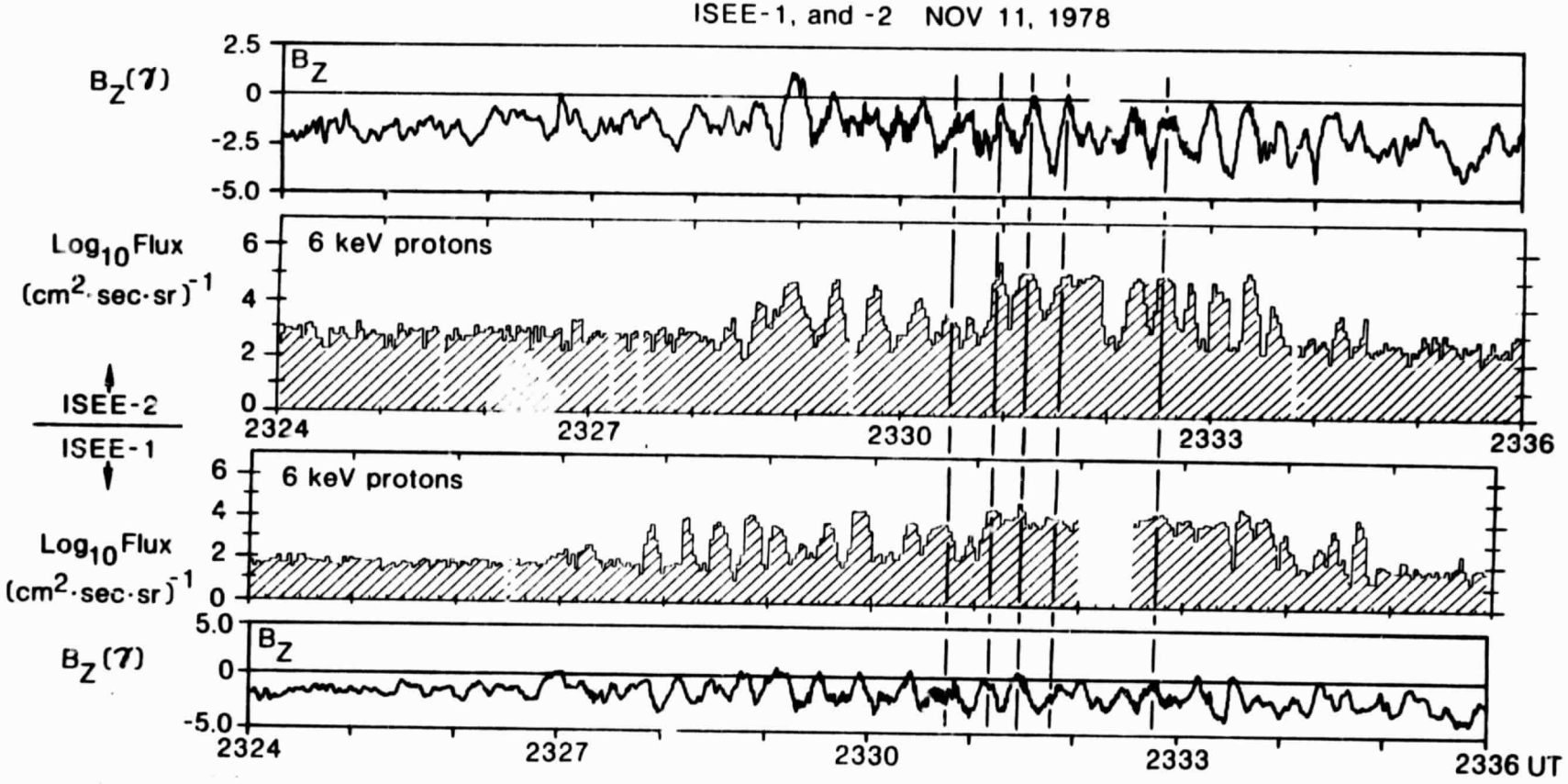


Figure 17

Figure 18: Electron Drifts and Ion Acoustic Waves: ISEE-3

The large electron heat fluxes in Figures 6 and 7 would lead to a strong parallel current unless the core electrons drifted relative to the ions in a direction opposite to the halo electron drift. The top panels compare the electron current carried by the halo electron model distribution with the current carried by the core electrons. The extent to which the two profiles are mirror symmetric indicates the degree of current neutrality. Note that the core electrons drifted with a parallel speed of about 200 km-$s^{-1}$ after bubble entry at 2228 UT. The bottom panel shows 5-min average (bar graph) and peak (dots) 1.78 kHz ion accoustic electric field amplitudes for the same time period. The origin of solar wind ion acoustic turbulence has been puzzling, because it is generally believed that the electron-to-ion temperature is too low for instability during such events. Indeed, the 200 km-$s^{-1}$ measured drift was below ion acoustic threhold for this event; it is possible that the ion wave activity was thermal fluctuations enhanced by the large electron heat flux. On the other hand, the measured core drift was near or at threshold for the ion cyclotron heat flux instability.